ROTATIONAL SKIN STRETCH FEEDBACK: A NEW APPROACH TO WEARABLE HAPTIC DISPLAY

A DISSERTATION
SUBMITTED TO THE DEPARTMENT OF MECHANICAL ENGINEERING
AND THE COMMITTEE ON GRADUATE STUDIES
OF STANFORD UNIVERSITY
IN PARTIAL FULFILLMENT OF THE REQUIREMENTS
FOR THE DEGREE OF
DOCTOR OF PHILOSOPHY

Karlin Young Ju Bark

March 2009

I certify that I have read this dissertation and that, in my opinion, it is fully adequate in scope and quality as a dissertation for the degree of Doctor of Philosophy.

(Mark Cutkosky) Principal Adviser

I certify that I have read this dissertation and that, in my opinion, it is fully adequate in scope and quality as a dissertation for the degree of Doctor of Philosophy.

(Larry Leifer)

I certify that I have read this dissertation and that, in my opinion, it is fully adequate in scope and quality as a dissertation for the degree of Doctor of Philosophy.

(Joan Savall)

Approved for the University Committee on Graduate Studies.

Abstract

We live in an increasingly technologically mobile environment where personal devices fit easily in our pockets and information is literally at our fingertips. However, while the information is *at* our fingertips, we obtain almost none of it *with* our fingertips, i.e., via tactile or haptic feedback from the devices. In contrast, haptic cues are an essential means by which humans and all other animals receive information about the world around them.

The work in this thesis is motivated by the idea that new modes of haptic interaction are needed to expand the range of activities and applications for wearable electronic devices. In applications ranging from motion training and physical rehabilitation to teleoperation of a remote system, haptic feedback can provide valuable information about forces and motions, particularly when vision and audition are otherwise occupied.

Today, by far the most widely used haptic technology for portable devices is vibration, as commonly found in cell phones. Vibration is easy to implement, but is best suited for transient event cues and is less effective when used continuously. It can lead to desensitization and many users find the stimulus annoying after a prolonged period of time. In addition, sensitivity to vibrations can be reduced when people are in motion. An under appreciated component of haptic sensation, particularly for applications involving portable devices, is skin stretch. Skin stretch is a known part of the normal physiological apparatus for proprioception, contributing to our sense of motion and location of our limbs. The motions and velocities necessary

to impart skin stretch can be low, allowing for the design of compact, low-power, wearable devices. With this motivation, the work in this thesis has focused on skin stretch for the display of proprioceptive information associated, for example, with the motions of a person's limbs. Two skin stretch devices are described. The first is a highly adjustable benchtop device for controlled testing; the second is a compact, wearable device to test skin stretch feedback in applications similar to those that might ultimately be encountered in motion training or proprioceptive feedback for amputees.

The major sections of this thesis are focused on understanding and quantifying the ability of humans to use and interpret rotational skin stretch. A series of psychophysical tests were completed to quantify the resolution of the devices. Our ability to interpret the feedback depends heavily on the setting and task. In an isolated environment, users are able to discriminate between different rotational displacements of stretch within 2-5 degrees, depending on the reference stimulus. In a more realistic setting where users are able to use the feedback to actively orient a virtual object, they are capable of positioning the object within ± 6 degrees on average. However, when users sit passively and are asked simply report the position of an autonomously moving object which they do not control, performance degrades. There is also a region of stretch near zero degrees, in which subjects have difficulty in interpreting the feedback accurately, which we call a "region of uncertainty". The size of this region depends on the details of the skin stretch end effector that is in contact with the skin. A three-dimensional analysis of skin motions, using visual tracking of markers on the skin, provides additional insight into the region of uncertainty and the factors that contribute to it.

A final set of experiments considers skin stretch in applications related to rehabilitation, or to the control of a prosthetic or teleoperated device, where skin stretch feedback substitutes for normal proprioception. Skin stretch feedback is compared to vibration feedback and to a baseline case of no haptic feedback. The results suggest that subjects can use skin stretch feedback to improve their control of a virtual

device. A particular benefit of skin stretch feedback in comparison to vibration is that it provides subjects with a sense of velocity as well as postion.

Acknowledgements

I have many people to thank, so let's just get started, shall we?

First and foremost, I thank my advisor, Mark Cutkosky for all of his support. I have always been in awe of how far his knowledge stretches and am grateful for his guidance and kind nature. Not everyone can say that their advisor took time from their Thanksgiving vacation to help a student prepare their defense. Thank you for teaching me not only how to research new ideas, but for giving me the opportunity to experience engineering through a unique, diverse learning environment.

To my reading committee, Larry Leifer and Joan Savall. Ever since I was an ME310 student, I have known Larry to ask insightful, out-of-the-box questions that no one else could possibly think of. His questions during my defense did not prove otherwise. His honesty, words of encouragement, and feedback were most greatly appreciated. I thank Joan Savall for his mentorship and expertise in design. Many students talk about how "luck" or "things falling into place" have a great effect on the PhD experience, and it was certainly a fortuitous occasion for me when Joan decided to come to Stanford. Not only has his relentless pursuit of good, efficient work and constant feedback given me the tools to succeed and believe in myself as a researcher, but I look to him for guidance in life.

I also thank my defense committee, Scott Klemmer who acted as the Chair and Sheri Sheppard. They both volunteered their time to hear about my work and also provided useful feedback, making the defense a surprisingly enjoyable experience. I was also lucky enough to have been a classmate of Sheri's in Designer in Society (the

first time I ever heard of a professor taking a regular class!). She has been such a fantastic role model for so many of us women in engineering, and for me personally, she simply always knew when to listen, offering to talk whenever I needed to, never failing to say hello and check in on me when our paths crossed in CDR. Her quiet support was palpable.

To the BDML. Who would have thought I would know so much about cockroaches, geckos...and fish? Will Provancher provided early guidance and continues to do so, Trey (who's Arthur?) McClung, Motohide Hatanaka, and Sean Bailey provided the foundation for the helpful, giving nature of the members of the lab. I owe much of my Labview and PIC programming knowledge to Dan Santos, Sangbae Kim's creativity and talent was an inspiration, Yong Lae Park has been a good friend, testing my Korean skills, Alan Asbeck and Matt Spenko were always at the ready for a skin stretch study, even documenting the torture, Noe Esparza and Sal Trujillo were my mechatronics experts, and the many other lab members, too numerous to name were a constant source of good natured ribbing and participated in so many of my studies. Much of my gratitude however, goes to two people, my fellow haptics researchers, Li Jiang and Jason Wheeler. Li helped me get started on this skin stretch adventure and our talks as we worked closely together in our early projects helped define this work. I am indebted to Jason, as his ideas for haptic applications just happened to be perfect for skin stretch. Our many discussions and collaborative efforts have improved this work immensely and I could always count on him for thoughtful insights.

My undergraduate advisors, Suman Das and Brent Gillespie. Professor Das (this was before I felt comfortable calling my professors by their first name), was instrumental in my decision to go to graduate school and provided me with my first opportunity to do actual research. He advised me to attend graduate school outside of Michigan, possibly the best advice I could have received. Brent (he insisted we call him Brent, though it made me uncomfortable) introduced me to the field of haptics. Through my project with Brent, I combined my engineering background

with my love of music and thus realized that not all mechanical engineers worked in the auto industry. It was the first time I felt motivated to do research. It was his guidance in my senior year that ultimately led me to Stanford.

Others who have had a significant role in the completion of this work are Professor Scott Delp, Sam Hamner, and Dustin Hatfield who assisted in the motion capture studies. I was fortunate (though unfortunate that it was the winter time) to have spent some time in Finland, visiting the University of Tampere for our collaborative research project. I thank Roope Raisamo, Veikko Surakka, Rami Saarinen, and Jukka Raisamo for their hospitality. I will never forget my time in Finland. To my undergraduate advisees, in particular Melody and Gayle, I thank you not just for your contributions to my research, but for showing me how to be a better mentor and advisor. Finally, I thank Judith Lee and Densie Curti, the administrative staff without whom none of us would be able to complete any research.

Lest you think the PhD was all academic, it would also not have been possible without the support given by family and friends.

To my family, I owe so much. My parents have instilled in me a strong work ethic and have been exemplary in their consideration for others through their giving, loving nature. Their constant, undying love and support of whatever I chose to do, has allowed me to flourish. Though it has been difficult to be so far from home, their happiness, pride, and love was never far from my heart. I thank my brother Ken ("oh bbah") for his constant support, advice on life decisions, medical advice, and moments of brotherly pride. Who else would buy six copies of Popular Mechanics? I also thank my cousin, Won Kyung for always listening to my problems and calling to check in on me. I love you all.

My friends, Judy, Aneeta, Julie, and Shantal. I would most certainly not have survived these last six years without each and every one of you. Your support through the difficult times, humor, concern for my wellbeing, are all unparalleled. You have shown me how to be confident and successful, all while having fun. I know it hasn't been easy and that I can be stubborn, but thank you for allowing me to be who I

am and for pushing me to believe in myself. Judy, I have no words that can express how glad I am we went to get your hair "approved" for a haircut that day. You have made me a better person, taught me to take better care of myself (and fed me), and shown me that I can do anything. None of this would have been possible without you.

Aaron and Sanjay - not only labmates (did you think I left you out earlier?), but good friends. Whether it was softball, euchre/doppelkopf , dumping water from Aaron's overflowing kitchen sink, or eating all of Sanjay's food, we all had some great times together. But Aaron, can I take my earmuffs off now? Suresh, Shad, Chris, James, Brett, Jeremy, and Edward - you were my family my first year at Stanford, helping me through the transition and providing me with opportunities to try new things and step outside of my comfort zone.

The folks at CDR - Barbara, Jonathan, Micah, and Michael, our conversations never failed to inspire me and recharge, giving me the final push to finish this work.

Yuko and Hahna - You both have been two of my closest friends for years. Yuko, you're one of the most considerate people I know and I wouldn't have gotten the NSF (and then wouldn't have stayed in grad school) without your drive to help your friends in any way possible. I'm "Ph.inally Done" and could not have done it without your friendship. Hahna, no one has known me longer than you have and there are times when you're the only person who knows just exactly how I'm feeling and thinking, which sometimes is all I need.

Team 1700, Gatorbotics. The experiences I had mentoring this spectacular group of young women were unforgettable. As much as they thank me for mentoring them, I feel owe them just as much, as it was through this endeavor that I finally found value in the skills I had learned and grew to love teaching. Your enthusiasm was inspiring and I feel lucky to have worked with you and everyone involved with Castilleja robotics.

And as we come to the end, I thank the National Science Foundation for their graduate fellowship, the NSF SGER (IIS-0554188), the Finnish Funding Agency for

Technology and Innovation (Tekes), decision 40219/06, and the Stanford Mechanical Engineering Department for sponsoring this work.

Contents

List of Tables

List of Figures

Chapter 1

Introduction

1.1 Motivation

Take a moment to close your eyes and move your arm about. Without opening your eyes, do you know where your arm is? Imagine if you didn't. Imagine that you couldn't feel your arm move and had no idea where it was unless you opened your eyes to watch it move. This how most amputees control their prosthetic arm. They can move and control their prosthetic, but they cant "feel" it. Consequently, they rely heavily on vision when using their arms for all kinds of daily tasks. Part of the reason for this condition is that developments in prosthetic technology have focused primarily on improving the actuation, dexterity and control [1,21,27,33,35,132], with much less work directed at providing feedback channels outside of vision [18, 37]. Promising research targeted at improving feedback focuses on developing invasive or expensive devices [70, 85]. What if an inexpensive wearable haptic device could be added to provide users with reliable feedback regarding the motions of their prostheses? This type of device could provide beneficial proprioceptive feedback, reducing the visual demand required to operate the prosthetic arm and aid in the user's ability to control of the arm. This is just one example of the growing interest in developing small, wireless haptic displays for portable or wearable use.

Although humans and animals use touch extensively to obtain information about the world that they interact with, it remains a small part of the human/machine interaction field, dwarfed by visual and acoustic display. The easiest and by far the most widely used technology for portable haptics is vibration, as found in cell phones, pagers etc. and incorporated into haptic vests, sleeves, and other accoutrements [10, 61]. However, vibration is best suited for transient event cues and is less effective when used for sustained stimuli due to adaptation effects. [5]. It can lead to desensitization and subjectively can be annoying when prolonged. In addition, sensitivity to vibrations can be reduced when people are in rapid motion because the background levels of acceleration mask the vibration signals [99]. Kinesthetic displays, which provide grounded reaction forces to the user, avoid the limitations of purely vibrational feedback. They can provide realistic interaction forces for extended periods of time and allow users to distinguish among different contact types based on the dynamics of the interaction forces they produce [40, 79]. Several investigations have shown that force feedback can enhance user performance in appropriately chosen training exercises and collaborative activities [15, 40, 120, 125]. However such force feedback devices are comparatively encumbering, bulky, and have a high power consumption. All of these factors make them difficult to adapt to individuals moving freely.

In this thesis, a new method of providing haptic feedback, working on the principle of imparting localized skin stretch, is presented. For unencumbering wireless displays, skin stretch is especially appealing as it does not require much power; motions and velocities can be low. Part of the motivation is also that skin stretch is known to be a contributing factor to our sense of proprioception, particularly for the distal joints but also at the elbow and knee [23, 31], and it is therefore intuitive that such a device could help subjects in motion tracking tasks associated with physical therapy, motion training, amputee feedback, etc. It has also been shown that mechanoreceptors respond quickly and accurately to skin strain changes [9, 32, 34, 96, 122]. In other work, skin stretch has been used for fingertip displays [7, 15, 91, 101, 102, 126];

however little has been done on devices that apply large strains to the hairy skin. In contrast to the previous devices, we are interested not in creating fine patterns of skin stretch at the fingertips but in applying skin stretch at discrete points on a persons limbs and torso, as in some applications (e.g. amputees) the hands are not available to provide tactile feedback. The results of this work characterize the effectiveness of localized skin stretch as an element of haptic display and provide a framework for developing future skin stretch haptic displays.

Other possible applications benefiting from improvements in tactile devices include physical therapy and motion training. For example, following orthopedic surgery, a patient's gait is often different than it was pre-surgery, and it may even be necessary for the patient to re-learn how to walk. Physical therapists can observe the patient and provide oral feedback, giving instructions such as "Lift your foot a little higher." However, such statements do not clearly specify to patients how much they should move their joints. However, a wearable device that is programmed to detect and track the motion of a patient could be used to guide the exercise, providing the patients with direct feedback regarding the speed and extent of motion of a limb or joint. Moreover, this device could be used routinely in the person's home.

1.2 Thesis Outline

This thesis is organized into six chapters.

Chapter 2 provides background information regarding the basic properties of human mechanoreception and skin relating to skin stretch. Initial studies that indicate our ability to detect skin stretch are also discussed. A brief introduction to psychophysical methods useful for evaluating human performance is provided as a reference, and the current state of wearable haptic devices is presented.

Chapter 3 discusses the design development of rotational skin stretch devices used in the experiments described in the following chapters. A number of design criteria are presented in the context of designing an adjustable, benchtop skin stretch device

and a second wearable skin stretch device. Pilot tests were conducted to choose a pattern of skin stretch (e.g., how many contact points and how to move them).

Chapter 4 investigates rotational skin stretch from a mechanical viewpoint. What happens at the skin surface when rotational stretch is applied? A three-dimensional motion capture system is used to measure skin displacements as rotational stretch is applied. The displacements form the basis of skin strain calculations. Correlating these with applied torques leads to insights regarding the pattern of skin stretch and how it corresponds to our perception of skin stretch. These findings, coupled with perception studies presented in Chapter 5, also motivate the design of a new, improved skin stretch end-effector.

Chapter 5 quantifies our ability to perceive rotational skin stretch. First, a traditional psychophysical test to determine our difference threshold of skin stretch is performed. The effects of changing the reference rotational position and angular velocity of stretch on the difference threshold are analyzed. Finally, for more practical purposes, the ability of users to correlate rotational skin stretch feedback to the position of a virtual object is tested for two different cases. The first case is one in which the users control a virtual object and receive skin stretch feedback correlating to the object's position. The second case is one in which users must report the perceived position of an autonomously moving object through passive perception of skin stretch feedback. The results of these experiments indicate that skin stretch feedback is better suited for applications in which users rely on it to provide feedback for voluntary motions (i.e., over the motions of a device over which they exercise control).

Chapter 6 examines the use of rotational skin stretch feedback as a substitute for proprioceptive feedback in a motion control task. Users were instructed to move a virtual object to a desired location with no visual feedback of the object's position. Haptic feedback concerning the object position was provided in the form of either vibration or skin stretch. The dynamics of the object were sufficiently complex that simple open-loop strategies were not sufficient for moving it accurately. Under these

circumstances, participants performed significantly better with either skin stretch feedback than with no haptic feedback. Overall, most users performed best with skin stretch, particularly when it was valuable to have a sense of velocity as well as static position. This finding highlights what may be one of the main advantages of skin stretch in motion training, prosthetics and related applications: it provides a sense of velocity and of position within a single haptic modality.

Chapter 7 summarizes the results of this research and suggests future extensions of this work.

1.3 Contributions

The main contribution of this thesis is the development of a new method of haptic feedback, using rotational skin stretch, to communicate information to a user. Under this heading, specific contributions include:

- a novel, wearable haptic device that uses the sensation of skin stretch to communicate information. The device imparts rotational skin stretch on the surface of the user's skin and is intended to be worn on the body. It is relatively lightweight and compact, is easily strapped to a variety of users, and can provide effective feedback to even naive users. This device is also the first known skin stretch device designed to be worn on the body.

- an evaluation of skin stretch feedback in providing proprioceptive information to a user. The implications of this experiment are that skin stretch can be useful, particularly because it can convey a sense of motion (position and velocity) at once. These studies strongly suggest that skin stretch feedback can be used for positioning of prosthetic limbs or robotic arms.

- understanding basic psychophysical characteristics of skin stretch. Our difference thresholds are lower at higher rotations, indicating greater sensitivity at

increased magnitudes of stretch. Our sensation of the velocity of stretch does not impede our ability to distinguish between static positions. In addition, skin stretch appears to be best suited for tasks in which the feedback is related to the commands the user inputs to the system for control. Passive perception of the feedback is poor.

- providing a framework towards understanding what mechanical aspects of rotational skin stretch contributes to our perception of skin stretch. The torques measured during skin stretch, the strain energy of the system, the overall displacement of skin, all contribute to activating our mechanoreceptors to signal skin stretch. The results from these studies can lead towards optimization of a skin stretch end effector that can provide ample resolution and range, yet remain comfortable for a user for long term use.

Chapter 2

Background Information

There are many aspects of touch that we take for granted everyday. Take for example the task of shaking another person's hand. People are often told that upon meeting someone new, you must smile, make good eye contact, and shake their hand firmly. Yet how is it that we can grasp another hand accurately, with appropriate force, while our visual attention is focused on maintaining eye contact? Why is it that we do not mistakenly grasp too firmly or aim poorly and run our hand into their stomach? We use our proprioceptive and kinesthetic senses to control the movement of our arm and hand. Our muscle contractions, skin stretching around our joints, and tendons lengthening provide us a sense of where our limbs are located and years of training allows us to control our movements and position our hand appropriately without vision. Mechanoreceptors in our fingers inform us that we have made contact with the other hand, convey the amount of pressure we are applying, provide feedback regarding the firmness of the other person's shake, and can convey the warmth of their hand.

As demonstrated by this simple example, our sense of touch is comprised of a complex combination of modalities which can include motion, force, vibration, texture, thermal conductivity, and even pain. The sense of touch is even further affected

by the method in which we explore objects and interact with the environment, classified as *passive* and *active* touch. Active touch, in which users retain control of their own movements and haptic feedback correlates to their commands, whereas passive touch occurs when a stimulus is imposed on the user with no direct correlation to their motor commands.

A challenge in providing haptic feedback for many applications is that several of these modalities should ideally be provided and the context in which it is provided (passive vs. active) can influence our performance. When we look at the relevant literature for any application, we find that it spans several research areas including robotics, teleoperation, haptic feedback devices, physiology, ergonomics and psychophysics. The work presented here focuses on skin stretch as a component of proprioceptive feedback. Therefore, the relevant literature includes studies of the properties of human skin, of mechanoreception, of perception and psychophysics, and of haptic interfaces. The following sections attempt to summarize and organize the literature in each of these areas. Additional references are cited in context as they occur in the following chapters.

2.1 Mechanoreceptors

Our skin contains a combination of different mechanoreceptors; each specialized in terms of the parameters they sense and the rate at which they adapt to changes in stimuli. In the human hairy skin, which excludes skin covering the fingerpads and the soles of your feet, there are 5 main types of mechanoreceptors [122]. The receptors are grouped into categories of Type I vs. Type II. Type I receptors are found closer to the surface of the skin, while Type II receptors are found deeper in the dermis layer of skin. Receptors are further divided into fast adapting (FA) types, which are sensitive primarily to transients, and slow adapting (SA) types, which are capable of registering steady state (DC) signals. A cross sectional illustration of the skin and location of these mechanoreceptors is seen in Figure 2.1.

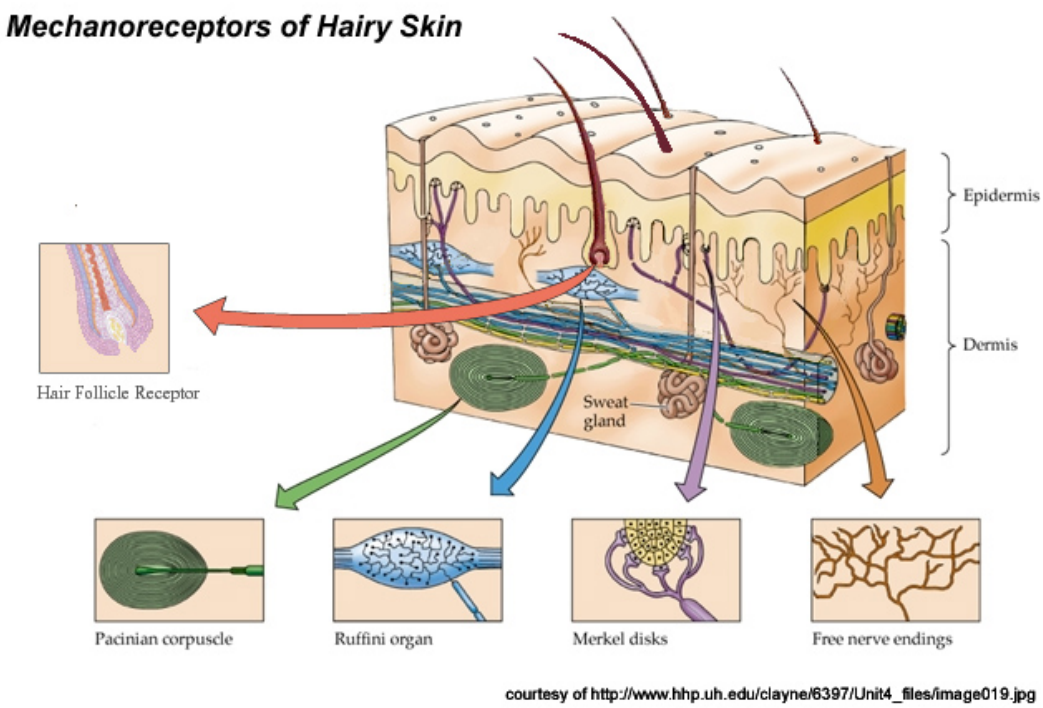

Figure 2.1: Mechanoreceptors found in hairy skin. Image taken from [73].

Receptor	Receptor Type	Median Field Size (mm^2)	Sensed Parameter
pacinian corpuscle	FAII	n/a	vibrations
hair receptor	FAI	113	hair displacement
ruffini ending	SAII	1.4	skin stretch
merkel disks	SAI	11	pressure and texture
field receptors (not pictured in Fig.)	FA	78	skin stretch and joint movement

Table 2.1: Characteristics of mechanoreceptors found in human forearm skin [122]. Sensed parameters suggested by Gilman 2002 [49].

Though much research has been done to characterize the receptors in the human hand [121], there is less known about the receptors found in hairy skin. The hairy skin of the human forearm contains slowly adapting type I receptors (SAI), slowly

adapting type II receptors (SAII), and three different types of fast adapting receptors including hair, field and pacinian receptors [122]. Though the FA units contribute to our sense of touch, the primary units that contribute directly to our sense of skin stretch are the SA receptors [49, 96, 122]. SAI receptors are responsible for forces and pressures. SAII receptors, typically associated with the Ruffini Endings found in glabrous skin, are responsible for directional skin stretch information. Several investigations have found that these SAII receptors are sensitive to directional movements and are sensitive to specific directions of stretch, possibly contributing to our ability to discern different movements of skin [17, 95, 97]. Both SAI and SAII receptors respond to both velocity and displacement [17]; though at sustained displacements, the SAII units respond continuously while the SAI responses are more intermittent.

Hair units in the skin respond to individual hair movement and are also sensitive to frictionless contacts such as air or bursts of wind over the surface of the skin. Hair units typically have larger, irregular receptive fields as compared to the other receptors. Vallbo [122] estimates the receptive field area to be between 45 and 213 mm^2, with no preference to direction of stimulation. Field units have similarly large receptive fields, though they are more closely packed together than hair units. In comparison to glabrous skin, hairy skin has extensive stretching capabilities as the connective tissues below are only loosely connected to the skin.

2.2 Skin Properties Related to Haptics

Though skin stretch for haptic feedback is a relatively recent area of research, skin stretch is a natural part of our sense of touch and has been studied outside of the haptics domain. It has been known for some time that skin stretch is an important contributor to our overall sense of touch, and several scientists have been interested in our ability to detect stretch. Here we discuss previous research related to our perception of skin stretch on non-glabrous skin.

2.2.1 Tactile Directional Encoding

In addition to studies designed to understand the biological factors contributing to our sensation of skin stretch, there has been considerable interest in quantifying our sensitivity to skin stretch and what factors contribute to our ability to detect directions of stretch. Tactile directional sensibility can be attributed to two separate types of stimuli: stretch caused by friction induced contact and spatial cues that vary with time [95, 98]. In other words, our receptors may detect the intensity of stretch through friction based displacement, or through displacement of a moving contact and activation of a series of mechanoreceptors, referred to as spatio-temporal stimulation. In general, humans are remarkably sensitive to movements of skin and stretch induced by a contact point attached to the skin. Studies have found that on the forearm, humans can report the direction of skin stretch with movements as small as 0.13 mm, movements that are barely detected through vision [97]. In contrast, when using only spatio-temporal stimuli such as a low friction air jet moving across the surface of the skin, the smallest distance of movement necessary to report the direction of the stimuli is approximately 60 times higher [95]. However, a drawback of lateral stretch sensitivity is that it is highly dependent on a variety of factors such as the normal load applied to induce stretch [94], the velocity of stretch, and varying skin stiffness [98]. In particular, as the body moves, the skin surface properties change, which has a large influence on our sensitivity to skin stretch. The minimum stretch necessary for a user to detect direction reliably when the skin is stiffer increases significantly [98]. In addition, when stretch is applied locally to the skin, a larger field of receptors is activated, as evidenced by Olausson [97], in which receptors located more than 25 mm from the contact point could signal the direction of skin stretch. Specifically, our SAI and field units are important in providing spatio-temporal cues whereas our SAII units are responsible for our encoding of the directions of lateral skin stretch [52, 96]. This work regarding our sensibility of directional skin stretch further points to the importance of skin stretch in contributing

to our kinesthetic and proprioceptive sensations [127].

2.3 Skin properties

The work completed by Olausson and Norrsell [98], stating that our perception and ability to discern different amounts of skin stretch changes and adapts with body movement can be attributed to the complex nature of skin tissue itself. Human skin is a non-homogeneous, anisotropic, non-linear viscoelastic material whose properties also vary with age, from site to site and per person, all of which makes it a very complex biological structure to study. Some challenges related to applying skin stretch and skin stretch perception can be attributed to the mechanical properties and biological structure of skin. An extensive review of the biomechanical properties of skin is found in Hendriks literature review [56], and brief summary is provided here.

Skin can be divided into two separate layers, the epidermis and dermis. In most studies, though the epidermis is stiffer than the dermis, its contribution to the mechanical properties of skin is neglected [56]. The dermis is primarily made of collagen, elastin and reticulin fibers, which all contribute to the mechanical behavior of skin. Collagen and elastin fibers are considered to be linear elastic, yet the stress-strain curve for skin is non-linear (Figure 2.2). The curve can be divided into phases. At small strains (section A), the skin stress-strain relationship is roughly linear as collagen fiber response is neglected. As the strains increase (section B), the relationship becomes non-linear as the effects of collagen fibers straightening cause the skin to stiffen. The last portion of the stress-strain curve (section C) before failure represents the phase when all the collagen fibers have straightened. The amount of strain arising from the application of skin stretch on the body for haptic applications and proprioception is thought to be within the first two phases of the stress-strain curve. Strain analysis from Chapters 3 and 4 indicate that the on average, the principal tensile strains are between 20 and 30 percent.

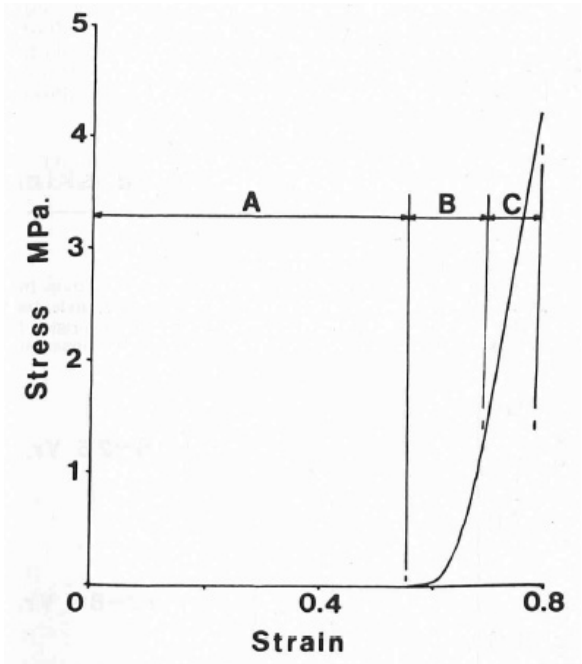

Figure 2.2: Stress strain curve for skin taken from Daly [25]. A = initial deformation (collagen fibers carry no tensile load and are not aligned in preferred directions), B = intermediate strain (fibers begin to straighten and align in direction of tensile force), C = near maximum deformation (all fibers are aligned).

In addition to their contribution to the stiffness of the skin, the collagen fibers in the skin may play a large role in our capacity for tactile direction discrimination. As skin also exhibits anisotropic behavior in which the properties change with direction, it is possible that there is an optimal direction to apply skin stretch, which may vary with location. Collagen fibers are known to display a preferential direction of stretch and maximum tensile stiffness, which have been characterized by Langer's lines [71, 72]. Langer determined these lines by puncturing small circular holes into cadaver skin and noting the resulting elliptical shape to determine directions of maximum and minimum tension. The direction of the long axis corresponds to Langer's lines, as seen in Figure 2.3, along which the extensibility of the skin is lower and results in higher stiffness, as the elastin and collagen fibers are more stretched along these lines than across these lines. These lines may provide insight

into developing the optimal orientation for applying skin stretch.

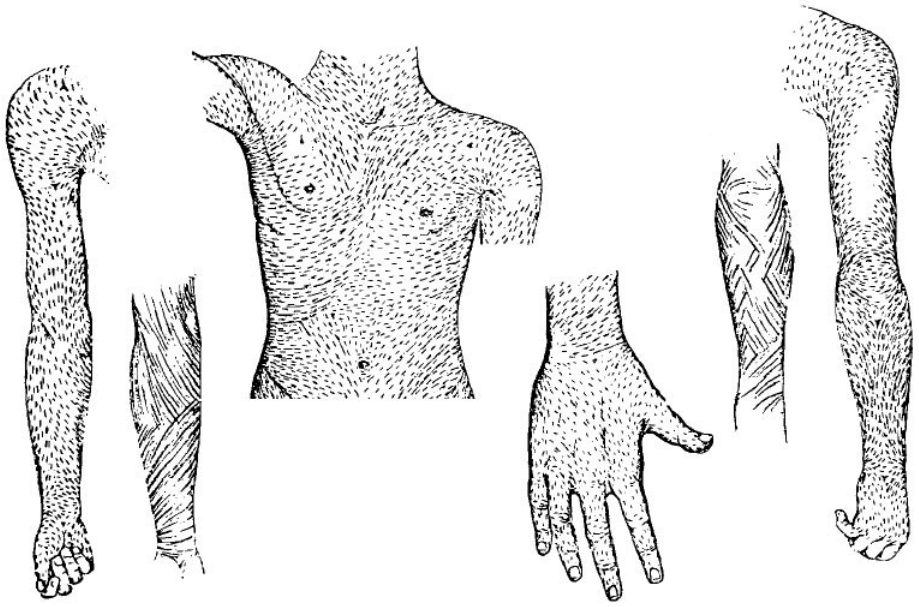

Figure 2.3: Langer Lines [71] indicating directions of maximum tension in collagen fibers of the skin.

Difficulties in determining skin properties and modeling its behavior have not prevented research on local stress and strain properties of skin. Subsequently, researchers have tried to replicate Langer's lines using various methods. Reihsner et al. [106] studied skin properties *in vitro* by excising human skin samples from various anatomical sites and attempting to re-create its in-vivo characteristics by re-stretching the skin to match its in-vivo geometry. As incremental strains were applied to the skin, the stresses were measured to obtain the skin's two-dimensional stress-strain relationship. A testbed that was constructed allowed them to estimate the direction of maximum in-vivo stress on 16 different locations of the body. Reihsner found that the angle between Langer lines and the stresses at that location ranges from -10 to 10 degrees, indicating that the Langer lines do coincide with the preferred orientation of the collagen fibers in the dermis. In addition, Reihsner et al. found that the maximum strain necessary to restore the skin to in-vivo geometry

changed approximately 40-50% with age. Younger subjects required larger amounts of strain, while older subjects required less, showing how skin properties and collagen content may change with age. Other work regarding the changing skin stiffness as humans age that agrees with Reihsner's findings include Agache and Sanders [2,109]. Finally, the degree of anisotropy is most pronounced at the patella, abdomen, and shoulder, where there is low in-vivo tension, perhaps indicating that these sites may require significant calibration and pilot testing to apply skin stretch for haptic feedback [106]. Finlay [38] also describes a device that uses a servo-system that was constructed for the specific purpose of measuring dynamic skin properties in-vivo. Finlay proposes that the straining of human skin in torsion causes a residual orientation of some of the tissue fibers in the skin. This type of behavior may be captured in the perception of skin stretch, in which a subject's perception of skin stretch adapts over time, directly correlating to the re-alignment of skin fibers. Meijer [86] has completed work to characterize the anisotropic behavior of skin, developing parameters to fit a skin model when strains are applied longitudinally and along a transverse direction.

A summary of various studies to measure skin strain and their major findings, as well as the shortcomings are listed in Table 2.2, taken from Bethke [6].

Authors	Year	Main Findings	Shortcomings
Langer	1861	Find directions of maximum in vivo skin tension by examining round punctures deform into ellipses.	Not quantitative; considers pre-tension state of skin only; neglects the effect of joint motion on skin.
Iberall	1970	Find directions of minimum skin extension during joint motion by observing marked circles of skin deform into ellipses.	Not quantitative or easily repeatable. Time consuming. Not readily transferable to computer data or to manufacturing devices.
Faga	1981	Determine directions of maximum in vivo skin tension by observing stream lines of hair.	Not quantitative or readily transferable to computer data. Small sample size (n = 8). Methodology not verified.
van Ratignen	1983	Find lines of maximum tension in dog skin by stretching and carrying out digital image analysis on small excised skin samples.	Invasive (requires excised skin samples). Method only applied to dog skin.
Reishner	1995	Measure anisotropy of human skin as function of anatomical region, using small cadaver skin samples.	Only 16 anatomical sites studied. Invasive measurement apparatus (requires excised samples).
Douven	2000	Optically measure displacement of markers on small sample of skin, during forcible stretching with attached pads.	Considers externally-applied loading; neglects the effect of joint motion on skin. Small (1 cm by 2 cm) samples rather than entire body surface.
Vescovo & Varchon, et al	2001, 2004	Map strain fields for excised sections of human skin subject to applied deformation, through photo analysis of initial and deformed samples.	Requires excised samples. Considers externally-applied loading; neglects the effect of joint motion on skin. Digital strain field mapping algorithm does not yet apply to curved surfaces.

Table 2.2: Summary table of experimental studies of skin stress and strain, and their shortcomings, taken from Bethke [6]. Langer [71], Faga [36], van Ratingen [123], Reihsner [106], Douven [29], Vescovo & Varchon [66, 84].

Finally, skin also exhibits viscoelastic behavior, where significant hysteresis, relaxation, and creep can be observed. Skin tissue shows stress relaxation under constant strain and creep under constant stress [112]. To further complicate matters, the viscoelastic response of skin is non-linear and varies between uniaxial and biaxial modes of tension. Thus, skin is anisotropically viscoelastic. Variations in skin behavior due to time dependent factors such as creep and relaxation can have a large effect on the adaptation of our mechanoreceptors and our ability to perceive haptic stimuli. Due to the highly time dependent nature of skin, it is largely unknown how such biological properties affect our perceptual capabilities.

2.4 Psychophysics

Psychophysics is a subfield of psychology that studies the relationship between human perception and stimuli, whether visual, audio, or tactile. It was founded on the principle that understanding and quantifying how humans sense and perceive various stimuli would provide psychologists the basic tools for understanding how the mind worked. In haptics, psychophysics has been used to design and develop new tactile interfaces, guiding the selection of appropriate parameters and providing insight into the strengths and limitations of the system. For a comprehensive overview of the field of psychophysics, see Gescheider [48].

The fundamentals of psychophysics lie in determining how strong a stimulus must be for a user to detect or identify it, if a user can differentiate one stimulus from another and how great that difference must be, and how a user can describe the magnitude of a stimulus. Absolute thresholds are the minimum stimulus levels necessary to perceive the stimulus while difference thresholds, also commonly noted as the just noticeable difference (JND), represent the minimum difference necessary to distinguish between two signals. Magnitude estimation tests are used to determine the subjective perceived strength of a stimulus. As skin stretch is a relatively new topic, understanding these basic psychophysical parameters was of interest. These

perceptual characteristics would motivate the design and usage of skin stretch stimuli in practical applications and provide intuition on how accurately users could interpret the feedback. Therefore a background on the common psychophysical methods used in these studies is presented here.

2.4.1 Difference Thresholds

Though there are many classic psychophysical methods that are used to determine difference thresholds (method of limits, method of constant stimuli, method of adjustment [48]), there are some major drawbacks, particularly in experiment design and execution, that make using these methods undesirable for skin stretch. The classical methods often require a large number of trials to determine a difference threshold accurately and are not particularly time efficient. The methods are also very repetitive, requiring a huge amount of concentration from the test subject, which can be unreasonable and lead to data error. In several studies since the 1970's, it has become more common to use adaptive psychophysical methods as described by Levitt [76]. The studies presented in this thesis used the adaptive techniques. However, the principle behind the adaptive procedures requires an understanding of the classical method upon which it is based. Therefore a brief explanation of one of the classical methods (method of constant stimuli) and theory are presented here as well as details regarding the adaptive method.

2.4.2 Method of Constant Stimuli

In the method of constant stimuli, the main task of the test subject is to examine pairs of stimuli and report which of the two stimuli was perceived to be larger than the other.

Difference threshold experiments typically require a subject to be presented with two stimuli and subjects are then asked to report which of the stimuli was greater in subjective magnitude. A reference stimulus level is chosen and kept constant

during the trials, and the secondary stimulus is referred to as a comparison stimulus. The comparison stimulus is typically any one of 5 to 9 different levels of stimuli, all varying in magnitude with an equal number of larger and smaller stimuli relative to the reference. In this method, the comparison stimulus changes in magnitude from trial to trial, and the order in which the comparison stimulus and reference stimulus is presented to the subject is varied to reduce presentation order bias. The comparison stimuli are chosen such that the largest stimulus is almost always recognized as being greater than the reference stimulus and the smallest stimulus is almost always recognized to be less than the reference. Each of the comparison stimuli are paired with the reference and presented in random order and the subject simply reports which of the two stimuli had a greater magnitude.

The results of the difference threshold test can be plotted in terms of stimulus intensity vs. percentage of "greater" responses, in which case, the higher the stimulus intensity, the higher the expected percentage of "greater" responses. A sample plot of typical data can be seen in Figure 2.4, which produces a psychometric curve. Psychometric functions typically resemble an "S" shape, called an ogive.

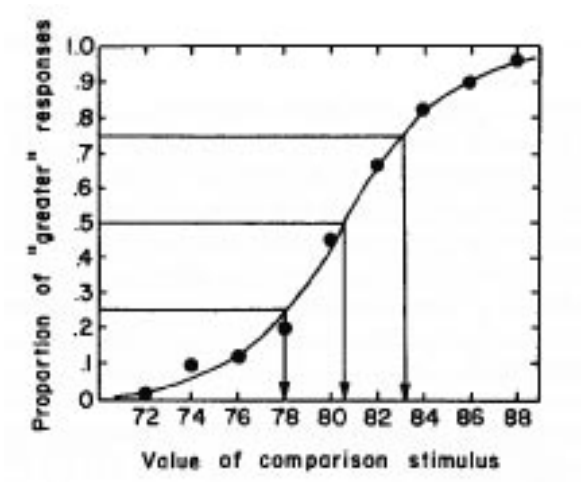

Figure 2.4: Typical psychometric function obtained using the method of constant stimuli. An ogive curve has been fitted to the points [48].

To determine the difference threshold, the 0.75 and 0.25 proportion points on

the psychometric function are used. The upper difference threshold is the difference between the reference stimulus level and the level at 0.75, and the lower difference threshold is difference between the reference level and the 0.25 point. Sometimes the two thresholds are averaged, but if the difference between the two are great enough, the difference thresholds are presented as separate parameters.

This method is acknowledged to be one of the most accurate methods, yet is extremely time consuming and requires significant amount of pilot testing to determine the levels of the comparison stimuli. Selection of the correct range and level of stimuli is crucial to the experiment and for producing accurate results. In addition, in most cases experimenters are only interested in finding one or two points on the psychometric curve, in which case the method of constant stimuli is extremely inefficient because there are several other stimuli placed far from the region of interest. For these reasons, more efficient methods have been adopted for testing.

2.4.3 Transformed Up-Down Method

Due to the problems in experiment design and inefficiencies of classical methods, adaptive methods were developed. Adaptive procedures by definition are experiments in which the stimuli presented to the test subject are dependent on previous trials and responses. In addition, these methods are designed to target specific points on the psychometric function, making the experiment more time efficient compared to the classical methods. The most basic of these methods is the Simple Up-Down method, aimed at finding the 50% level of the psychometric function. In simple up-down methods, the comparison stimulus level decreases at a fixed step size after a subject correctly identifies it to be greater than the reference stimulus, a positive response. After an incorrect or negative response, the level of the comparison stimulus is increased. The experiment continues until at least six or eight reversals are obtained. A reversal occurs when the change in stimulus level switches from decreasing to increasing and vice versa. A typical data set resulting from this method can

be seen in Figure 2.5.

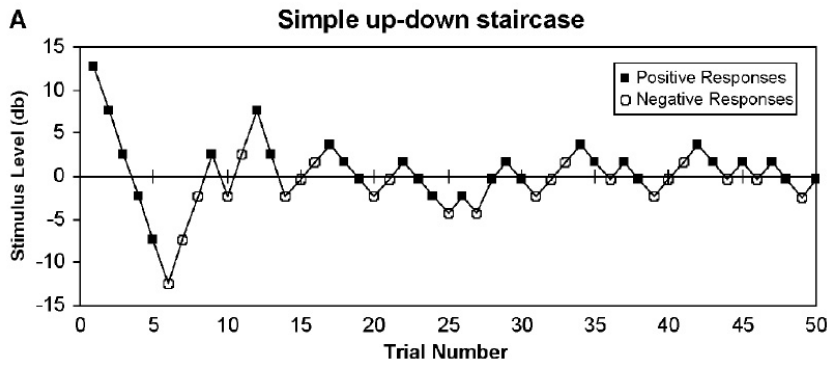

Figure 2.5: Typical data for the simple up-down procedure, estimating the 50% point on the psychometric function [74].

The increment by which the stimulus level changes is the step size. Often, to converge more quickly to the point of interest, the step size is large at the beginning of the trial. After two or three reversals, the step size is decreased to more accurately find the point of interest. Though the method is good at estimating the 50% level and can account for stimulus adaptation, it is not well suited for finding any other points on the psychometric curve which are of interest in difference threshold tests.

To target other points, Levitt [76] and Leek [74] describe a transformed procedure in which points other than the 50% level can be found easily. In these transformed methods, observations or sequences of observations are placed into two separate groups, termed UP and DOWN groups. How these observations are grouped depends on the point of interest. Table 2.3 displays a variety of sequences that lead to different points on the psychometric curve. Similar to the simple up-down procedure, the comparison stimulus changes based on the subject's response. However, the stimulus level changes only if a sequence of events as defined in the UP or DOWN group occurs. For example, entry 2 in Table 2.3 corresponds to a two-down, one-up procedure. The stimulus level is increased (UP group) whenever a [+ -] or [-] sequence of responses is obtained, corresponding to one incorrect recognition of the stimulus level. The stimulus level increases only if a series of two correct responses [+ +] is obtained,

Entry	Response sequences: UP group increase level after:	Response sequences: DOWN group decrease level after:	Response groupings: Probability of a sequence from DOWN group = P[DOWN]	Response groupings: Probability of positive response at convergence
1	−	+	$P(X)$	$P(X)=0.5$
2	+ − or −	+ +	$[P(X)]^2$	$P(X)=0.707$
3	− −	− + or +	$[1-P(X)]P(X)+P(X)$	$P(X)=0.293$
4	+ + − or + − or −	+ + +	$[P(X)]^3$	$P(X)=0.794$
5	+ + + − or + + − or + − or −	+ + + +	$[P(X)]^4$	$P(X)=0.841$
6	− − − −	− − − + or − − + or − + or +	$1-[1-P(X)]^4$	$P(X)=0.159$
7	Any group of 4 responses with 1 or more negative responses	+ + + +	$[P(X)]^4$	$P(X)=0.841$
8	− − − + − + − −	+ + + − + − + +	$[P(X)]^2[3-2P(X)]$	$P(X)=0.5$

Table 2.3: Response groupings for transformed up-down strategies, taken from Levitt [76]. Entry 1 is the simple up-down procedure and Entry 4 is the method used in experiments described in Section 5.2.

as specified in the DOWN group. Transformed up-down methods converge to the stimulus level where the probability of an UP sequence is equal to the probability of a DOWN sequence ($P(x) = 0.5$). If this is true, for the two-down, one-up method, the condition of $P([+\ +]) = 0.5$ must be satisfied. If p is the probability of a positive response, then p x p = 0.5, and $p = \sqrt[2]{0.5}$. $p=0.707$. Therefore, the transformed up-down method converges to the point where $p=0.707$, or the stimulus level at which the probability of obtaining a "greater" response is 0.707, corresponding to the 0.707 point on the psychometric curve (see Figure 2.4).

Similarly, a three-down, one-up method (entry 4 in Table 2.3) requires three correct responses to decrease the stimulus level and again only one incorrect response to increase the stimulus, and corresponds to the 0.794 point on the psychometric curve ($p = \sqrt[3]{0.5}$). It has been suggested that this particular criterion for the

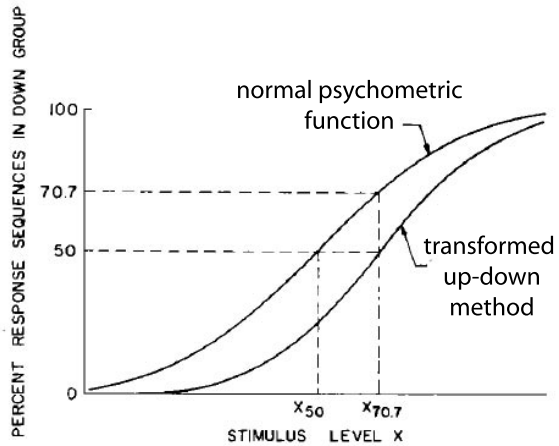

Table 2.4: Transformed response curves, showing the typical psychometric function and the transformed response curve corresponding to the 70.7% level for a two-down, one-up procedure. Taken from [76].

transformed up-down procedure is more efficient than the two-down, one-up groupings [68, 110], and it has subsequently been used in a variety of haptic perceptual studies [12, 53, 105, 114]. It is the method used in the following sections to determine the skin stretch detection threshold parameters.

2.5 Different Methods of Providing Wearable Haptic Feedback

As technology improves and electronic handhelds increase in complexity and become smaller in size and weight, haptic device designers must also work to develop smaller, wireless haptic displays that are portable or wearable as opposed to fixed on a benchtop. Portable and wearable devices are ideal to allow for freedom of movement and the development of such devices and corresponding applications can push us towards achieving a truly ubiquitous interaction environment. As outlined in [118], in general, wearable devices should be lightweight, not interfere with a user's daily activities, be useful for persons with varying degrees of sensitivity to tactile

sensations, require little training, and integrate seamlessly with our sense of vision and sound. Currently, the two most general methods of providing haptic feedback to a user are through vibration and force, with a few additional examples based on other phenomena such as skin stretch or temperature. Vibration and force feedback have been developed for portable and wearable applications. Skin stretch devices have been primarily been restricted to display at the fingertips, in some cases with portable devices in mind [102]. This section discusses the current state of wearable haptic devices and outlines our approach to using skin stretch to develop a new method of wearable haptic feedback.

2.5.1 Vibrotactile devices

For portable devices, the easiest technology to implement is vibration feedback. Previous investigations have demonstrated that small vibration devices can provide cues about events and that individuals can distinguish among patterns of vibration to receive orientational cues, etc. [13,43,60,104,115,116,118]. There has been considerable effort to develop various types of vibrotactile displays in the forms of belts [93], vests [61,63], and body suits [77]. Jones and Nagel [61,63,93] have developed vibrotactile assistive displays for navigational purposes, and Lieberman and Breazeal [77] have developed a wearable vibrotactile suit for motor learning and kinesthetic feedback. Unfortunately, the display of sustained contacts with continuous vibration can become annoying to users and can lead to desensitization [5,57]. In addition, in dynamic situations, (e.g. while dancing or jogging) the threshold of detectability for vibration feedback can suffer [99].

2.5.2 Force Feedback Devices

In contrast to wearable vibrotactile devices, wearable force feedback devices, beyond a few force feedback gloves, has remained under-developed as force feedback often

requires the use of heavy, bulky actuators with high power consumption. Nevertheless, as force feedback provides high quality feedback, groups have studied various methods to mobilize the technology through use of passive actuators for interaction with virtual environments [87, 108]. Voyles Jr. [64] developed a tactile finger/glove using electro-rheological gel for actuation while Caldwell [14] built one of the first multi-modal haptic gloves, providing force, tactile, and thermal feedback simultaneously. In a different application, Panasonic [100] has developed a force feedback suit for rehabilitative purposes.

Other alternative wearable haptic displays utilize a variety of methods to provide tactile feedback, in the form of pressure, temperature, and small amounts of vibration. The TapTap is a wearable scarf for asynchronous distributed touch therapy. The TapTap [11] itself is embedded with sensors and vibrotactile actuators as well as thermal elements for users to communicate with one another virtually through the sense of touch. Similarly, the Hug+Shirt [24] and Huggy Jacket [119] are systems that promote physical interaction through remote communication between persons.

Chapter 3

Developing a Rotational Skin Stretch Device

How can skin stretch be applied for tactile feedback? What is an effective method, specifically keeping in mind that the device should be compact, lightweight, and provide users with information beyond simple event cues? In comparison to other haptic displays, few devices utilize skin stretch and none has been developed for stretching hairy skin. The challenges in developing any haptic device are numerous, but developing a skin stretch device is complicated by the issue that our ability to perceive skin stretch is largely unknown. This is in contrast to vibrotactile or force feedback devices, for which considerable research has been done to quantify our capabilities to perceive vibrations or forces and use them in a control loop. Our sensation of skin stretch can vary depending on the size of pads inducing the stretch, the location where stretch is applied, the direction of stretch, the number of contact pads, the amount of normal force applied to the skin, the variations in skin stiffness from user to user, and more. A series of prototypes led to the design of a benchtop rotational skin stretch device for controlled testing and a wearable skin stretch device for use in more practical settings. This chapter outlines the design process, detailing the decisions that were made and the final device characteristics.

Although rotational stretch is ultimately a good method to induce skin stretch and future chapters validate the benefits of using such feedback, this design is by no means optimal. Future chapters also outline the pros and cons of these devices and ultimately suggest further improvements that can be made.

3.1 Previous Work

Though there is relatively little literature on skin stretch haptic devices, particularly for the hairy skin, important exceptions include the work of Hayward and colleagues [54, 75, 126] and [7, 41, 101] who have developed fingertip displays that include skin stretch. These displays use small piezo-electric actuators that can bend to compress and stretch local skin on the fingertip in different patterns. Several investigators [32, 75, 91] have also studied the mechanisms behind skin stretch. Makino [81] has developed a suction-based display that produces illusions of pressure on the skin, at least in part by producing localized skin stretch. However, non-glabrous skin stretch displays have been largely unexplored and, in the context of wearable haptics, skin stretch has not been utilized. Combined with our knowledge of mechanoreceptor properties and responsiveness to skin stretch as outlined in Chapter 2, skin stretch shows promise in being used as a method of haptic feedback. In contrast to the devices mentioned here, we are looking to apply skin stretch at discrete points on a person's limbs and torso.

3.2 Rotational Skin Stretch Design Development

Throughout the design process, the primary goal was to develop a portable haptic device that was capable of conveying information beyond simple event cues to a user. Keeping this in mind, design requirements were determined to aid with the design and development. Various early prototypes ($\sim$15) were constructed and modifications to the design were driven by qualitative observations from users in testing the

functionality of the prototypes. Using these observations, a benchtop skin stretch device was designed and built to study and test the feedback in a controlled manner. After further testing and prototyping with the benchtop, a wearable device was also constructed and tested.

3.2.1 Design Requirements

In developing a wearable, portable device, the following initial set of design requirements were determined.

Physical Requirements

The device

- must be capable of being strapped to the body,
- must be lightweight; ideally, no more than the average weight of a cellular phone (∼120g),
- must not be permanent; the user must be able to move the device without discomfort,
- must be reusable,
- must accommodate various user's body shapes (e.g. arms from 5 cm to 12 cm in diameter),
- must be durable.

Functional Requirements

The feedback

- must be reliable and consistent - specifically, once calibrated, it should produce repeatable perceptual effects (ideally within 10%) for a given level of actuation,

- produce a large range of perceived magnitudes (e.g. 2-3 bits of information),
- must produce smooth motion (humans are extremely sensitive to vibrations as small as 0.1g for frequencies of tens or hundreds of Hz [124]),
- must not cause discomfort to the user so that it can be worn continuously for a few hours.

3.2.2 Linear Motion vs. Rotational Motion

There are a variety of motions that can produce lateral stretch on the skin. A contact pad attached to the skin may move linearly in an infinite number of directions, or the point may deviate from linearity and move in an arc or pre-determined path. Qualitatively, there appears to be a difference in the perceived magnitude of stretch depending on the path of the pad, where perceived magnitudes are higher when the contact pad rotates versus moving in pure translation. These two basic motions can be grouped into forms of linear or rotational motion. To quantify which of these two motions would produce the greatest perceived magnitude, a preliminary strain analysis was conducted. The differences in strain and forces applied using the two methods were determined.

Preliminary Strain Analysis

Setup and Methods

An analysis of the forces and strains applied to the skin with a single contact pad for linear and rotational stretch motion was completed. A testbed was constructed to allow a single contact pad to move in a linear or rotational motion. A digital camera was mounted to the top of the testbed to take images directly above the region of skin being stretched. In order to measure the displacement of the skin as stretch was applied, a grid of lines and dots was drawn on the forearm. Reasons for choosing this location are outlined in Section 3.2.4. The grid lines were spaced 5

mm apart from one another and covered a large surface area of the forearm (90 mm x 140 mm). The grid was applied using a temporary tattoo printout to ensure that the distances between the points were consistent. The contact pad, also attached to a 6-axis load cell, was glued to the skin using cyanoacrylate adhesive to ensure that no slipping would occur.

Linear skin stretch was defined to be stretch applied along the long axis of the forearm with no rotational component. The contact pad moved linearly from its resting point towards the wrist. Rotational stretch, not to be confused with twisting, was defined to be stretch applied as the contact pad rotated about a central axis point, defined to be 12.7 mm (0.5 inches) from the center of the contact pad, resulting in a combination of translational and rotational motion. This radius was chosen as it did not produce any discomfort but still provided a qualitative difference in perceived stretch as compared to linear stretch. For both types of stretch, the pad started from the same resting location. Lead screws were used to move the contact pad incrementally in both cases. The initial normal force applied by the contact pad was 2N, a small force. At each incremental move, the digital camera captured the displacement of skin. Sample images from the two motions can be seen in Figures 3.1 and 3.2.

To compare the two methods of stretch, a similar amount of displacement was applied. For the linear motion, a contact pad displacement of approximately 9 mm was applied. For rotational motion, the pad rotated approximately 40 degrees, which resulted in an arc length of 8.8 mm, close to the distance moved in the linear case.

Analysis

Displacements of the grid dots were determined by calculating the difference in location of the grid points from the previous image. For analysis, a very localized region of skin was studied (35 mm x 80 mm area) as the displacements of skin far from the contact point were small. By measuring the relative displacement of each of the points, the strain at each point was estimated. A curvature correction factor to

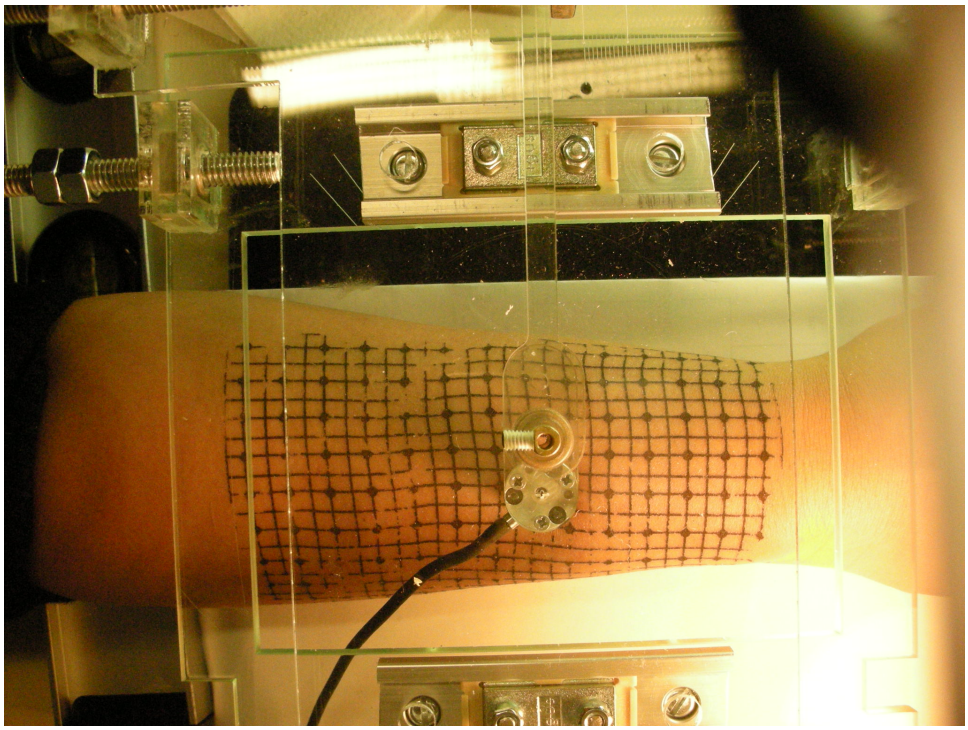

(a) Neutral position(no stretch).

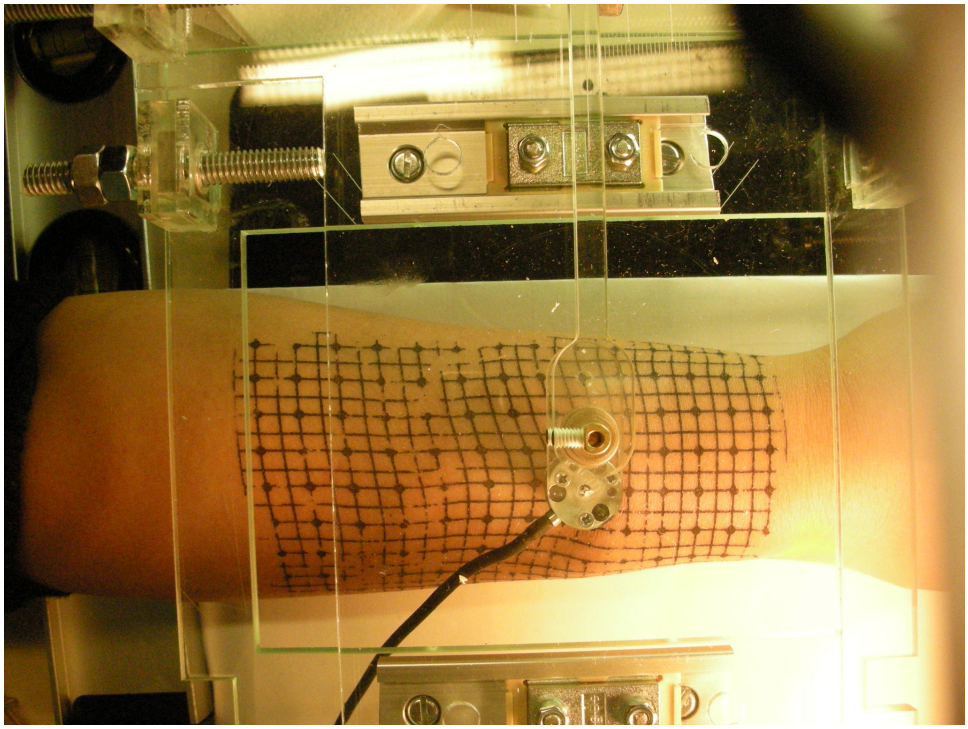

(b) Linear stretch at 9.3 mm of displacement.

Figure 3.1: Linear skin stretch images.

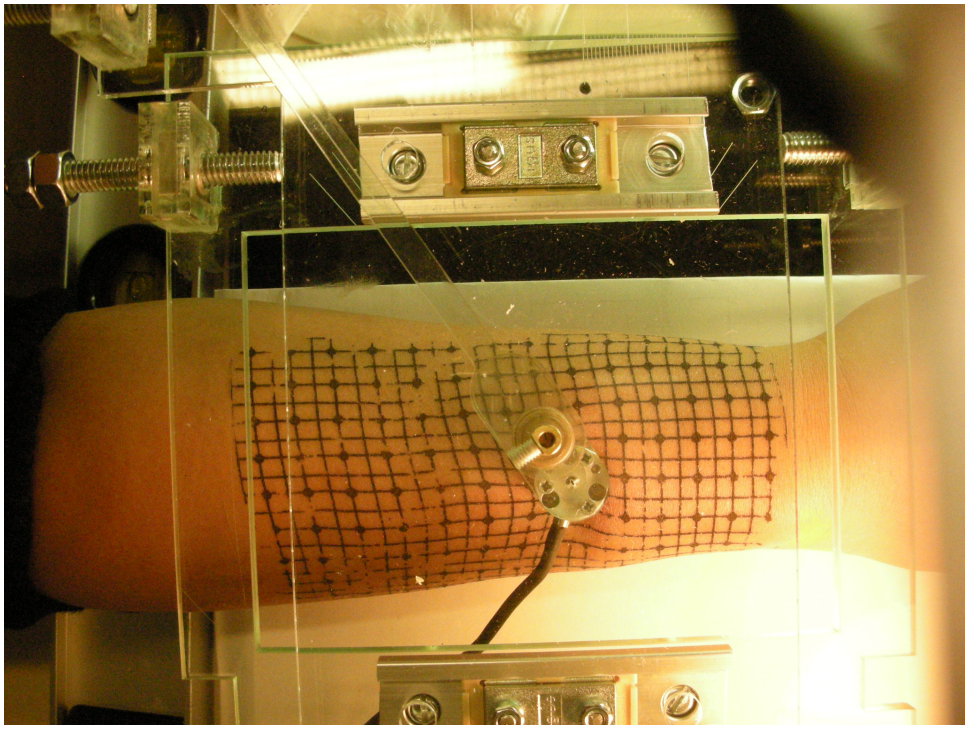

Figure 3.2: Rotational skin stretch at 40 deg of rotation (8.8mm arc length).

compensate for the curved surface of the arm was applied to the grid points to obtain planar 2D X-Y coordinates of each grid point of interest. Detailed explanation of the calculations can be found in Appendix A.

Results

Of particular interest were the principal strains. A vector field of the principal strain axes and magnitudes can be seen in Figures 3.3 and 3.4 for linear stretch and rotational stretch, respectively.

As the contact pad moved, intermediate images were taken and the average and peak principal strains as the skin was displaced from 0 to 9mm, and rotated from 0 - 40 deg were computed (Figures 3.5 and 3.6 where the rotational angle has been converted into an arc length (mm)). As seen in the figures, at each distance, the rotational motion has higher average and peak principal strains. This shows that although the contact pad was moving a relatively similar distance in each case,

rotational motion may produce a greater amount of local strain.

In addition to higher strains, the net force in the X-Y plane applied to the skin was measured with the load cell. The forces can be seen in Figure 3.7. It can be observed that the forces measured in the rotational case were much higher compared to linear motion. These results matched the qualitative observation of many pilot users who stated that the rotation motion resulted in "stronger" sensations.

Overall, this preliminary study indicates that rotational skin stretch may provide some perceptual benefits over linear motion. In these pilot studies, rotational motion required a greater range of force, which would potentially allow users to perceive a greater range of magnitudes. In addition, rotational motion also appeared to produce a larger net amount of strain, potentially activating our mechanoreceptors to a greater extent than linear motion. However, it should be noted that a displacement

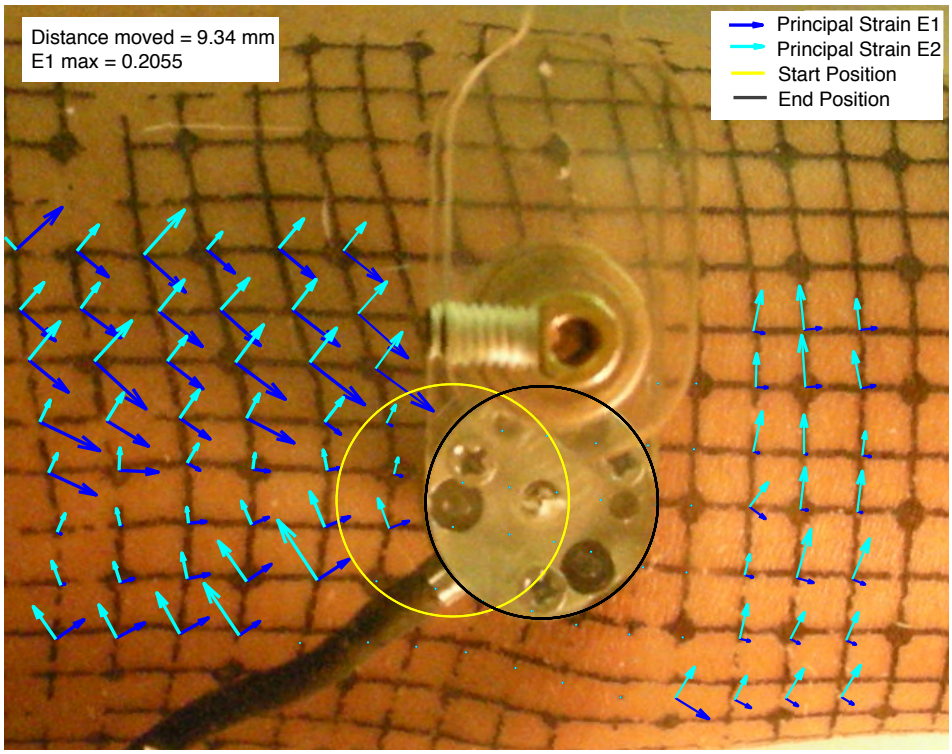

Figure 3.3: Principal strains for linear stretch.

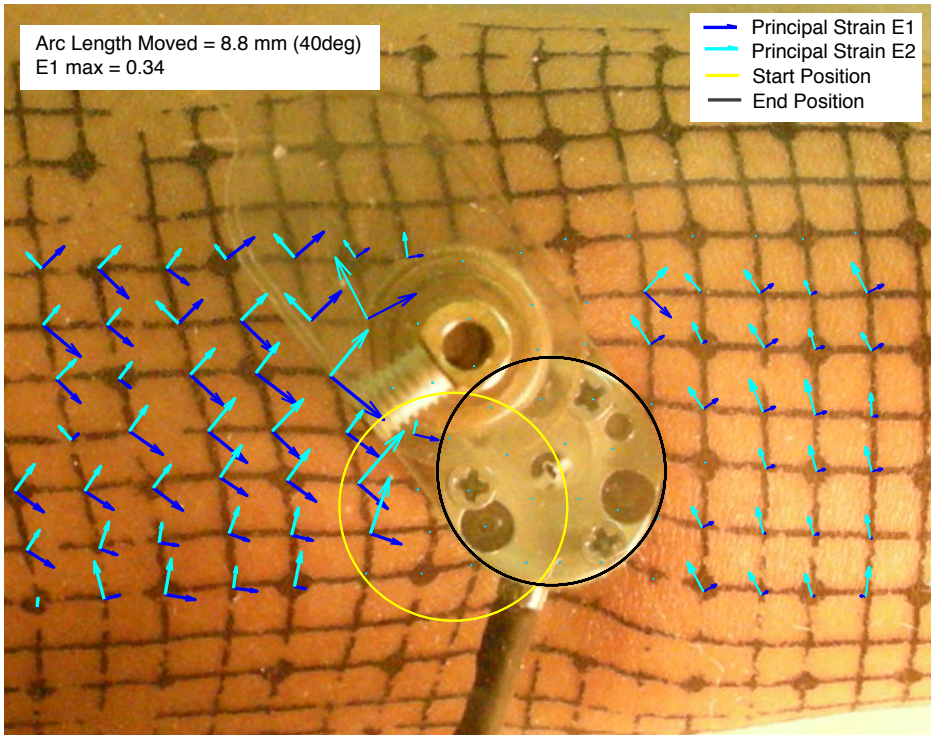

Figure 3.4: Principal strains for rotational stretch.

of 9mm in linear motion was not near the maximum displacement possible on a user. Stronger magnitudes and higher amounts of strain could certainly be induced by simply moving the point further. Yet, as our primary guidelines were to produce a large sense of magnitude while keeping in mind that the ultimate goal would be to produce a small, compact device, rotational skin stretch seemed to be the more promising method, producing higher strains and forces within a smaller area.

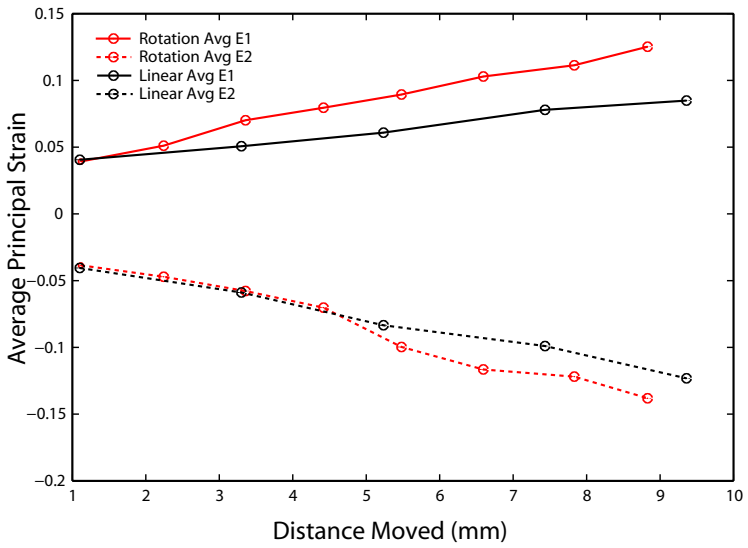

Figure 3.5: Average principal strains for linear and rotational stretch.

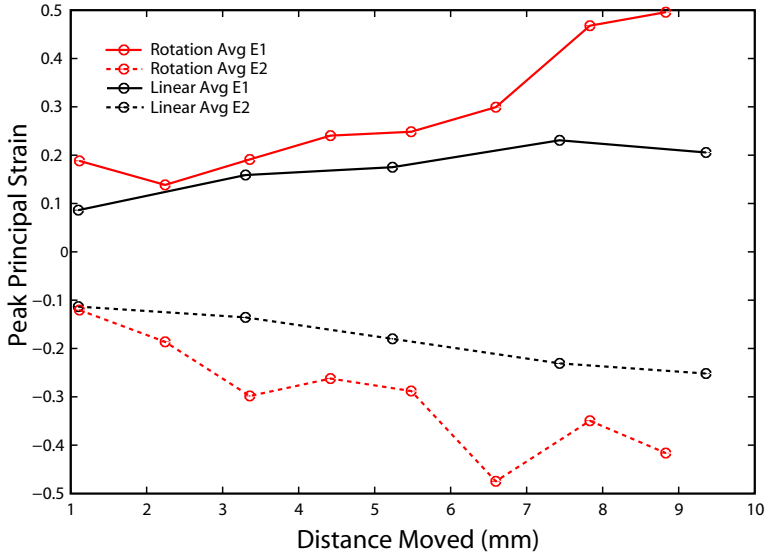

Figure 3.6: Peak principal strains for linear and rotational stretch.

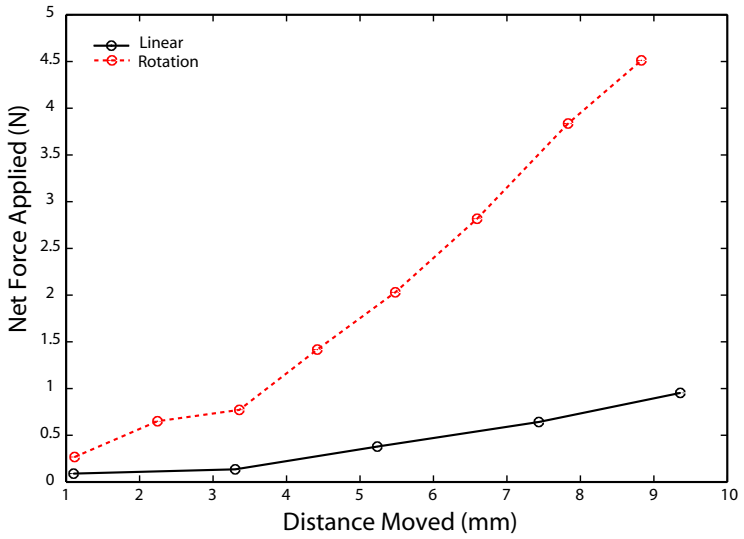

Figure 3.7: Forces applied during linear and rotational stretch.

Qualitative Observations

Several qualitative observations regarding different motions of stretch were also noted in separate pilot testing to support our theory that rotational skin stretch would be more beneficial compared to linear motion. A series of different types of skin stretch was applied to the user's forearm, as listed in Table 3.1. In testing a subject's ability to distinguish between different types of stretch, subjects were able to easily distinguish between the motions as described in Table 3.1. 3 subjects were asked to identify which type of stretch was being applied, and all were able to correctly identify the motions with 100% accuracy. However, the general consensus was that when two points were used, the sensation was stronger. This is not surprising, as we can assume that adding another contact point would activate a greater number of mechanoreceptors. In particular, when two points moved in opposing directions, the sensations were reported to be strongest. There were two general methods that produced this shear motion, one in which the points moved in opposing directions linearly, and another in which two points rotated about an axis.

Though it is possible that in applications where navigational information is necessary, a single point skin stretch device would be more than adequate, the goal for this device was to provide as many bits of information possible to a user through our ability to perceive different magnitudes. With this requirement, the two shear motions were leading candidates to produce the desired range of perceived sensations. When combining these observations with the preliminary strain results, it was decided that to obtain the greatest range of magnitude perception within the smallest surface area, rotational motion was the best method to pursue.

3.2.3 The end effector: How to apply stretch

Once a type of motion (rotation) was determined, the next design element of interest was the end effector, the area of the device in contact with the skin. One specific design requirement was that the normal force applied to the skin be kept low (0-2N)

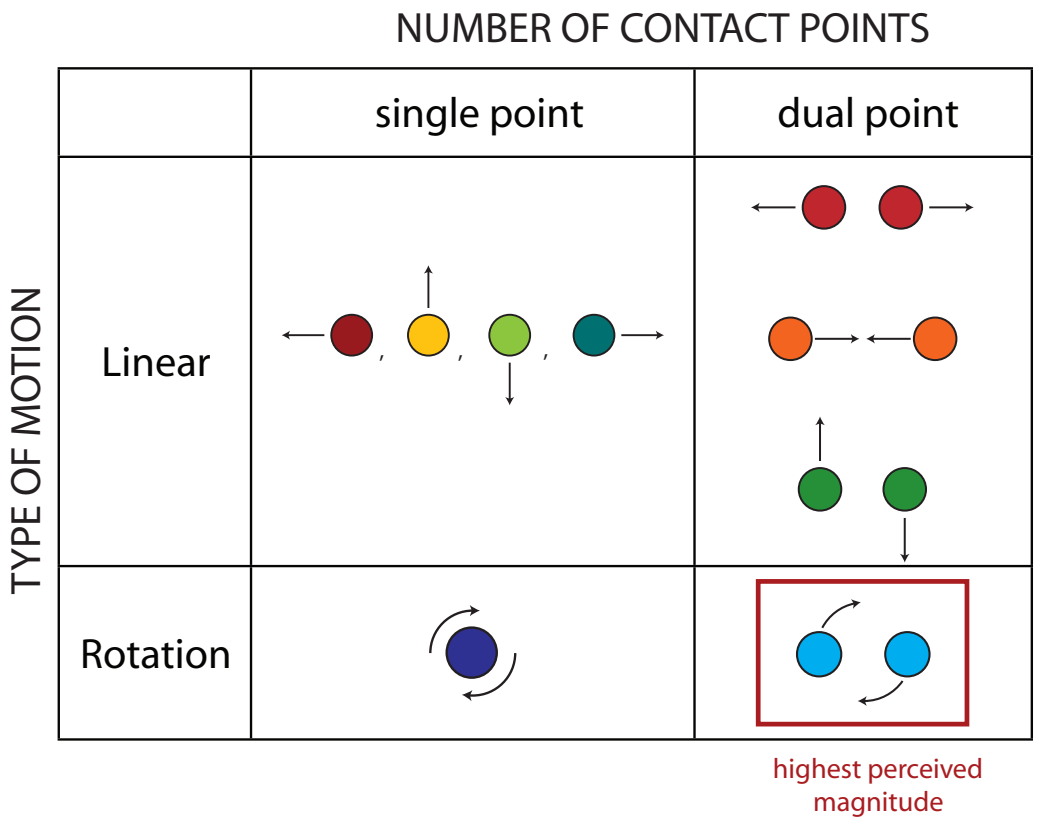

Table 3.1: Table of skin stretch methods tested with observations resulting from pilot testing.

as pilot subjects using initial prototypes found that an increased normal force led to less shear/stretch sensations overall and also limited the total amount of possible rotation; the sensation of the normal force also dominated the user's perception if too great and users reported concentrating more on the normal force as compared to the stretch sensations. Another design requirement was that the contact pads should be in the same plane as the surface of the skin to obtain good contact to help reduce the likelihood of slipping. If the contact pads were placed on the skin with an uneven distribution of pressure and misaligned with the surface of the skin, as the pads rotated, the end effector would lose contact with the surface easily.

The contact pads

Although in the pilot studies and initial prototypes, two contact pads were used, prototypes to test varying numbers of contact pads and patterns were built. If increasing the number of pads from one to two produced larger magnitude sensations, would increasing the number of contact pads beyond two create even greater magnitude sensations? Users who compared the stretch resulting from increased contact pads reported that the overall range of movement degraded and the overall intensity of the stimulus increased to the point of being uncomfortable. It is hypothesized that the increased shear strain and twisting of skin with greater numbers of pads resulted in a more pinching sensation, creating discomfort to the user. Prototypes testing various shapes, patterns, and numbers of contact pads were tested. A small sample of the patterns tested can be seen in Figure 3.8, however it was ultimately decided that a simple two point rotation would be adequate for our purposes.

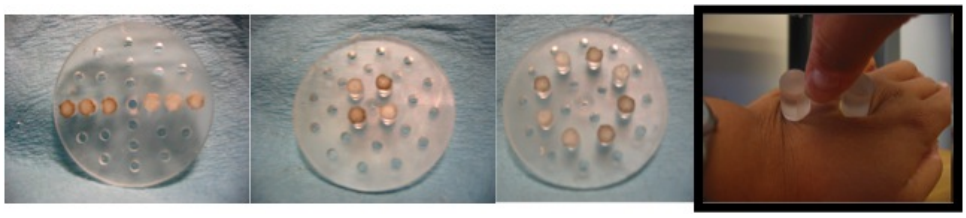

Figure 3.8: End effector prototypes.

The sizes and shapes of the contact pads were also tested. Because the device was envisioned to be worn on the body, the most natural locations discussed were the arms and legs. The curvature and smaller surface area of the arms in particular were considered in determining the shape and size of the contact pad. An end effector with a greater number of contact pads would be more difficult to conform to the curvature of the arm. Points that are too large in surface area would not fit on the arm, yet points that were too small were often painful and required higher amounts of normal force to be applied as they were more susceptible to slip. A surface area similar to the area of a fingerpad was deemed to be appropriate, as it allowed enough

area to adhere to the skin while minimizing slip, yet was small enough to be compact and fit on the surface of most users' forearms. In addition, the shape of the contact pads was circular, as any sharp edges or points, that would result with rectangular shaped pads, created discomfort.

Adhesion to skin

The skin is a difficult surface to adhere to. An ideal skin stretch device should contact the surface of the skin with minimal normal force as it was found that as the normal force increased, the perception of skin stretch diminished. It is also necessary to apply stretch with little to no slip between the surface of the skin and contact pad. In a practical application it is desirable to have a device that can easily be removed and re-attached with minimal effort.

A stiff contact pad to adhere to the surface of the skin is also desired. If a compliant material is used, the elastic properties would influence the amount of stretch applied to the skin. Skin is already a non-linear, viscoelastic [42], time-varying material, and adding another level of compliance would reduce the amount of stretch being applied to the skin.

It was decided that a rigid contact pad with some adhesive coating could attach to the skin. Low durometer silicones are readily available, have a naturally tacky surface and were tested for their ability to adhere to the skin with small amounts of normal force. The various types of silicone tested can be seen in Figure 3.9. While silicones were reusable and worked well with some types of skin, it typically required a high normal force (>2N) to prevent slip at high rotations of skin stretch. In addition, silicone did not present equally adhesive properties on all skin. The contact pads would simply slip during rotation on skin with a large density of hair, essentially producing friction/slip sensations rather than stretch. Though methods such as suction could provide potentially better adhesion, the goal to design a low-power, lightweight device made this option unlikely.

Ultimately, although there may be other materials that can adhere to the skin,

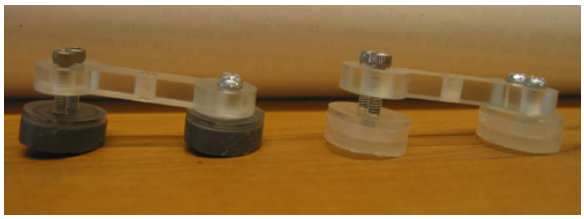

Figure 3.9: Silicone prototypes.

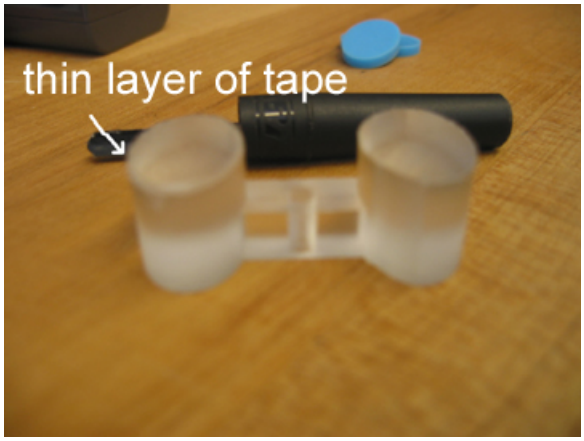

Figure 3.10: True Tape prototypes.

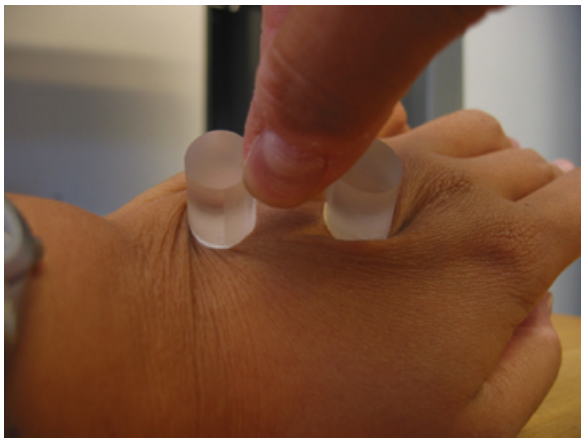

Figure 3.11: True Tape stretching skin.

for these experimental purposes, a skin-safe adhesive was discovered to provide a strong bond in rotational stretch (see Figures 3.10 and 3.11). Red-e-Tape, along with a polymer, Skin Shield, commonly used in medical applications and cosmetics, was used in all testing. This method was less susceptible to differences in hair density than other methods and allowed for uniform testing between a wider variety of subjects. The tape provides a strong bond between the end effector and skin to produce lateral stretch, but is a one-time use only method, and after the end effector has been removed from the user, a new layer of tape must be re-applied.

3.2.4 Where to apply stretch

While there are several locations on the body that skin stretch can be applied (virtually anywhere on the body), we ultimately decided to concentrate on the forearm. We suspect that the number of mechanoreceptors in the forearm is greater than other areas of the non-glabrous skin [95]. In addition, for applications and portability, it would be easy to imagine strapping a wearable device to the forearm/bicep. Though skin stretch perception on the different parts of the body can/should be studied, it is beyond the scope of this project to determine how different areas of the body result in different perceptual responses.

3.2.5 How to control the amount of stretch induced

The remaining critical aspect of designing the device was to determine the best method of controlling the amount of skin stretch applied. The two methods considered were controlling the torques applied to the skin, or controlling the amount of angular displacement of the skin. To estimate the amount of torque necessary to apply skin stretch, a single piece of tape was attached to the skin and to one end of a spring scale. The tape was pulled gently using the spring scale to measure the force applied to the skin and the user indicated when the force applied was near the preferred maximum limit. On average, this number ranged from 7-10 N of estimated

force, varying from user to user. Estimating a distance of approximately 25 mm between contact pads, this would result in 125 mNm of torque necessary to provide a wide range of skin stretch on a user. It was noticed qualitatively that a user's perception of the torque being applied was not constant. It appeared that the stiffness of skin decreased over time, and consequently as a constant torque was applied, the angular displacement of the skin stretch pads increased continually. In addition, the varying stiffness of skin between different users made it difficult to know if applying the same amount of torque on one user would result in similar perceptual interpretations of the feedback on another user. For these reasons, displacement controlled skin stretch was chosen. Applying a controlled displacement ensured that the same amount of skin displacement would be applied from subject to subject, even though the perceptual differences were unknown.

3.2.6 Device Design Requirements

Ultimately, the results of the prototypes and observations led to the design and construction of various skin stretch devices. Using data collected from pilot studies as well as in depth experiments, a set of mechanical design requirements building upon those listed in Section 3.2.1 were completed. The design requirements for the device were that it

- be capable of positioning end effector within 1 degree, exceeding human resolution of rotational skin stretch; Chapter 5 details perception tests showing humans can at best distinguish 2 deg differences in rotations,
- be capable of a reasonable range of speeds (5-200 degrees per second), not to exceed comfortable ranges of angular velocity,
- be capable of producing 0.2 Nm of torque,
- have minimal vibrations ($< 2.5\ m/s^2$ for 10-500 Hz [58]),

- have an operating range of ±60 degrees, exceeding the range of possible and comfortable stretch values as observed in studies detailed in Chapter 5,
- be adjustable to accommodate different limb sizes,
- be capable of adjusting normal forces applied to user with a range of 0-2N,
- be capable of measuring torques and forces applied during stretch (0-0.2Nm, 0-10N, with 1% accuracy),
- allow for easy testing of different end effector configurations.

3.3 Hardware Design

The primary device used in experiments and testing was a benchtop rotational skin stretch device. The main purpose of the device was to be used as a testbed to apply skin stretch on a variety of users and provide sustained, localized skin stretch.

3.3.1 Benchtop Rotational Skin Stretch Device

Three versions of a benchtop skin stretch device, in which the stretch pattern is induced with two contacts, were designed and developed for testing of controlled skin stretch. All of the devices (two are shown in Figures 3.12 and 3.13 while the third is shown in Section 4.2.1, Figure 4.3), allows us to vary the contact method and test different end effector configurations to evaluate perception and ability to induce skin stretch. The first device was designed for pilot testing and initial perception studies. The second benchtop was developed to test the technology suitable for developing wearable or portable devices, namely utilizing an ultrasonic motor. The second device also incorporated a method to test linear stretch. The third device was developed for use in 3D motion capture tracking. All operated on the same principles and basic design structures with only minor mechanical differences. The essential

specifications of the devices are outlined in the following sections with differences between the two devices specified where applicable.

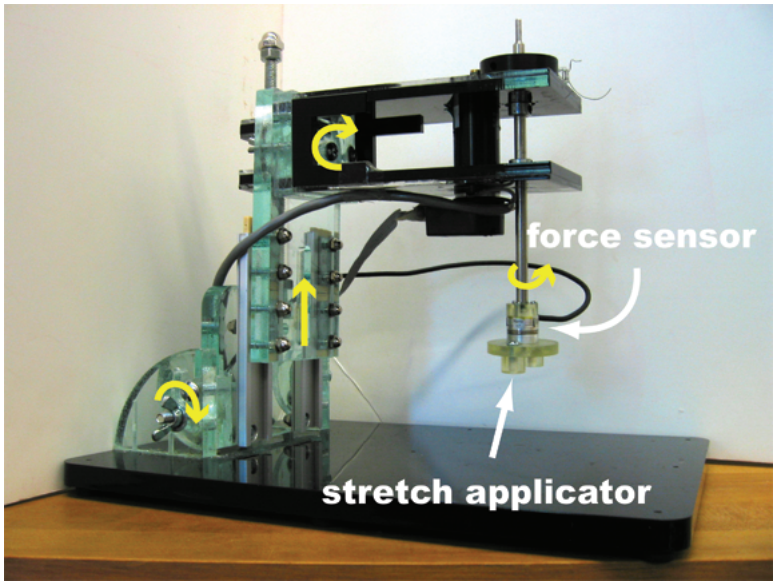

Figure 3.12: First skin stretch benchtop device. Arrows indicate directions device can be adjusted manually to be placed on test subject's limbs and utilizes an standard low-friction servo motor.

Actuation and Drive System

Device 1 uses a low-friction servo motor that applies torques to the rotating shaft and the stretch applicator disks, inducing skin stretch primarily in shear. The motor is coupled to the shaft of the stretch applicator through a capstan pulley with a 6.83:1 speed ratio which provides a low friction transmission. Devices 2 and 3 use a slightly smaller speed reduction ratio of 5:1 and an ultrasonic piezoelectric motor to apply stretch. Details for this design choice are outlined in Section 3.3.2.

Body

Early pilot tests also showed that maintaining flat contact with the skin was important in reducing the amount of slip and eliciting strong sensations. Therefore,

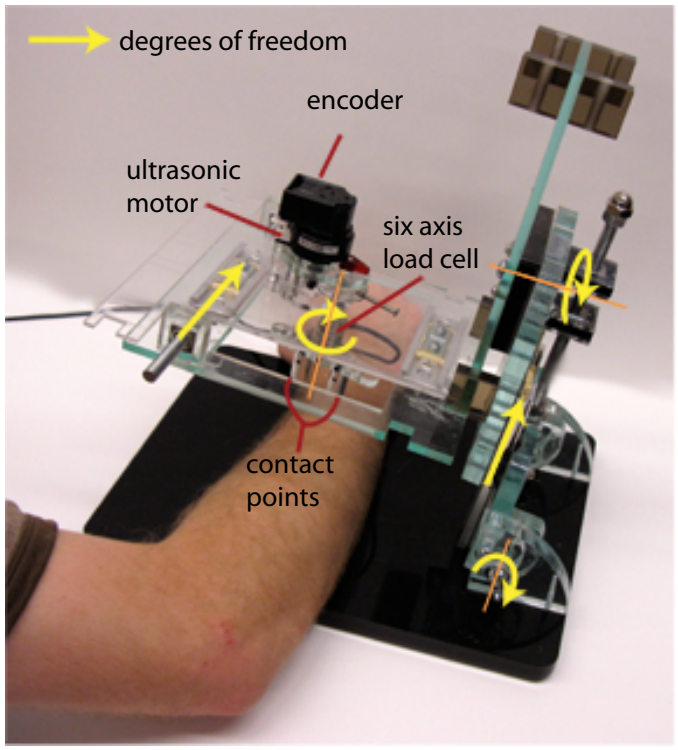

Figure 3.13: Second benchtop skin stretch device incorporating an ultrasonic motor and linear stretch capabilities. Arrows indicate adjustable degrees of freedom.

as indicated in the figure (yellow arrows), the device has three manually adjustable degrees of freedom to accommodate different sizes of arms and legs while keeping the stretch applicator and the axis of rotation perpendicular to the local skin surface. A lead screw to adjust the vertical height of the device allowed us to control the amount of normal force applied to the user.

End Effector

Following the observations in Section 3.2.3, the end effector is comprised of two circular contact pads (d = 13 mm) spaced 25.4 mm apart to attach to the skin, resulting in a contact area of roughly 2.5 cm^2.

Sensors

A six-axis force/torque sensor (ATI Nano 17) is mounted between the shaft and the stretch applicator to measure the overall forces and torques applied. The load cell is used to ensure that the same normal force (2N) is applied to each user prior to each experiment trial. Device 1 had an encoder resolution of 0.1deg/tick, while Device 2 had a resolution of 0.036 deg/tick, utilizing the encoder's quadrature capabilities.

Control

Based on the results of earlier pilot tests as described in Section 3.2.5, we determined that applying fixed rotations produced less subject-to-subject variability in the perceived skin stretch than applying fixed torques. Consequently, position controlled skin stretch was applied using a PID controller with feedforward components to reduce transient errors. The control is implemented using a PIC microcontroller running at approximately 800Hz. Under test conditions, the skin stretch applicator tracks commanded rotations with an accuracy of approximately ± 1 degree. The controller used for Device 2 is outlined in Section 3.3.2.

3.3.2 Wearable Rotational Skin Stretch Device

As the goal was to ultimately build a wearable, portable haptic device, a smaller, more compact device was designed and constructed.

The wearable skin stretch device is designed to be attached to, and provide skin stretch feedback on, non-glabrous skin. Initially, it was tested and optimized for attachment on the arm. The objective of the design was for the device to attach easily to any part of the human body, without interfering greatly with the skin stiffness and perception at the end effector location.

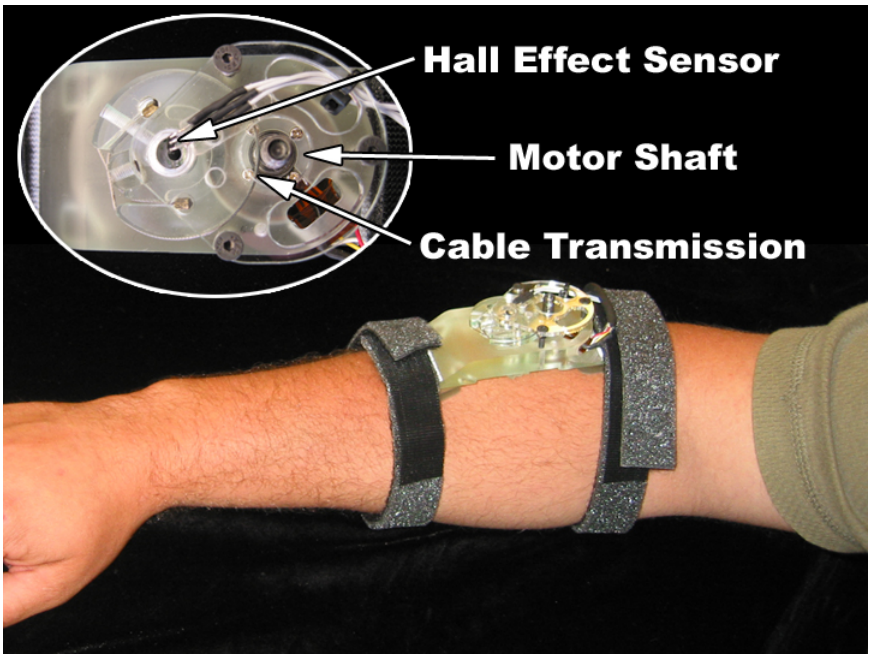

Figure 3.14: Wearable skin stretch device on arm.

Actuation

In typical haptic applications, a DC motor is used to provide vibration or force feedback to the user as used in the benchtop device. DC motors are readily available and can produce large vibrations and/or torques at relatively low cost. For force feedback applications, the backdriveable nature of DC motors used in direct drive or cable transmission configurations provides a low-impedance interface. However, producing large torques requires bulky and heavy motors and transmissions. For the wearable skin stretch device, we typically perform pure position control and backdriveablility is not important. In this application, a non-backdriveable motor is desirable because it requires no power to hold a position against an external torque. We therefore require an actuator which can deliver large torques at relatively low speeds in a lightweight, flat package. Though commercially available DC motors have the ability to produce the required torques and speeds, the power consumption and weight were not acceptable for a wearable skin stretch device. More importantly,

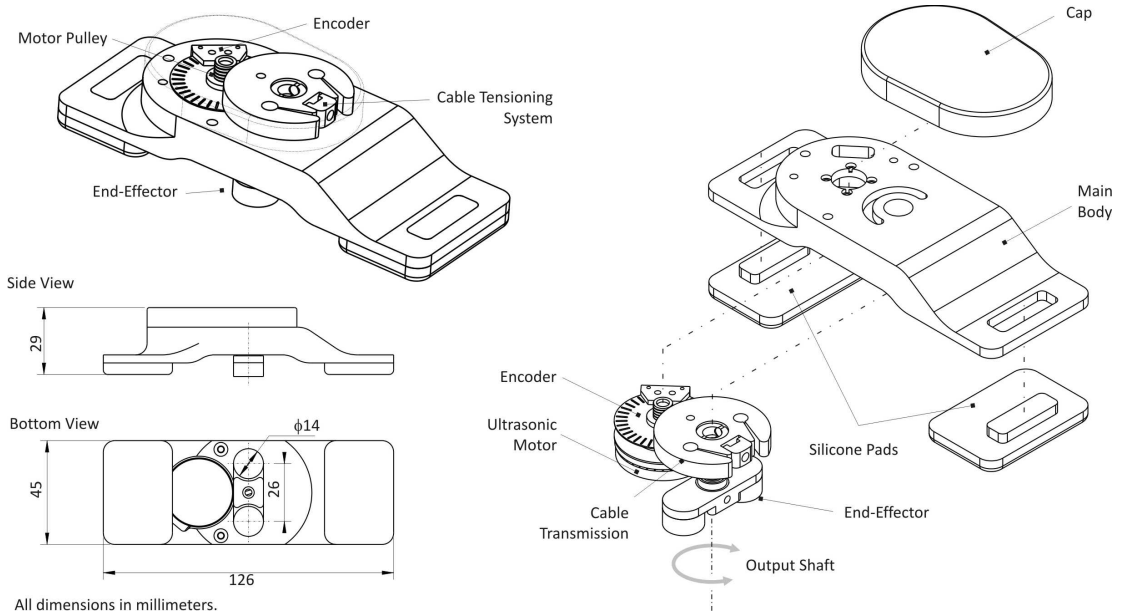

Figure 3.15: Wearable skin stretch device assembly layout and main dimensions.

to obtain the torques necessary within the size requirements, a gearbox would be required. While this is adequate for most applications, in haptics, where the user's sense of touch is exploited, any additional sensations such as vibrations from gears are highly undesirable. In addition, gearboxes can result in backlash which is easily detected by users through their sense of touch. A sufficient level of backlash can cause oscillations and be a limiting factor for precise movements. For this reason, an alternative method of actuation was investigated.

An ultrasonic piezoelectric motor (Shinsei Motors, USR30-B3) is used to fulfill the design requirements for a wearable skin stretch device. These ultrasonic motors use a piezoelectric ceramic element to produce small, high frequency (50 KHz) deflections in a stator structure. These displacements are converted into unlimited rotary motion of the rotor through intermittent frictional coupling [113] . Ultrasonic piezoelectric actuators can not only produce high torques at low speeds, but they are also non-backdriveable. Finally, these motors can be small, flat, and lightweight - ideal for our purposes. Consequently, the wearable skin stretch device was designed to incorporate

the ultrasonic motor. Specifications of the ultrasonic motor are outlined in Table 3.2.

	Motor Specifications
Diameter	30 mm
Thickness	9 mm
Maximum Torque	0.1 Nm
Holding Torque	0.1 Nm
Weight	20 g
Maximum Speed	150 rpm = 900 deg/s
Minimum Speed	15 rpm = 90 deg/s
Driving Frequency	50 kHz

Table 3.2: Ultrasonic motor specifications

Drive System

The power from the ultrasonic motor is transmitted to the rotational skin stretch end effector through a capstan cable drive system. To produce the torques and speeds necessary, a 6:1 speed ratio was employed. The effective range of speeds for the rotational end effector is then reduced to 15 - 150 deg/s. The maximum torque output of the end effector is 0.6 Nm, far exceeding the maximum torque necessary. The capstan cable drive is utilized to keep vibrations low and smoothly transmit torques from the motor to the end effector. The relatively small range of motion required (±60 degrees) also makes a cable driven system easier to implement. A braided steel cable is used to transmit the torques and a small tensioning block/lead screw system is implemented to minimize slip. To guide the cable, keep it within the confines of the motor shaft and increase the friction coefficient between cable and pulley and the output shaft, a threaded pulley is placed over the motor shaft (see Figure 3.15).

End Effector

The end effector used with the wearable device is the same as the one used with the benchtop device. Both devices are designed to easily accept changes in pad designs and configurations.

Body

The dimensions of the main body of the device (Table 3.3), specifically the width of the device, were constrained by the physical properties of the forearm, as we envisioned using the device primarily on the lower and upper arm extremities. The overall thickness of the device was minimized to reduce inertial effects felt by the user while the device was in use. Finally, the overall length of the body was chosen such that the supporting contact pads were sufficiently far from the end effector, so that the user's perception of skin stretch would not be altered significantly by the body of the device. The body is attached to the user using Velcro straps. The straps are easy to remove and allow the device to be attached to a wide range of limb sizes. To provide extra comfort to the user, silicone pads are placed between the contact areas of the body and the skin. Urethane plastics are used for the body and end effector. All body parts and pads were constructed using Shape Deposition Manufacturing (SDM) techniques, a fabrication method for creating multi-material robotic appendages [8].

	Design Requirements	Device Specifications
Size	small	29 x 45 x 126 mm
Max Torque	0.2 Nm	0.6 Nm
Speed Range	$\leq$ 200 deg/s	15-150 deg/s
Weight	$\leq$ 200 g	115 g
Sensor Resolution	1 deg	1 deg (Hall Effect) 0.05 deg (Encoder)

Table 3.3: Wearable skin stretch device characteristics

Sensors

Pilot studies indicated that position sensing and control were optimal for rotational skin stretch. In order to keep the device lightweight and compact, a hall effect sensor was placed above the pulley shaft to sense the rotational position of the end effector. Two miniature neodymium magnets were embedded 180 degrees out of phase into the center hold of the capstan pulley. Within the inner hole, a small hall effect sensor was positioned to sense the changing magnetic fields produced by the magnets embedded in the center of the pulley (Figure 3.16, left). Because a relatively small range of motion is used, the linear range of the hall effect sensor output was large enough to control the device to initial specifications, accurately positioning the device within 1 degree of the desired position. Though in typical applications this type of sensor resolution would be more than adequate, for research purposes, a more accurate method of position measurement was necessary. To evaluate the effectiveness of the wearable device, a position sensor with high resolution was implemented (see Figure 3.16, right). In the experiments presented here, the device is equipped with a standard quadrature optical encoder, mounted to the motor shaft for improved accuracy. This results in a resolution of 0.015 deg/encoder tick. The device itself is easily adaptable to different sensor configurations as seen in the Figure 3.16, and subsequent experiments may utilize either method of position sensing.

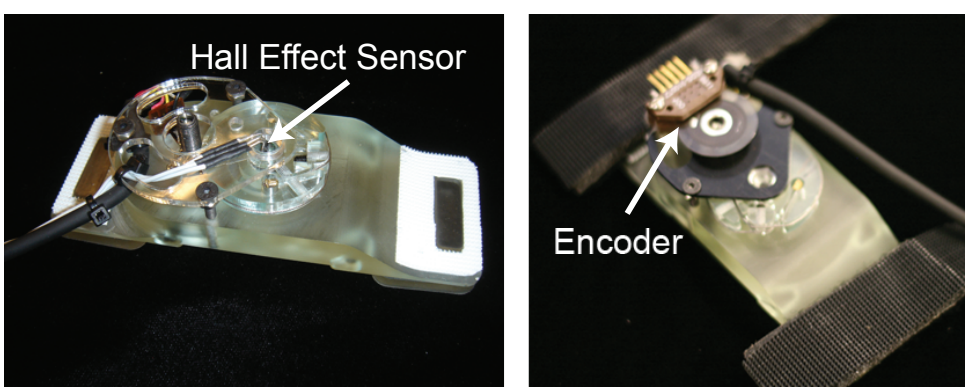

Figure 3.16: Wearable skin stretch device with hall effect sensor and/or encoder for position sensing.

Control

Due to the resonant characteristics of the motor, a non-linearity is present in the motor dynamics. The motor cannot rotate slower than a speed determined by the resonant frequency of the piezo-elements. We used a motor driver board supplied by the manufacturer to control the motor [89].

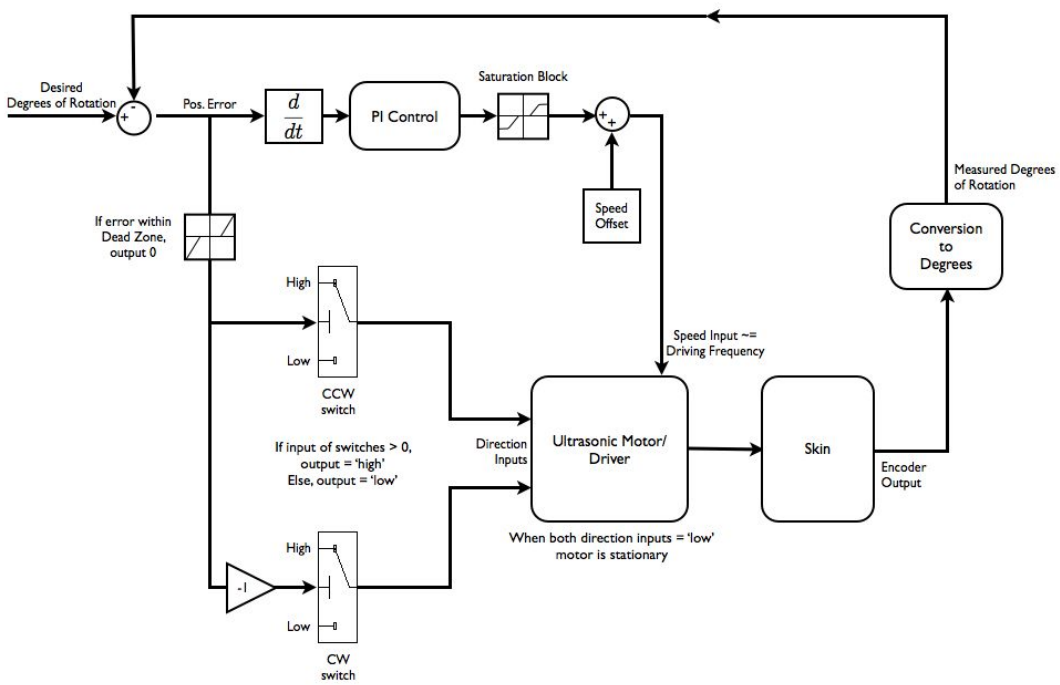

Figure 3.17: Wearable skin stretch device control block diagram.

The driver takes three inputs, two to specify the direction of motion (digital) and a third analog channel to set the motor speed. We used Matlab's xPC real-time toolbox with a multifunction data acquisition board to control the hardware. Logical operators in the computer code were used to set the appropriate direction of motor rotation. To avoid chattering around desired position due to the non-linearity

in speed, a deadband in the position controller was implemented. A simple linear PI controller was used to drive the motor. For the experiment described below we used a deadband of ±0.05 degrees, a proportional gain of 0.8, an integral gain of 0.4 and a sample rate of 200 Hz. The position and integral position errors are fed back through the appropriate gains to the speed channel of the motor (Figure 3.17).

Second wearable device

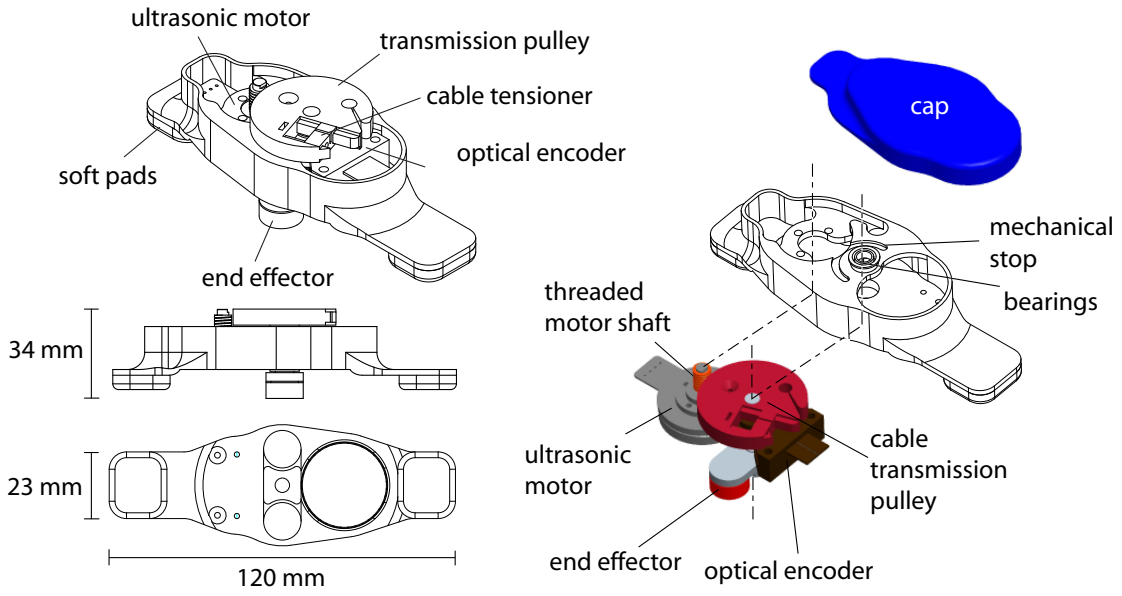

Figure 3.18: Second wearable skin stretch device schematic and dimensions.

A final wearable skin stretch device was designed and manufactured to reduce the overall size and weight, place the encoder in a more robust location, improve the cable tensioning system, and increase the safety of the device by designing mechanical stops to prevent the end effector from rotating beyond ±90 degrees of rotation. CAD drawings of the device can be seen in Figure 3.18. The body of the device is constructed using a three step SDM process. The new device weights 82 g and the overall height is reduced to 34 mm. Photos of the device are in Figure 3.19. This

new device will be used for future experiments using rotational skin stretch feedback.

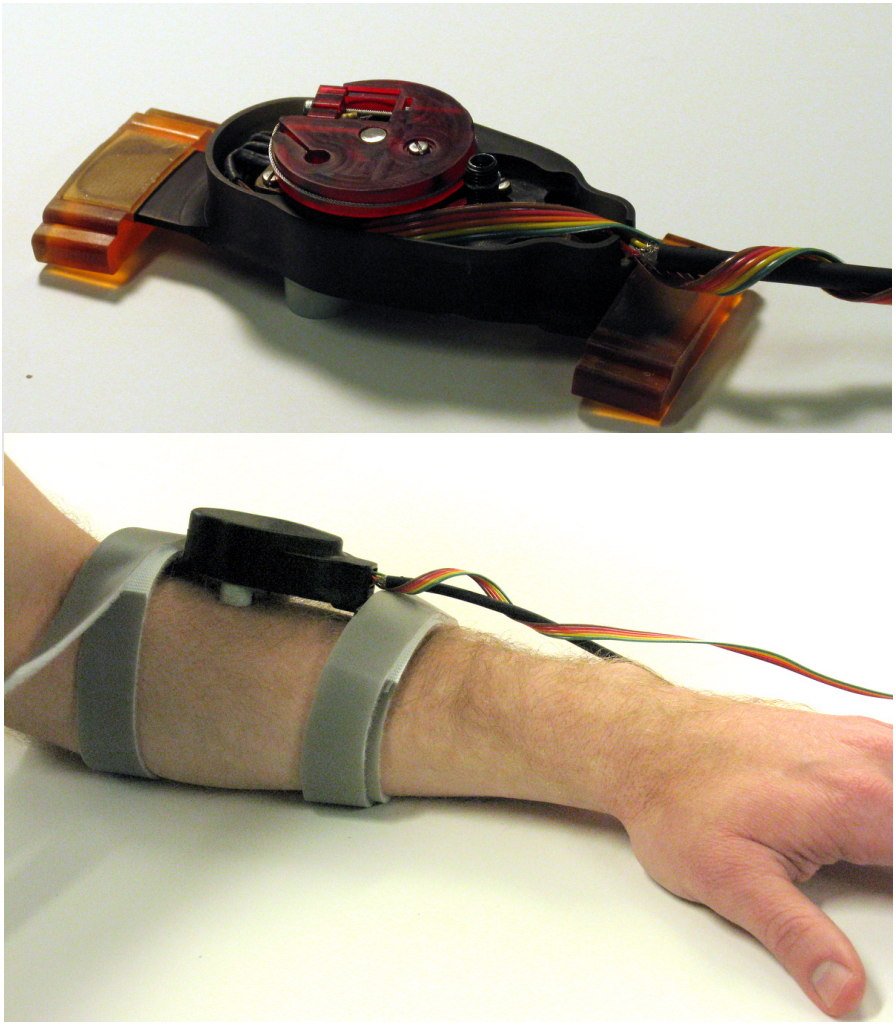

Figure 3.19: Second wearable skin stretch device (above) and placed on arm (below).

3.3.3 End Effector Design

The primary end effectors used in the studies are described earlier (Section 3.3.1), however a secondary design was used in several investigations as well. Pilot studies indicated that the perceptual qualities of skin stretch are heavily influenced by the strain patterns around the end effector. In particular, local shear strains imparted by rotation of the pads can cause a stronger sensation of intensity but can also become uncomfortable for large rotations (Figure 3.20, left). A solution was to design free rotating contact pads to reduce the amount of shear strain induced by the end effector. In this design, the pads were equipped with bearings so that they could rotate freely as they tracked the circular arcs defined by the end-effector arms (Figure 3.20, right). An end effector was designed to allow fixed or free pads, as seen in Figure 3.21. A small set screw is inserted into the cylinder to prevent rotation when desired. In initial tests, it appeared that with freely rotating pads, users felt more comfortable with large rotations but had more difficulty in detecting small rotations. The perceptual qualities of these two different end effector designs were evaluated in following studies to determine what, if any, difference was produced by the two configurations.

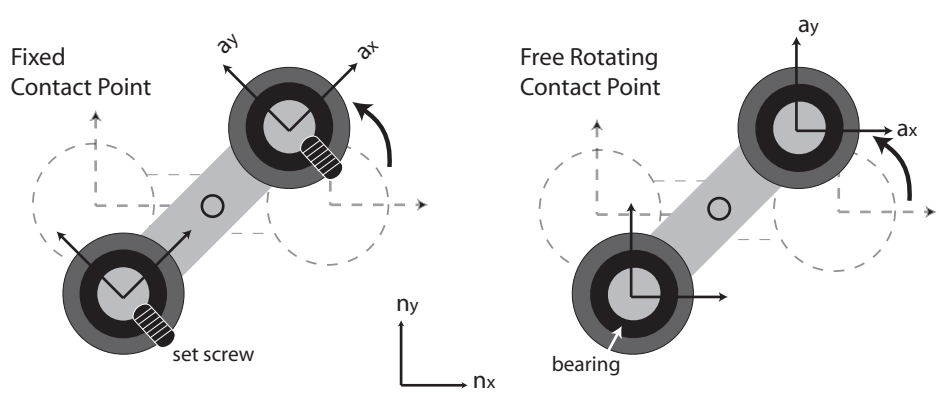

Figure 3.20: Fixed versus free end effectors: A coordinate frame (a_x, a_y) is embedded in the contact pad and either rotates rigidly with the end effector arms (left) or pivots and remains aligned with a stationary reference frame (right).

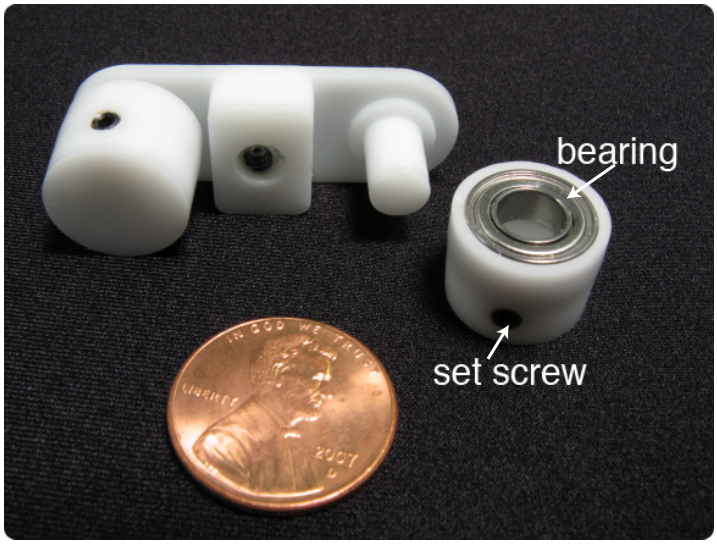

Figure 3.21: End effector used in experiments to switch from fix to free configuration quickly and easily.

Chapter 4

Rotational Skin Stretch Measurement

We are applying lateral deformations and displacement of skin to elicit responses from our mechanoreceptors and, while the motion produced is a simple rotation, the deformation and movement of skin at the surface is much more complex. What mechanical factors can we measure at the skin surface, and how do these correlate to our perception of stretch? For our studies, we are not interested in determining precisely what each individual stretch receptor is sensing, but in understanding what occurs at the skin surface when a two point rotational stretch is applied. In particular, it is of interest to compare skin stretch using the two different end effector congurations, with fixed and freely rotating contact pads, respectively. Qualitatively, it has already been observed that the fixed contact pads result in slightly higher magnitude sensations particularly at higher degrees of rotation. It would be beneficial to know what mechanical factors lead to this observation and to quantify these perceptual differences in future experiments as well.

4.1 Previous Work

The literature does not agree on what specific mechanical properties contribute to our perception of skin stretch. Experiments and their analysis are complicated by the fact that skin is anisotropic, non-linear, and viscoelastic [42]. While some studies have shown that stresses correlate to mechanoreceptor activity [52, 65], others have shown that compressive strains or strain energy correlate to receptor activity [26, 103]. The general issue is that these various experiments are rarely completed on human skin, as testing tends to be quite invasive. As a compromise, researchers often use animal skin such as on rats or cats for understanding receptor behavior, yet it cannot always be concluded that animal receptors react in a similar manner to human receptors, as the authors acknowledge [52]. The region of skin that is tested is also varied in these experiments, using the hands or legs of animals, further confounding the results. What can be agreed upon is that SAI and SAII receptors respond to various types of skin stretch, and in particular, SAII units are directionally sensitive, with increased activity when stretch is along a preferred orientation or axis [26, 30, 52, 65].

Early work to characterize skin properties varied in the type of stretch applied and the location of stretch. Manchott [82, 83] performed uniaxial tensile tests on human calf, both across and along the tibial axis. Two square tabs (10 mm $\times$ 10 mm) were attached to the skin with cyanoacrylate adhesive with a distance of 5 mm in between. In tensile testing, this procedure of attaching two tabs to the skin and pulling apart is common. Meijer [86] performed similar uniaxial testing of the skin on the forearm in order to obtain parameters to develop a skin model. A strain field was obtained using optical tracking techniques.

Agache, Finlay, and Sanders [2, 38, 109] all studied skin properties under torsional twist of a single contact point on the forearm, though the precise location of applied stretch is unclear. It is clear from these studies that the modulus of elasticity of skin is not simply a constant. In all cases, different moduli were obtained for various subjects, and were found to be highly dependent on the age of the subject, as well as

the experimental conditions. In addition, these studies focused on studying the local stress and strain of the skin at a single point, with small strains applied, staying in the linear region of the stress-strain curve. In our studies, large scale deformations occur and the strains resulting from the lateral deformations most likely surpass the linear region.

In the last 10+ years, non-invasive techniques to measure skin properties in-vivo have been developed. Digital image correlation (DIC), an optical method that can provide accurate 2D and 3D measurements of deformations, displacement, and strain from digital images [20], for skin measurements has been employed by a few researchers. Douven [29] placed markers on a small patch of skin on the arm to measure the forces and displacements as two pads were moved apart from one another and Marcellier and Khatyr [66, 84] also subjected small samples of skin to tension or extension and measured the strains resulting from the displacement field. Khatyr developed a viscoelastic model for forearm skin and estimated Young's modulus of the skin on the inner forearm. However, these studies either required the excision of skin, measured very small areas of the skin, or did not account for 3D movement. Bethke [6] used a laser scanning technique to track markers across a large surface of skin covering the entire knee joint. The strains as the knee joint bent were estimated, and it is this work that serves as a guide for the analysis presented in this chapter.

As mentioned previously, skin properties are extremely difficult to measure. Several studies have investigated skin strain using optical and laser scanning methods [6, 29, 66], yet except for [6], all other test methods were looking at very small regions of stretch where 3D capture of the curvature of the skin was not important. For our purposes, as the region of stretch was large, as was the percent strain applied, a method that would capture the complete movement of the skin surface in all directions was desired.

4.2 Methods

4.2.1 Motion Capture Setup

To measure the displacements of the skin as rotational skin stretch was applied, a 3D motion capture system was used. In the previous strain study using 2D images, the main drawbacks were having a limited view of the motion of skin near the contact points and the failure to measure and account any motion in the z-axis. In addition, while the 2D images provided static measurements of strain, the 3D system allowed us to capture the dynamic motion. Another advantage of this system was that the full dimensionality of the curvature of the arm was captured in a non-invasive manner. A diagram of the entire setup can be seen in Figure 4.1. Four Eagle/Hawk digital cameras from Motion Analysis Inc. were set up in a rectangular orientation. The cameras were placed so that one was directly behind the subject, aligned with longitudinal axis of the forearm and another camera was in front of the user, also aligned with the longitudinal axis. The other two cameras were placed orthogonal to the long axis, and viewed the forearm from the sides. This placement allowed at least two cameras to view any one of the markers placed on the forearm at one time. The accuracy of this set up and calibration was on average, ± 0.2 mm. Cameras recorded data at a sample rate of 100 Hz.

1.5 mm diameter markers were placed on the forearm in a 7 x 9 grid pattern, with a few extra markers placed to measure general displacements far from the contact points (Figure 4.2). A gap in the markers occurred where the contact points were to be placed. The markers were placed on the arm manually with the aim of keeping a 10 mm spacing between the markers. Small amounts of rubber cement were applied to the markers and attached to the skin to ensure the markers would stay on the skin throughout during the study.

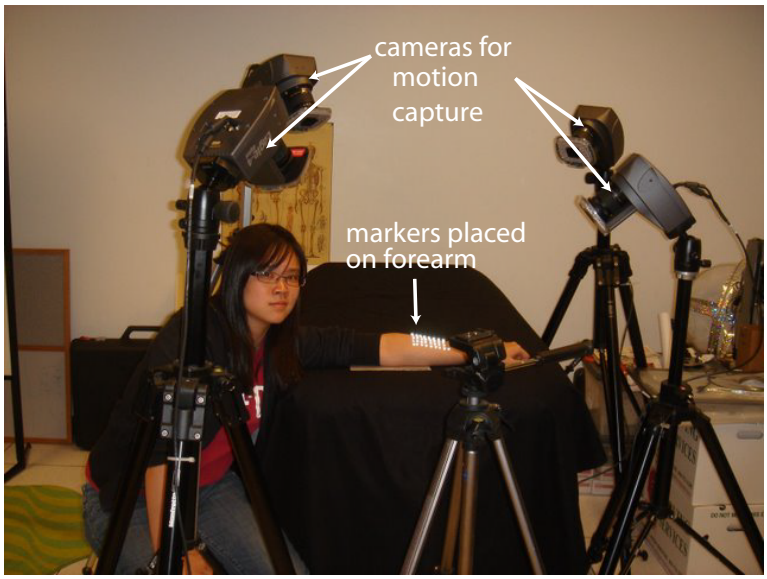

Figure 4.1: Setup of motion capture cameras. Reflective markers visible on arm in center.

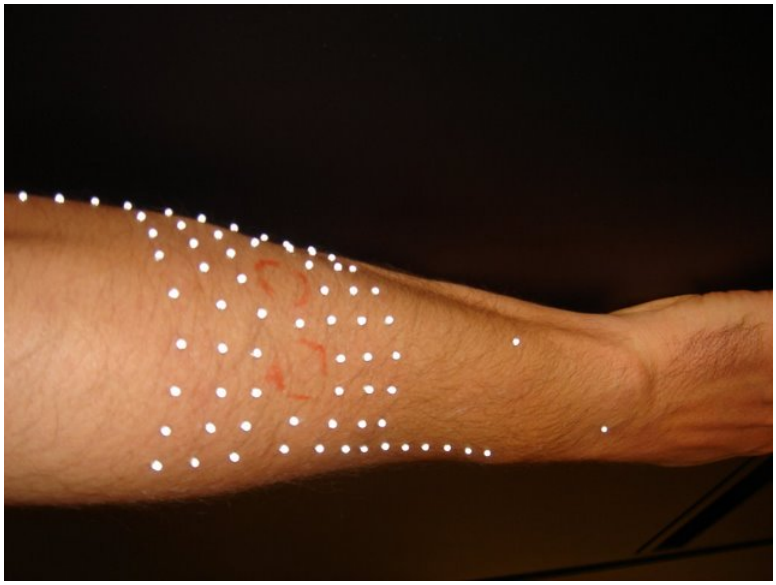

Figure 4.2: Grid pattern of markers placed on arm.

4.2.2 Device

Modifications to the existing benchtop device design were made to accommodate the motion capture environment and to improve the visual field of the forearm. The

capstan pulley and ultrasonic motor configuration used in the benchtop device were removed and attached to a tripod. This configuration reduced the width and allowed the cameras to view a larger area of the arm (see Figure 4.3). The six axis force sensor was also attached to measure the forces and torques applied throughout the study. Several markers were placed on the end effector to measure the movement of skin in contact with the end effector and monitor the motion of the device.

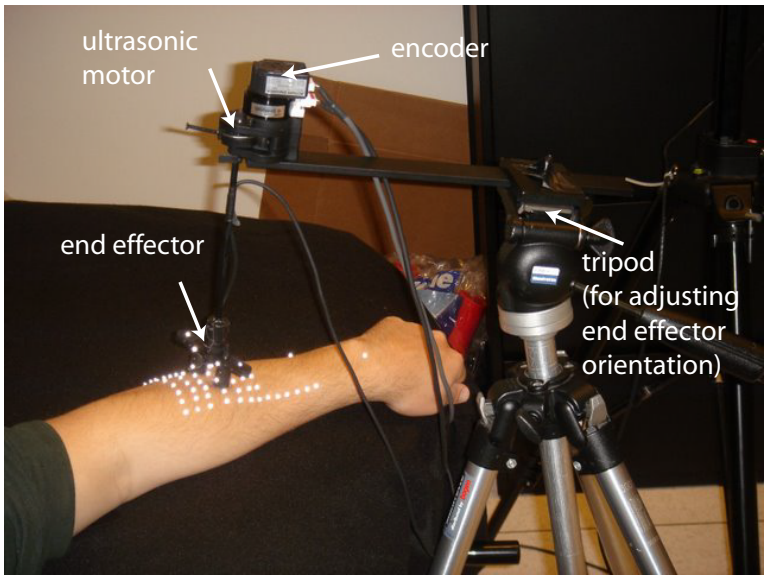

Figure 4.3: Skin stretch device used in motion capture experiments.

The end effectors were modified to switch easily from freely rotating to fixed contact pad end effectors. A small rod was inserted into the contact points and attached to the main structure of the end effector, held in place by set screws. When these set screws were loose, the contact points rotated freely about the shaft. The entire system was painted over with black, matte spray paint to prevent any extraneous reflections from confounding the motion capture marker identification process.

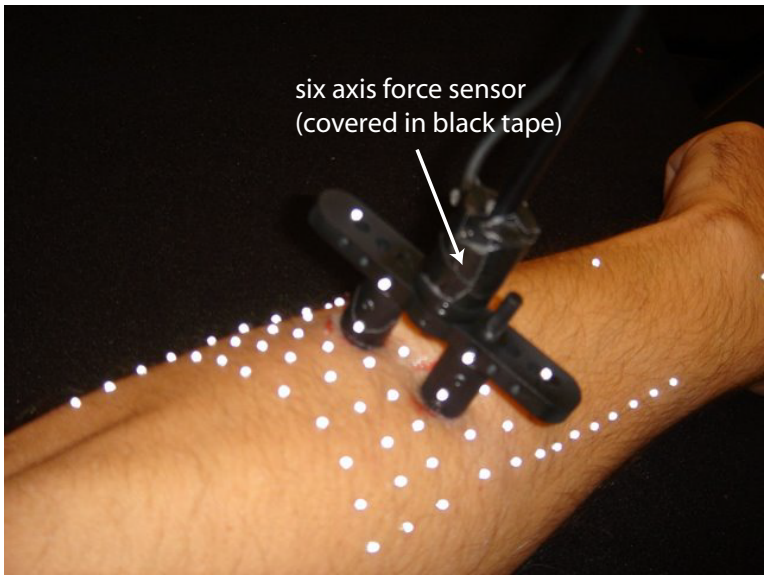

Figure 4.4: Skin stretch device attached to arm with markers.

4.2.3 Experiment Protocol

Rotational skin stretch at various degrees and directions was applied using both end effectors. A sequence of rotations starting from 0 and ramping to 10, 20, and 30 degrees of rotation was applied. After each ramp up, the device rotated back to the neutral position. The nominal speed of skin stretch was 80 deg/s for the ramp stimuli. Torques and end effector rotation were measured with sensors integrated into the device. The procedure was completed with the fixed and free effector pads.

4.3 Results

The main purposes of the experiment were to determine what differences were occurring in stretch with the two different end effector configurations and to examine what led to the perceptual differences evident from the positioning experiments. A variety of parameters were studied and the results of these analyses are presented.

4.3.1 Absolute Displacement

The most basic parameter of interest is the overall displacement of the skin. Using Motion Analysis' EvART 4.2 software, the X, Y, Z coordinates of each marker were output. As the skin is stretched, the absolute displacement of each marker relative to its starting point is calculated for the duration of the movement. The extra displacements measured when using the fixed contact pads (Figure 4.5) indicate that there is overall greater movement of the skin. These findings indicate that a greater amount of rigid body displacement is occurring in the fixed case, plausibly activating a greater number of mechanoreceptors. A surface color map to display the magnitude of displacement for each marker in both cases is presented in Figure 4.6

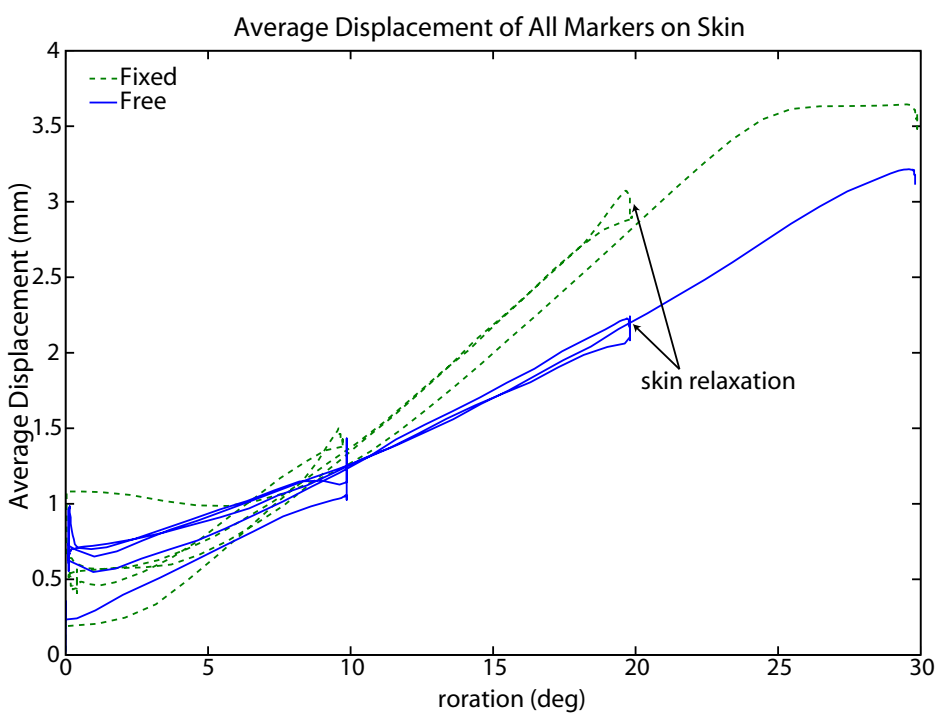

Figure 4.5: Average displacement of points.

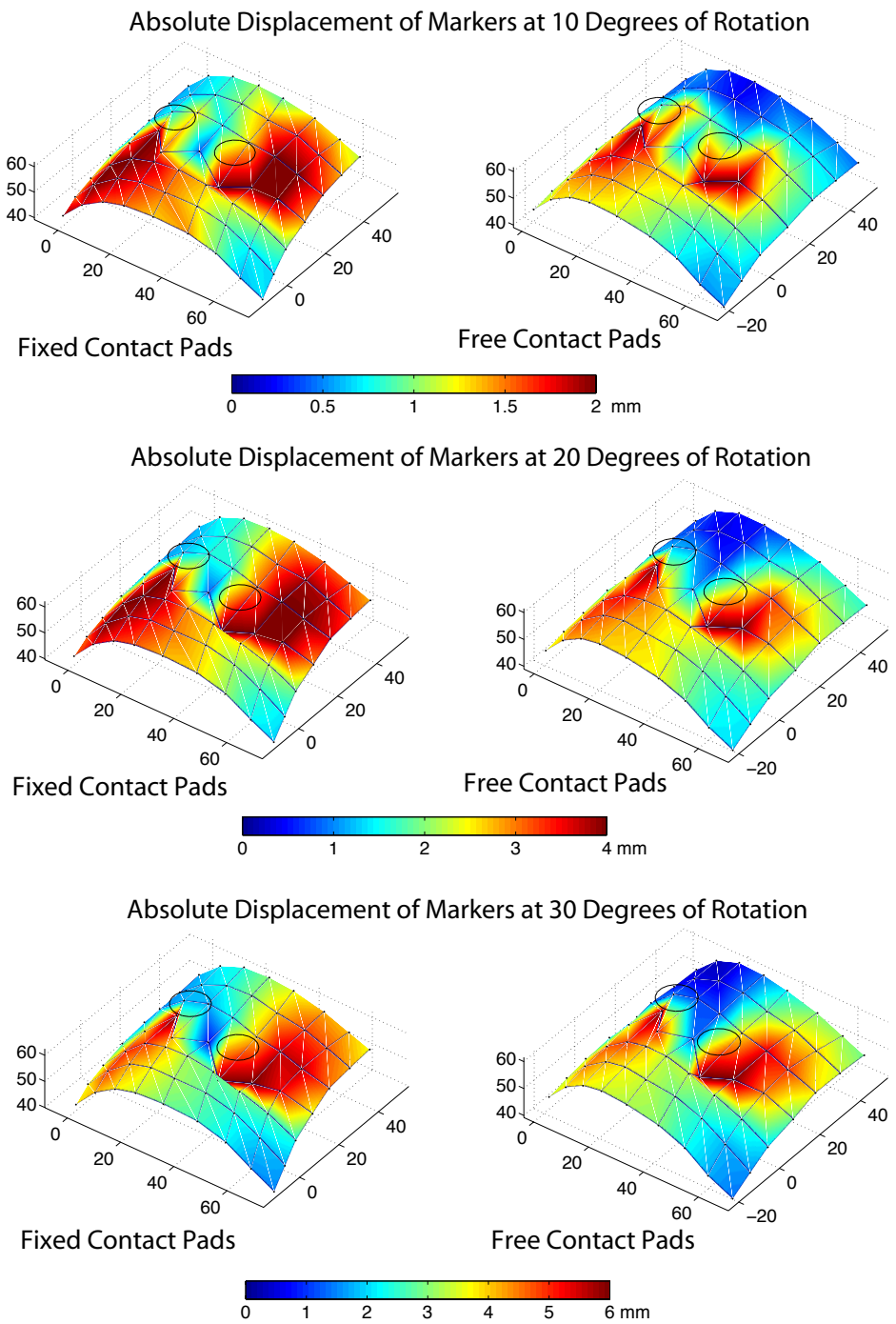

Figure 4.6: Displacement of a point approx. 6 cm from contact pad as pads rotate to 10, 20 and 30 degrees. End effector rotates clockwise.

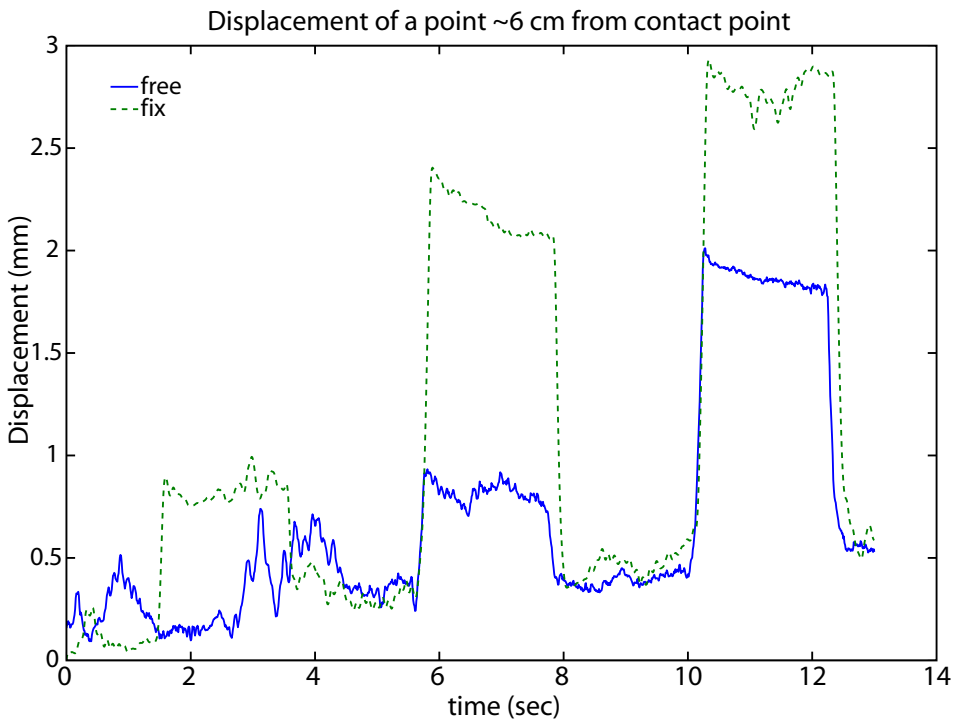

Figure 4.7: Displacement of each point when rotated at 10 degrees. End effector rotates clockwise.

Though at first glance the average displacement at low degrees of rotation appears to be similar between the two cases, when the absolute displacement of each individual point is displayed (Figure 4.6), it is clear that there is 0.5-1.0 mm extra displacement of markers in the fixed case, particularly in markers located further from the end effector contact points. In an absolute scale, an extra 0.5 - 1.0 mm of movement or displacement would not seem to be large, but it is known that humans are capable of sensing skin pulls of distances between 0.13 mm and 0.3 mm [97] and even have direction sensing capabilities with displacements corresponding to these minute movements. Olausson [97] also showed that receptors located as far away as 15 mm from the location of stretch were responsive to these displacements. The extra displacements measured when using the fixed contact pads indicate that there

is overall greater movement of the skin. To further substantiate this, the displacement of a point 6 cm from the contact pads was measured. This lone marker's displacement over the course of the trial is seen in Figure 4.7. The aggregate of these displacement findings indicate strongly that a greater amount of rigid body displacement is occurring in the fixed case, plausibly activating a greater number of mechanoreceptors. It has been inferred that a displacement as small as 2 mm can activate up to 16-17 SAII receptors located in the forearm [96], and these receptors have receptive field sizes ranging from 6 - 135 mm^2 depending on the normal force applied, again supporting the theory that a greater number of mechanoreceptors are activated using the fixed contact pads.

4.3.2 Strains

Data Analysis

As displacements were measured, the strain at each marker point was estimated. A detailed outline of the analysis can be found in Appendix B. The average surface strain at each marker point was estimated by determining the initial distance between the marker and the 8 adjacent points; therefore the marker of interest is the center of a 3 x 3 grid. The deformation is estimated by measuring the change in distance between the marker of interest and its adjacent points over time. The 3 adjacent points to the east, northeast, and north are separated into one quadrant, the north, northwest, and west points are separated into another quadrant, and so on. Each quadrant's normal strains are calculated and used in strain gage rosette equations to transform these strains from an arbitrary reference frame to the x and y components of strain along the long and horizontal axis of the surface of the forearm. The horizontal axis is defined to be follow the circumference of the arm and the long axis is the axis from elbow to wrist, and therefore changes at each marker point and reference quadrant.

Measured Strains

The longitudinal and transverse strains for each of the rotations, 10, 20, and 30 deg, are shown in Figures 4.8, 4.9 and 4.10 respectively. Shear strains and principal strains were also calculated, but the longitudinal and transverse plots provide a more intuitive visual display of the strains occurring. The surface strains display the magnitudes of compressive and tensile strain along the two axes. Not surprisingly, the longitudinal strains display high regions of compression (red color) located between the two contact pads and along the surface of the skin that "opposes" the displacement of the pad. Transverse strains, as expected, as skin has often been described as an incompressible tissue, oppose this pattern. In general, in comparing the strain patterns of the two contact pads, there are greater magnitudes of tension when using the freely rotating pads, but higher magnitudes of compression when using the fixed pads. The maximum principal strains also follow this trend. As users indicated qualitatively that the fixed end effector configuration resulted in higher perceived magnitudes and discomfort, this strain analysis would lead us to believe that it is not the tensile strains that cause the discomfort at high rotations, but rather the compressive strains. However, as the direction of mechanoreceptor orientations is unknown, this statement cannot be made with confidence, as it cannot be ensured that the directions of maximum compression and tension line up with the principal axes of the receptor sensitivity.

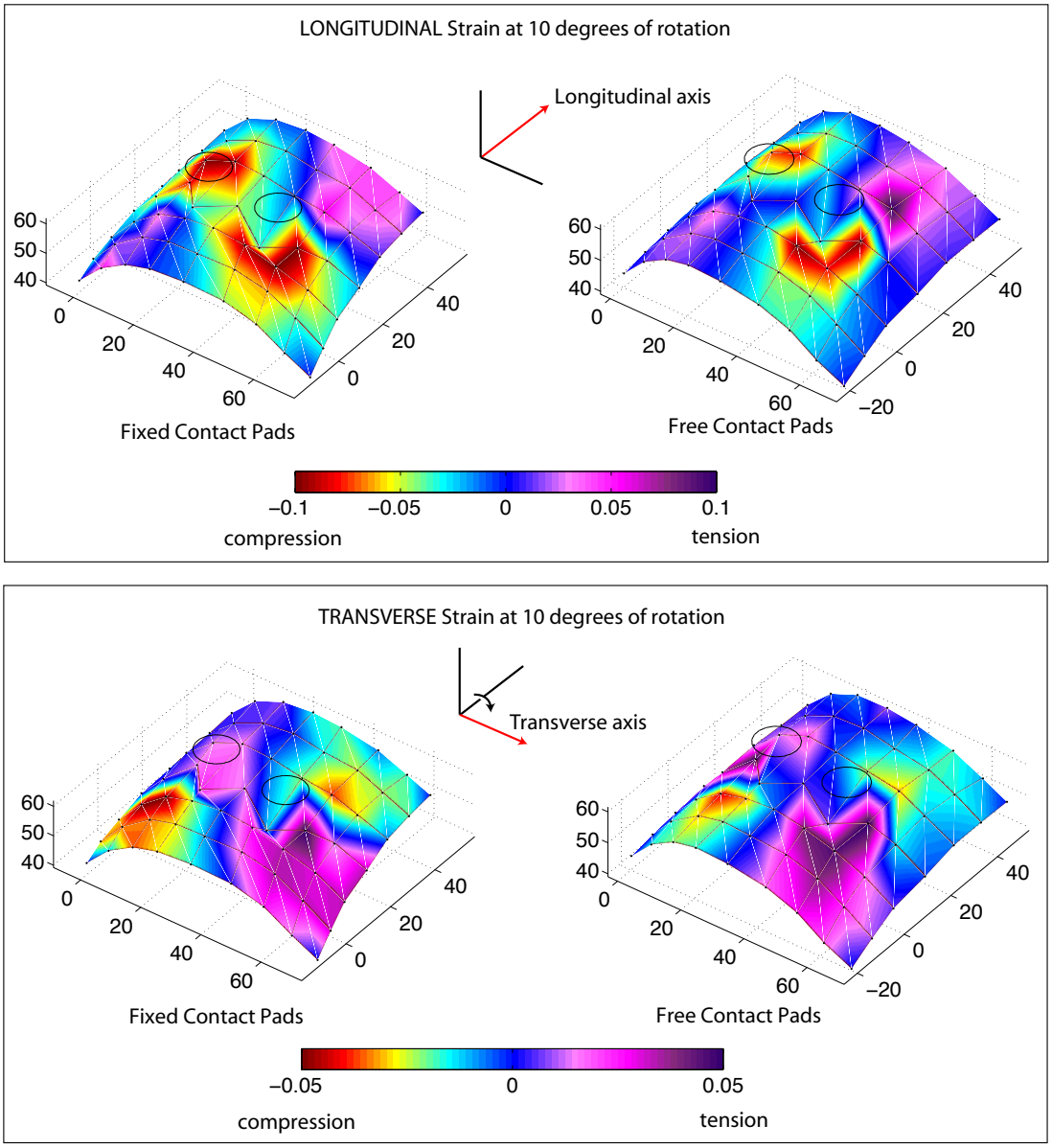

Figure 4.8: Surface strains measured at 10 degrees of rotation. End effector rotates clockwise.

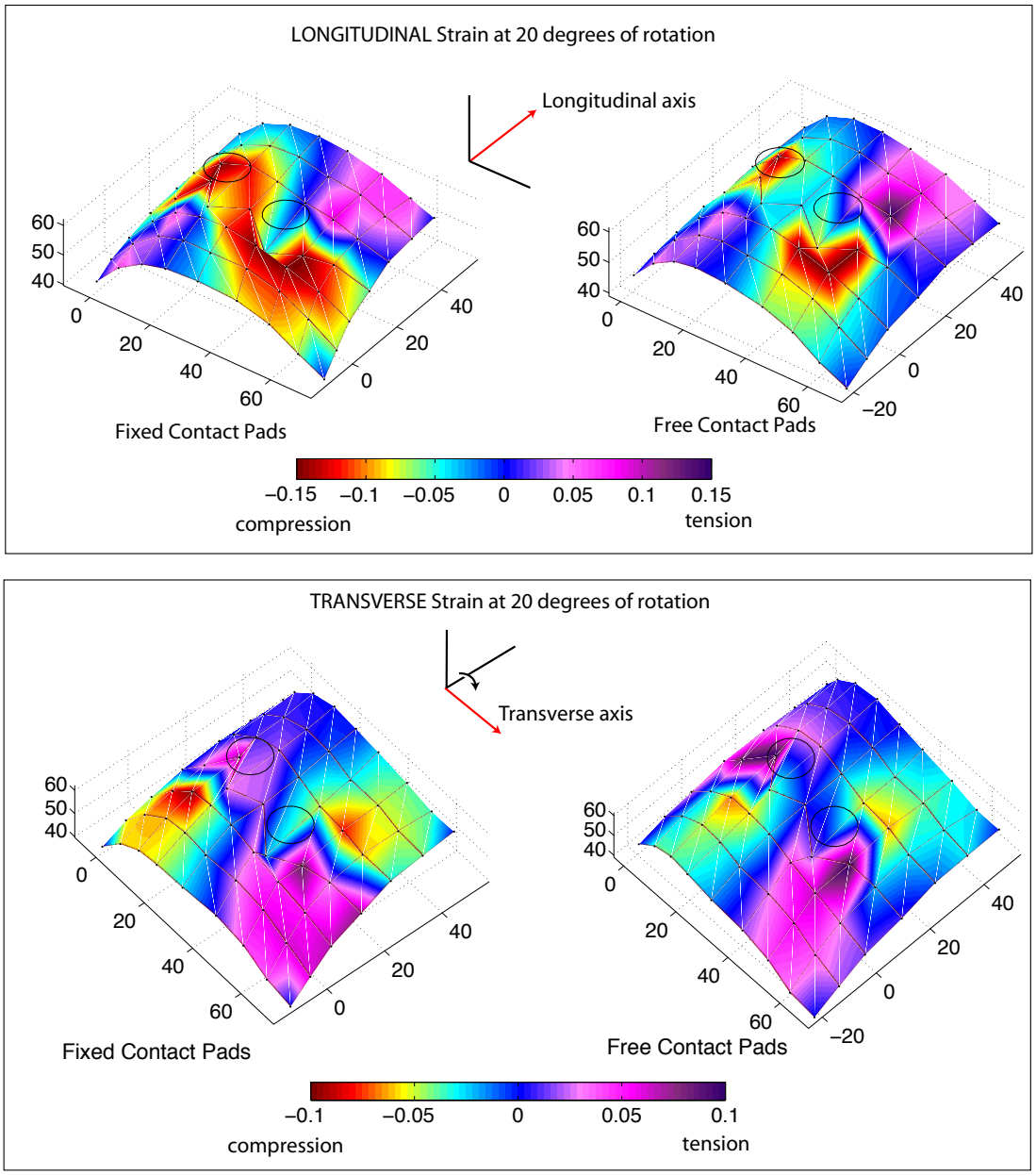

Figure 4.9: Surface strains measured at 20 degrees of rotation. End effector rotates clockwise.

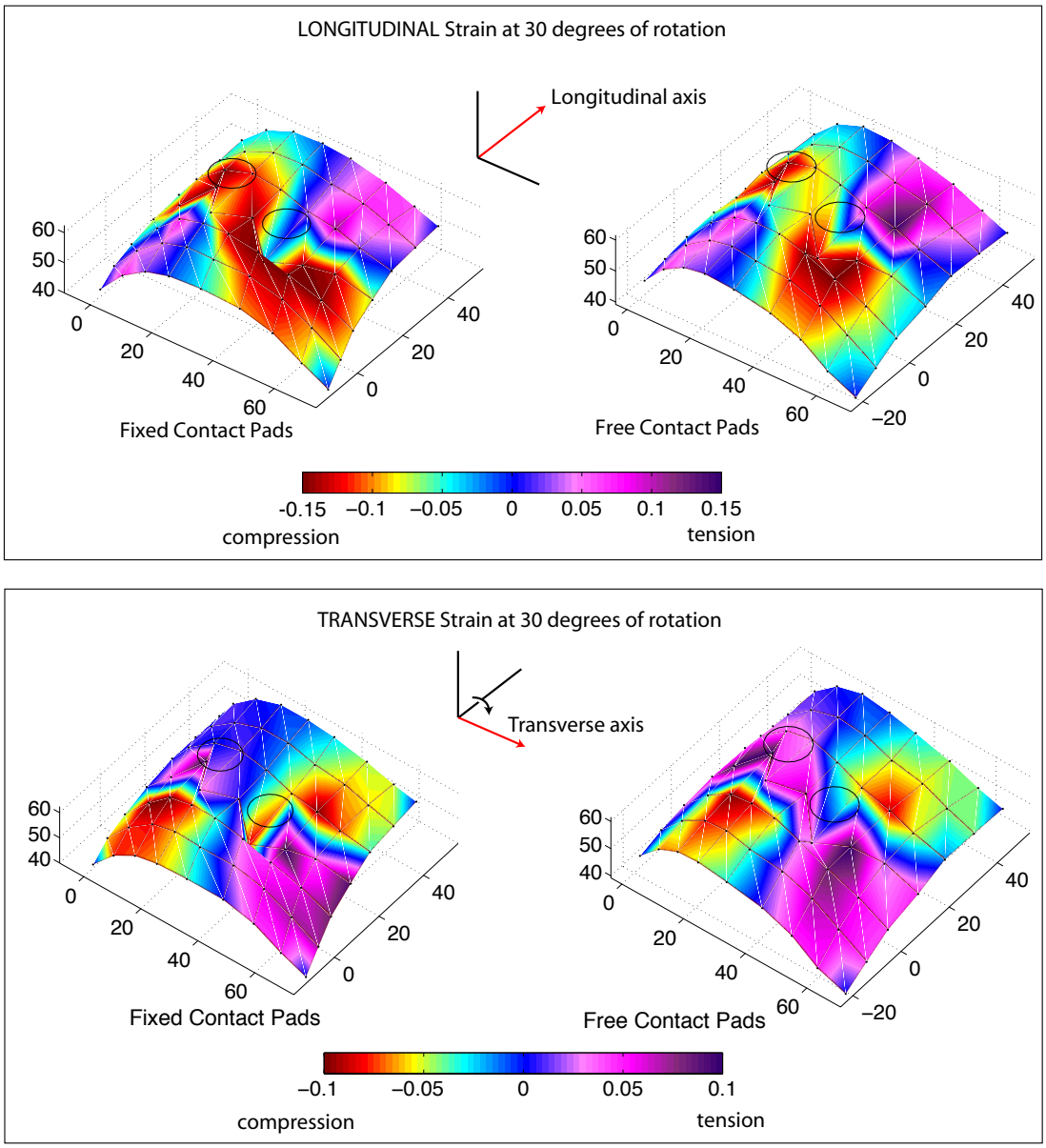

Figure 4.10: Surface strains measured at 30 degrees of rotation. End effector rotates clockwise.

Strain Energy

As the direction of the receptors is unknown, perhaps a better parameter to examine is the strain energy of the system. It has been suggested that some mechanoreceptor activity correlates best with strain energy density [26, 103], as strain energy is independent of direction yet is still a scalar measure of strain activity at a given location. If this is true, stain energy should also correlate with our perceptual observations that users are able to distinguish rotations of stretch with greater accuracy using the fixed end effectors. A plot of the overall surface energy of the surface of skin is seen in Figure 4.11. The strain energy of the system is estimated using the relationship from [4] and seen in Equations 4.3 and 4.4, where U is the total strain energy of the system. In order to estimate the stresses , σ_x, σ_y and τ_{xy}, using the strains, the relationship in Equation 4.1 is used, where a Poisson's ratio of $v = 0.5$, and a Young's Modulus, E, of 420 kPa [2] are assumed.

$$\begin{bmatrix} \sigma_x \\ \sigma_y \\ \tau_{xy} \end{bmatrix} = \begin{bmatrix} \frac{1}{E} & \frac{-v}{E} & 0 \\ \frac{-v}{E} & \frac{1}{E} & 0 \\ 0 & 0 & \frac{1}{G} \end{bmatrix} \begin{bmatrix} \epsilon_x \\ \epsilon_y \\ \gamma_{xy} \end{bmatrix} \tag{4.1}$$

$$G = \frac{2}{E(1+v)} \tag{4.2}$$

$$dU = \frac{1}{2}(\sigma_x \epsilon_x + \sigma_y \epsilon_y + \tau_{xy}\gamma_{xy}) \tag{4.3}$$

$$U = \frac{1}{2}\int_V (\sigma_x \epsilon_x + \sigma_y \epsilon_y + \tau_{xy}\gamma_{xy}) dV \tag{4.4}$$

Because the material properties of skin are difficult to characterize, the choice of modulus is somewhat arbitrary. Therefore, what is important is not the magnitude of the strain energy presented here, but rather the changes in strain energy with rotational displacement and the relative difference between the two cases. It is clear

that the fixed end effectors result in greater amounts of strain energy overall. It is possible that in our studies, the difference in strain energy had an overall effect on our perception caused by increased mechanoreceptor activity when using the fixed end effectors. The differences between the two cases are more clearly seen in the surface plots of the individual components of strain energy in Figure 4.12. Here, it is clear that the strain energy at points located near the contact pads differs more in magnitude, which correlates with the strain estimates, as that is where the largest differences in strain occur.

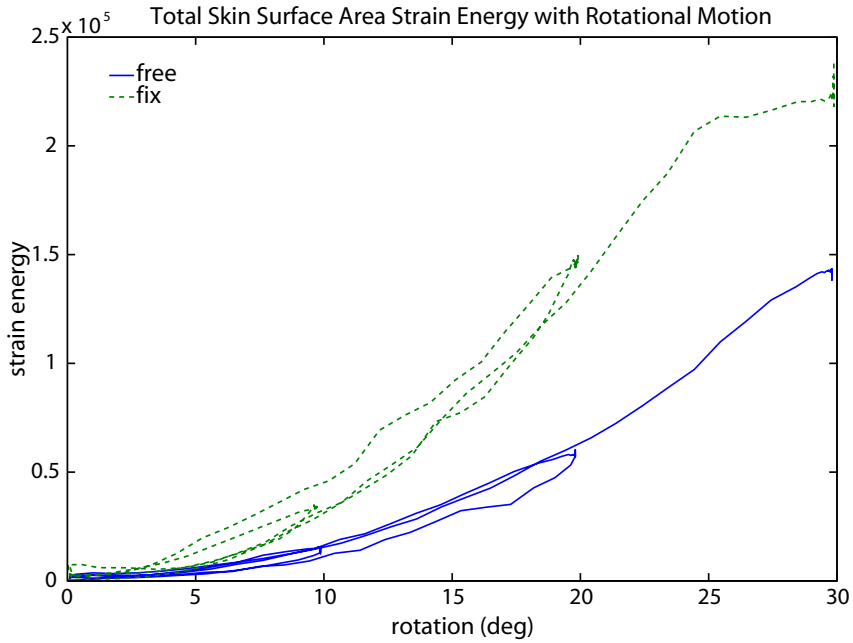

Figure 4.11: Total strain energy of measured skin surface as rotational stretch is applied.

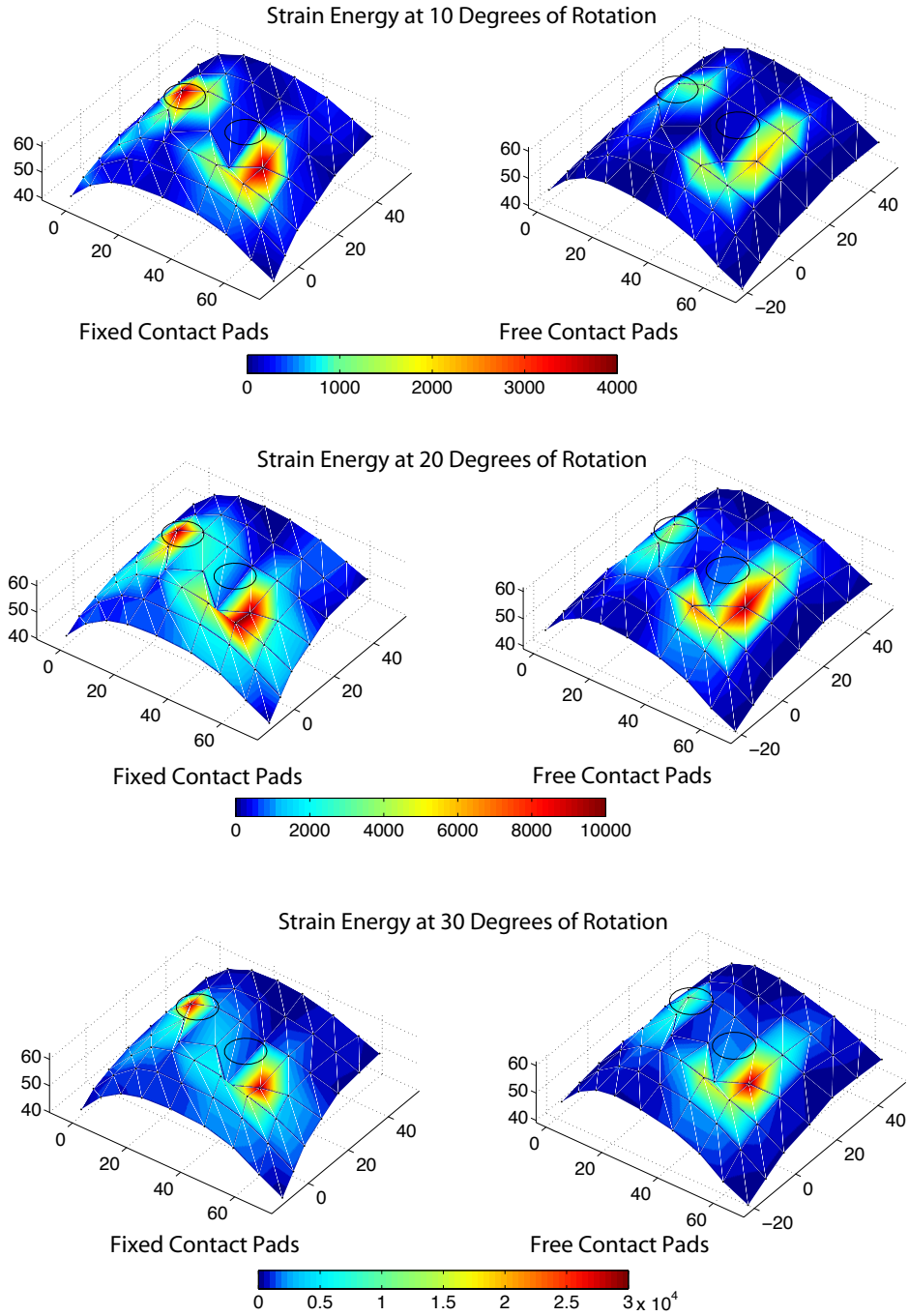

Figure 4.12: Strain energy of each point as pads rotate to 10, 20 and 30 degrees. End effector rotates clockwise.

4.3.3 Torques

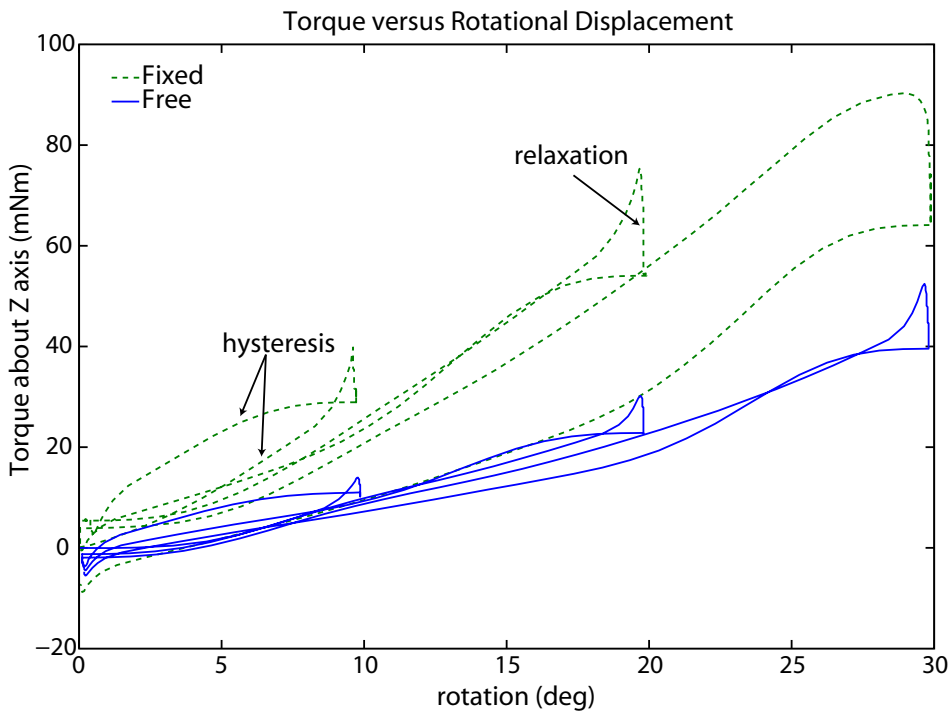

Figure 4.13: Torque measured as a function of rotational displacement.

Another measure of intensity is the torque required to produce a given rotational displacement. As seen in Chapter 3 with the linear and rotational stretch measurements, the forces applied to induce skin stretch varied greatly between methods, and appeared to correlate with the perceived magnitude of the stimulus. The comparison between these two methods of skin stretch follows the same pattern. Using the ATI Nano17 force sensor, the primary measurement of interest was the torque about the z-axis, or the torque necessary to rotate the skin. The torques measured as a function of rotational displacement can be seen in Figure 4.13, where relaxation and hysteresis characteristics are noted. As the skin reaches its desired rotation and remains stationary, the torque drops rapidly then slowly relaxes over a longer period of time. Hysteresis effects are less pronounced at higher rotations of stretch; the

changes in torques applied when ramping to 30 degrees and back to zero occur due to movements from the user that are detected in the motion capture analysis. This movement was observed after the device had reached 30 degrees. These results also correlate well with our strain energy observations as the energy is correlated to the work put into the system [4], which is also related to the torque and displacement of the system.

4.4 Conclusions

As evidenced by this analysis, there are a variety of factors that may cause the perceptual differences between the fixed and free rotating contact pad configurations. Different displacements, energies, and torques are observed in the fixed contact case, all of which may contribute to heightened perception. A combination of these factors induced at regions near zero degrees of stretch are important for subjects to perceive skin stretch accurately; but at high rotations, these factors cause discomfort to the user, and users prefer the free rotating contacts. It is possible that a combination of the two designs would produce an even more effective method of inducing skin stretch, where performance does not degrade at low rotations, but comfort is increased at high rotations.

Chapter 5

Skin Stretch Perception

As discussed in Chapter 2, the determination of absolute and difference thresholds is central to understanding our abilities to interpret sensory feedback. Absolute thresholds are the minimum stimulus levels necessary to perceive the stimulus while difference thresholds represent the minimum difference necessary to distinguish between two signals. Absolute or detection thresholds are typically the first parameter of interest when designing stimuli. However, it has been shown in previous work that humans are remarkably adept at detecting lateral skin stretch (see Sections 5.1.2 and 2.2.1), for movements as small as 0.13 mm. The skin stretch stimulus designed in these studies is large scale deformation, with strains up to 40%, far exceeding the detection threshold. Therefore, what was more relevant was determining the difference threshold of skin stretch. Determining the difference threshold provides a sense of our resolution of skin stretch detection, aiding in the design of skin stretch stimuli for practical applications.

Psychophysical studies, while useful for understanding our sensory abilities, are typically conducted under highly controlled environments. Outside distractions such as noise and visual aids are eliminated to focus on the pure tactile perception. This of course is unrealistic for practical applications. Therefore, another set of studies were completed to determine the feasibility of using skin stretch feedback in a more

practical setting. User studies to assess the ability of subjects to detect the rotational orientation of the skin stretch device end effectors using the wearable device were completed. This set of studies provide a better understanding of the types of applications rotational skin stretch is best suited for. Both the psychophysical and practical perception studies are discussed in this chapter.

5.1 Previous Work

Prior work regarding our perception of relevant haptic stimuli is presented here. Though little is known about our perception of skin stretch, we can use our perception of vibration as a baseline to place the results of our studies into context for the haptics community.

5.1.1 Vibrotactile Stimuli

In contrast to skin stretch stimuli, extensive research has been completed to characterize our perception of vibration, studying the effects of stimulus waveform, contact area size, frequency, amplitude, and various other factors. Jones and Sarter provide a comprehensive summary of relevant findings [62], covering the last 60 years of research on vibrotactile stimuli to aid in designing tactile displays. A brief overview is provided here.

Vibrotactile stimuli are characterized in terms of the frequency and amplitude of stimulation and the effects of changing both these parameters on our perception of vibration has been well documented. However, variations in results are evident and are attributed to differences in experimental conditions and methods, choice of stimulus waveform, and size of contact area [59,80]. In general [62] humans are most sensitive to frequencies in the 150-300 Hz range, though it varies slightly relative to the region of the body where the stimulus is applied. For example, humans are most sensitive at their fingertips, less sensitive on their forearms, and least sensitive in their

abdominal and waist area. This trend is even more apparent in the human ability to detect amplitudes of vibration, where detection thresholds vary considerably more. The amplitude for detecting vibration at any frequency varies from 0.07 μm to 4 μm [130].

Vibrotactile difference thresholds have been studied considerably less than detection thresholds due to the difficulties in modulating changes in frequency and amplitude. As the amplitude of vibration increases, even though the frequency is constant, there is a perceived increase in frequency [88]. In addition, perceived frequency varies greatly across different regions of the body. Jones and Sarter produce a chart summarizing the findings of several studies to determine vibrotactile difference thresholds (see Figure 5.1). Here it can be noted that differences in measurement technique and environment may cause variation in threshold results, as there is a large discrepancy in difference thresholds at the finger. Frequency discrimination thresholds are typically presented as a normalized function of the reference frequency, $(\Delta F)/F_{ref}$, where (ΔF) is the frequency difference threshold in Hz, and F_{ref} is the reference frequency.

Frequency difference thresholds for the forearm range from approximately 0.2 to 0.4, where the thresholds are higher at lower frequencies [80]. Changes in amplitude can also be used to vary vibration intensity. Though there are variations in data, in general, amplitude based difference thresholds decrease with increasing stimulus intensity [59]. Though the sensation of skin stretch is markedly different from vibration, we can use this knowledge to gain an idea of the variations in skin stretch perception with respect to amplitude, frequency, and location.

5.1.2 Skin Stretch Absolute Threshold

There is very little in literature that characterizes a human's ability to distinguish and detect different levels of skin stretch, with the exception of Norrsell and Olausson [94–98], who have completed research to determine detection thresholds of skin stretch

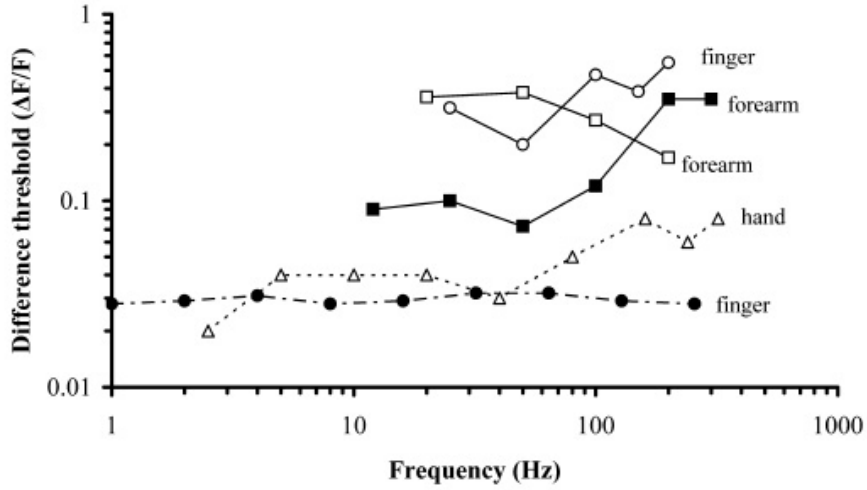

Figure 5.1: Vibrotactile difference thresholds as a function of frequency for pulses delivered to the forearm (filled squares, Rothenberg [107] ; open squares Mahns [80]), the finger (filled circles, Franzen & Nordmark [39]; open circles, Goff [50]), and the hand (triangles, Mowbray & Gebhard [90]). Figure taken from Jones [62].

.

on the forearm (0.13 mm). Skin stretch perception and sensitivity can be dependent on the location of stretch, the size of the contact point that induces the stretch, the normal force applied, the method of attaching the stretch applicator, and the number of contact points (see 2.2.1). In addition, most studies with skin stretch involve only a single contact point that moves linearly [95, 97] or twists [2, 38], yet our method uses a two point rotational motion to produce stretch. Though there are no studies that have determined the detection threshold of rotational skin stretch, the scale of movements for our purposes far exceed the detection thresholds, eliminating the need to perform a full scale absolute detection threshold study.

5.2 Difference Thresholds

How different does a stimulus have to be before we notice it is different from the previous one? What is the resolution of rotational skin stretch? Two different factors

could influence our perception. First, from prior observations, the velocity of skin stretch seems to play an important role in our perception. Pilot studies shows that subjects could easily detect changes in stimuli (sensing motion), yet felt no difference in stimulus magnitude. Second, the difference threshold may change as a function of the reference stimulus. For example, is it different at 10 degrees of rotation versus 30 degrees of rotation? Experiments to determine the effects, if any, of these main factors were completed.

5.2.1 Methods

Participants

Twelve subjects (4 female, 8 male) participated in this experiment. Four of the subjects were familiar with rotational skin stretch, while the remaining eight subjects were naive and had never used a skin stretch device previously. All participants volunteered for the study and experiment protocols followed the guidelines set by the Stanford Research Compliance Office (IRB Protocol 13172).

Device and Stimuli

The second benchtop skin stretch device (Figure 3.13) was used in these experiments.

To determine what effect the velocity of rotation and reference position had on the difference threshold of rotational skin stretch, 2 different reference positions and 2 reference velocities of rotation were chosen. A relatively low rotation of 10 degrees and a higher rotation of 30 degrees were chosen. 10 degrees of rotation produces relatively low magnitude sensations, yet is well above the absolute detection threshold. In pilot studies, the maximum amount of preferred rotation ranges from 35 to 40 degrees, therefore 30 degrees of rotation represents a stimulus near the absolute maximum threshold with relatively high magnitude sensations. Reference velocities of 20 deg/sec and 80 deg/sec were chosen as slow and fast velocities of skin stretch respectively.

Experiment

A three-interval, one up three down adaptive procedure was used to estimate the difference thresholds of rotational skin stretch (Figure 5.2). This method has been used previously [76, 114] for force discrimination and was determined to be the most time efficient method of data collection (see Section 2.4.3).

At the beginning of each trial, the subject is presented with three stimuli. Two are the reference position while the third is a stimulus greater than the reference, deemed the comparison stimulus. The three stimuli are presented in random order and the subject is asked to indicate which of the three is the test stimulus by indicating "1", "2", or "3" through a computer input. When a subject correctly indicates the test stimulus three times in a row, the magnitude of the test stimulus is decreased. If a subject incorrectly identifies the test stimulus, the magnitude is increased. For each session, the test stimulus begins at a value 4 degrees greater than the reference stimulus. The test stimulus is then decreased by 1 degree for the first three reversals. Afterwards, the test stimulus is decreased by an increment of 0.25 degrees. The test stimulus is increased at a larger rate early on to help reach convergence faster. The session is over after a total of fifteen reversals, where a reversal is any point the comparison stimulus changes from decreasing to increasing or vice versa. The first three reversals are used as practice trials and the last twelve reversals are used in data analysis.

To reduce bias these sessions for the various trials are typically interleaved, however in our case, when interleaving the reference positions, the time taken to complete the experiment increased beyond 60 minutes. Data from pilot subjects indicated that concentration was difficult to maintain over a period of time greater than 30 minutes, biasing the results. To reduce the time of the experiment and ensure that fatigue would not be an issue, it was decided to run each trial separately. This resulted in 4 separate sessions each consisting of 60 to 100 trials, lasting between 20 and 30 minutes (varied between subjects). Only a single session of data was recorded per

day, so data for each subject were collected over 4 days. In addition, to prevent the subjects from using audio cues of the motor to bias their results, headphones were worn throughout the experiments.

Stimulus

Typical haptic feedback stimuli can simply be turned "on" or "off" instantaneously; however, skin stretch is unique in its ability to convey both a velocity and static position at once. When testing a subject's ability to discriminate between two different stimuli, there are a variety of factors the subject can utilize to determine the difference. The purpose of the experiment was to determine the discrimination threshold in degrees of skin stretch. However, when applying skin stretch at constant speed, it is possible for participants to simply use their sense of timing to determine which stimulus is different. It was unclear whether subjects were able to use their sense of timing to determine which of the three stimuli was greater than the reference. To eliminate the ability of subjects to simply use timing, the duration of all three stimuli presented during each trial was kept the same. Therefore, as the test stimulus increases, the velocity of stretch increases. For example, at a reference of 10 degrees and velocity of 20 deg/s, the time taken for the stimulus to reach its final position is 0.5 seconds. Therefore, for a test stimulus of 14 degrees, the time to reach 14 degrees is kept constant at 0.5 seconds, resulting in a velocity of 28 deg/s, a 40 percent change in velocity. At 30 degrees and 20 deg/s, the total time is 1.5 seconds. A test stimulus of 34 deg is ramped up at a velocity of 22 deg/s, a 13 percent change in velocity. When two stimuli were close, the velocity of stretch was nearly equal. Though the change in velocity may be evident to the subject, because in a real application the subject would be able to use their sense of velocity to interpret the stimulus, the ability of subjects to use velocity sensing was maintained.

5.2.2 Data Analysis

For each subject and for each of the 4 trials, the peak and valley pairs occurring at a reversal were calculated. A peak reversal occurs when the test stimulus level changes from increasing degrees to decreasing, and vice versa for a valley reversal. These points in the data can be seen graphically in Figure 5.2. These peaks and valleys are then grouped into peak/valley pairs and averaged. The last six pairs are used in the data analysis. The mean threshold and standard error are determined from the six averages. This results in 6 samples per subject, per condition. These 6 samples are then averaged to determine an average discrimination threshold [114]. Repeated measure analysis of variance (ANOVA) with pairwise comparisons was then performed to analyze the effects of both velocity of skin stretch (20 and 80 deg/s) and reference position (10 and 30 deg).

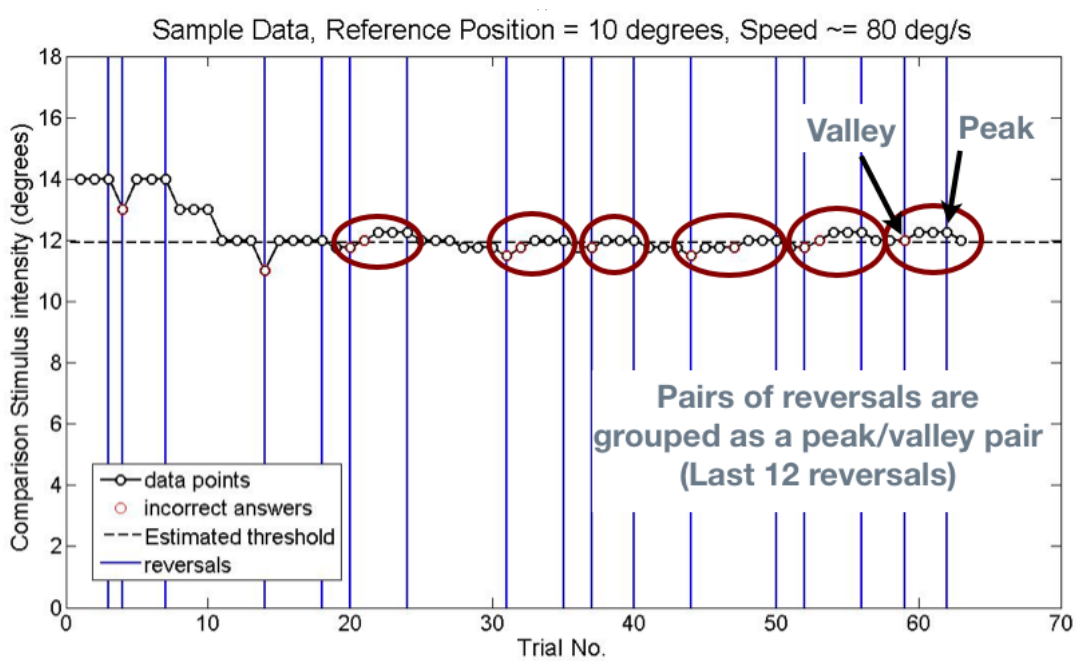

Figure 5.2: JND Data analysis- peaks and valleys used to determine discrimination threshold.

5.2.3 Results

The reference position had a significant main effect on the difference threshold (F = 21.979, p = 0.001), yet surprisingly, no signicant main effects were found due to velocity (F = 2.955, p = 0.114). This also validates our approach to keep the total duration of the stimulus constant while varying the velocity, as the changes in velocity likely had no effect on the subject's performance. At a lower reference stimulus of 10 degrees, the discrimination threshold was lower than at 30 degrees. However, changing the speed from 20 to 80 deg/s appeared to have little effect on subject's ability to discriminate between stimuli (Figure 5.3). The difference threshold is presented as a Weber Fraction (WF), $\Delta Deg/Deg_{ref}$, where ΔDeg is the difference between the threshold and reference stimulus and Deg_{ref} is the reference stimulus. On average, at a reference of 10 degrees, the discrimination threshold was 2deg, while at a reference of 30 deg, the discrimination threshold was significantly higher at 4 deg, resulting in WF's of 0.205 and 0.125, respectively.

A closer look at individual subject data indicates that subject to subject variation was high (Figure 5.4). However, it can be seen that though the variation between subjects was high, the general pattern of decreasing weber fractions with increasing stimulus intensity held true for most subjects.

Finally, the torques that were applied to the skin were measured for three subjects. The data in Figure 5.5 represents the torques measured from just one subject when the reference stimulus was 30 degrees and the nominal angular velocity was 80 deg/s. Though the actual measured torque for each subject varied, all three showed similar trends of decreasing stiffness as the trials progressed. It is clear that the torque applied decreased significantly over the course of the experiment, which was approximately 20 minutes. Interestingly, this appeared to have no effect on the discrimination threshold as there were no signs of increasing comparison stimulus levels due to decreased torque.

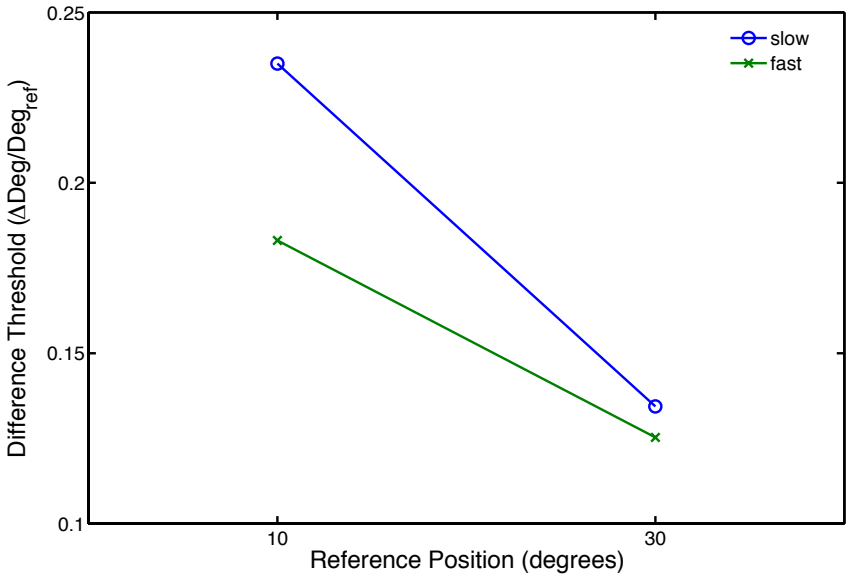

Figure 5.3: Difference thresholds for all subjects at the two different reference positions. The blue line (with open circles) is for slow rotations (20 deg/s) and the green line (with "x" symbols) is for faster rotations (80 deg/s). Changing the rotational velocity does not have a strong effect on difference thresholds, but as the reference stimulus level increases, the Weber Fraction decreases.

5.2.4 Discussion

Though subjects were in general able to discriminate between stimuli with higher resolution at 10 degrees of stretch compared to 30 degrees of stretch, subjects also tended to report qualitatively that they felt they were overall, less sensitive to the stimulus at lower rotations of stretch. The trend of higher weber fractions at smaller reference stimuli does follow observed psychophysical trends with other types of stimuli such as vibration [59, 62, 80] as discussed in the beginning of this chapter. One factor that may have contributed to the subject's perception was the ability to detect a change in velocity. Because we were initially concerned with the ability of subjects to time the duration of the stimulus, as explained previously, the velocity of the test stimuli varied in order to keep the duration of the stimuli constant. At a reference of 10 degrees at 20 deg/s, a test stimulus of 14 degrees would move at

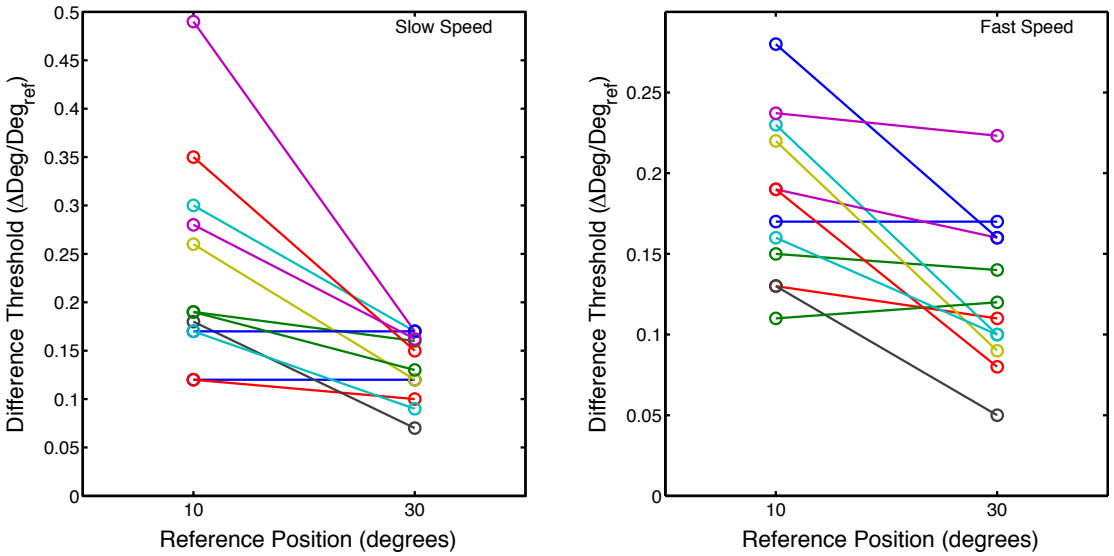

Figure 5.4: Individual subject discrimination thresholds. Each line represents one subject. The plot on the left is thresholds taken at slow rotations, and the plot on the right is for faster rotations. Though variation is high, in general subjects have smaller weber fractions at 30 deg.

a speed of 28 deg/s, a change in 8 deg/s. However, at a reference of 30 degrees at 20 deg/s, a test stimulus of 34 degrees would move at 22.67 deg/s, a change of only 2.67 deg/s. It is possible that subjects were able to subconsciously detect changes in velocity as well as change in overall stimulus level to help them determine which of the three stimuli was the test stimulus.

To explore this hypothesis, the study was repeated for a few subjects where changes in velocity were more difficult to detect. One method of hindering the subject's ability to use the velocity portion of the stimulus is to test the stimuli at very high speeds, where changes in speed are more difficult to detect. For two subjects, the trials were repeated using a high speed (200 deg/s), but results and trends were similar to their previous individual results. The other method of removing the sense of velocity is to move the stimulus at a very slow speed, where the rate of skin stretch is imperceivable. This would require moving the stimulus at a speed less than

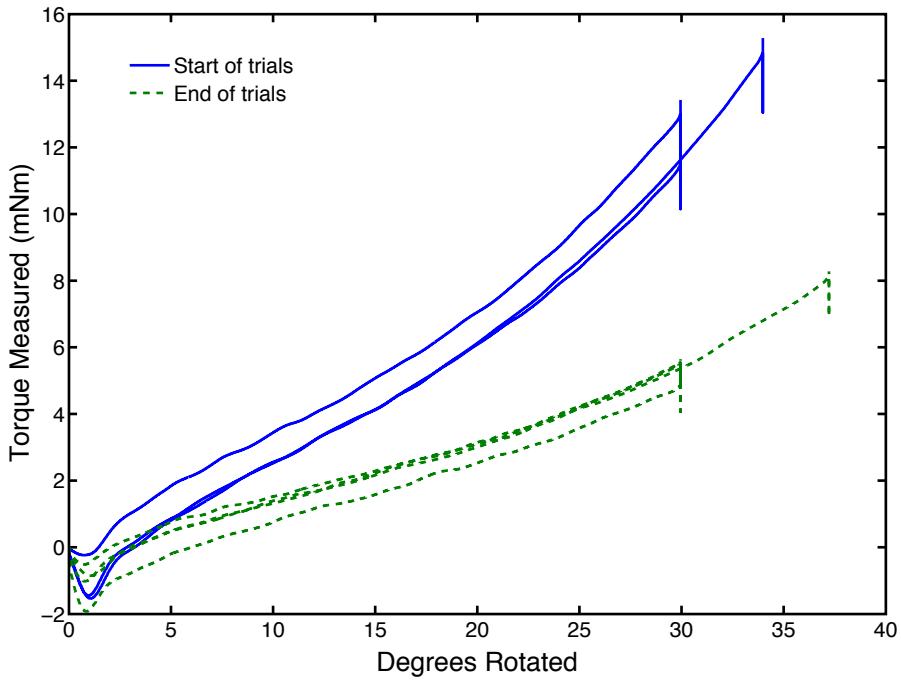

Figure 5.5: Variations in torque measured during the experiment. This is the torque measured from one subject during one of the four trials (Ref = 30 deg, Speed = 80 deg/s). The solid blue lines indicate torques measured at the beginning of the trial and the dashed green lines indicate torques measured at the end of the trial, after approximately 20 minutes.

1 deg/s, close to 0.5 or 0.25 deg/s. However, to do so, this would increase the time of the experiment greatly and fatigue would again be a factor. It is also very unlikely that in a practical application, the stimulus would move at such a slow speed and subjects will be able to use their sense of the rate of stretch to perceive rotations. So while it is possible that subjects are simply detecting changes in velocity in addition to static position, in practical applications this is not an issue, as subjects should use whatever strategies are available to them to decode the stimulus signal. Another approach to hinder a subject's ability to use the velocity and dynamic portion of the stimulus to determine the static location is to use non-constant speeds and also move

in a quasi-random path before coming to rest at the desired stimulus level. Studies using these strategies were not completed, but may provide insight into what portion of the stimulus is important for users.

It is also interesting to note the change in torque that occurred throughout the experiments. Either the skin properties change over time, which would not be surprising, or there is significant slipping occurring at the contact site. It is unclear which of these factors dominates the change in torque measurement, yet regardless of which of these factors influence the outcome more, neither appears to have biased the results in any way. If users were purely sensing torque, one would expect the comparison stimulus level to increase, as the torques applied were decreasing while the experiment progressed. However, no such pattern was detected in any of the subjects. Though there may be areas of fatigue occurring near the end of the trials, there are no clear patterns or trends that would lead us to believe the change in torque was significantly influencing the user's response. One reason why this method may have been robust to these changes in torque is that subjects were asked to compare three stimuli. If the subjects were asked to report the perceived magnitude with no reference stimulus, it is possible that the changes in torque would effect the outcome.

It should be noted that the results of this study do not indicate a full scale resolution of rotational skin stretch, nor would subjects be able to perceive differences of 2 degrees of skin stretch in a practical setting. This study was completed in an isolated environment and only tested our ability to distinguish comparison stimuli that were greater than a given reference. To prevent fatigue, each trial also only tested one reference stimulus and subjects could easily learn and memorize the reference stimulus. In a more practical setting, the stimulus is constantly changing, hindering the subject's ability to discriminate between stimuli. This study provides a best case scenario resolution but a different study to determine the true ability of users to use skin stretch feedback was necessary to test the practicality of the feedback and is described in the following sections.

5.3 Absolute Positioning

To determine the feasibility of using the feedback in a more practical setting, a user study was done to assess the ability of subjects to detect the rotational orientation of the skin stretch device end effectors. If subjects are able to detect the orientation of the end effector, the feedback could be used to convey position and motion information of an external object. For example, for a person driving a car or truck, we could present the distance of the nearest car behind them (assuming vision is either obstructed or devoted elsewhere). Or, as mentioned previously, subjects can use skin stretch feedback to position a robotic arm or a prosthetic device. A set of user studies assessed the ability of subjects to detect the rotation of the skin stretch device. The wearable skin stretch device was used for this set of studies. In addition, the difference in performance between the two end effector designs as described in 3.3.3 was studied. The following sections describe experiments conducted to determine how well subjects could use the feedback *actively* and *passively*. In the former case, subjects used the device to provide feedback for desired motions; in the latter case they were asked to assess the magnitudes of arbitrary amounts of skin stretch imposed on them. Previous research indicates differences in perception resulting from the different modes of touch [78], in which subjects have better accuracy with active touch. The results of these studies provide a preliminary indication of how accurately users can interpret the feedback to position an external object or interpret the position of an object passively, providing insight into which practical applications and interaction methods this feedback is best suited for.

The studies were repeated using both fixed and free end effectors in random order for a total of 4 data sets. The active control study was always completed prior to the passive study. Ten subjects overall (3 female, 7 male) were tested, and all subjects completed both studies. Ages ranged from 22 to 37, with a mean age of 27.5. The studies were approved by Stanford's Institutional Review Board (IRB Protocol 13172).

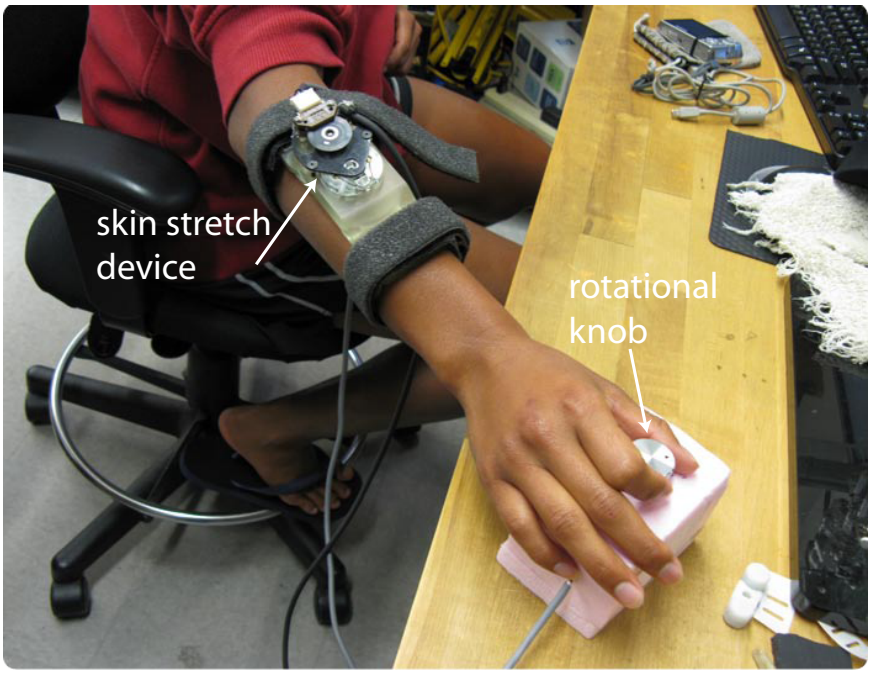

Figure 5.6: Wearable skin stretch device and knob used to control rotation of the device or input perceived positions.

5.3.1 Methods

In all studies, the device was placed on the outer forearm as shown in Figure 5.6. The two contact pads were placed across the narrow width of the forearm. This location was chosen due to the relative high density of slow adapting mechanoreceptors [122].

Training

A training procedure was first performed to determine the appropriate range of skin stretch rotations for each subject and to allow them to become accustomed to the feedback. After the device was placed on the subject's forearm, they were given the opportunity to control the motion of the skin stretch device using a small knob. The knob was simply a potentiometer that produced a desired position for the skin stretch end effector where 1 revolution of the knob resulted in 1.4 revolutions of the end effector. During this training period a virtual environment was also displayed on

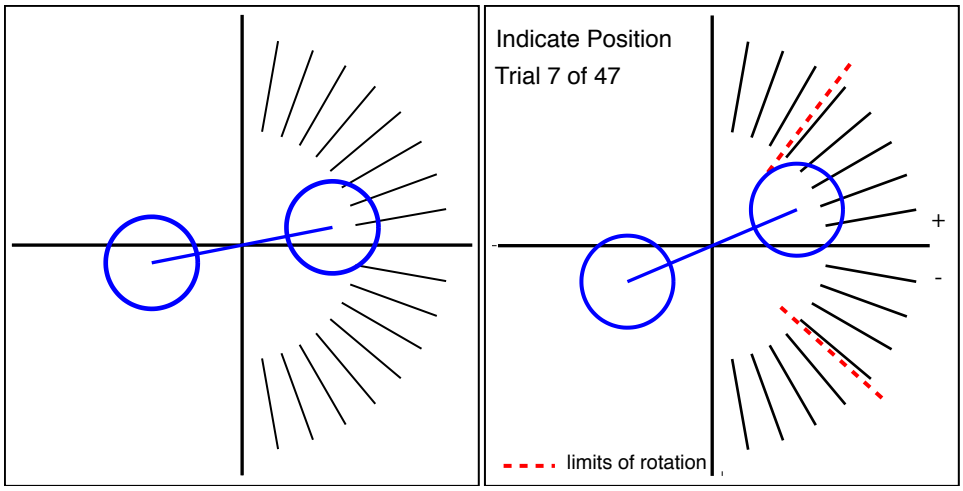

Figure 5.7: Display shown to subjects during trials. The left is the screen displayed during the training phase (showing the actual location) and on the right is the desired location as shown in the experiment trial. Dashed lines indicate the limits of rotation specified during the training phase.

a computer screen, consisting of a dial representing the position of the skin stretch device (Figure 5.7). A line with two circles representing the contact pads is shown to make the display intuitive, correlating the virtual environment with the device end effector. The subjects were instructed to move across the workspace at various speeds and to move the device to the maximum comfortable rotations in both positive and negative directions. Subjects were given as much time as they desired in this training phase though subjects typically spent only 1-2 minutes to complete this exercise. At the end of the trial, the maximum positions in each direction were recorded and corresponding lines were placed on the screen in subsequent trials so that responses were constrained to fall in this range. This training procedure was completed each time the end effector configuration changed.

Active Positioning Study

The purpose of this study was to determine how well subjects could position the skin stretch end effector to a desired rotation. Using the range of motion set by the

subject in the training phase, a data set of desired locations spanning the range in increments of 2 degrees was determined (e.g. a range of -37 to 43 degrees results in a data set of -37, -35, -33...43). Because the data set was dependent on each individual subject's range of motion, the number of trials varied from subject to subject. The desired locations were randomized and displayed visually to the subject. Red lines indicating the subject's specified range of motion were also displayed on the screen to provide the subjects with a reference (Figure 5.7). The subjects were asked to move the skin stretch device to match the position shown on the screen. As in the training phase, subjects were able to control the device using the knob, however the gains were changed such that 1 revolution of the potentiometer resulted in 0.23 revolutions of the skin stretch device. This gain was chosen so that participants would not be able to simply use the proprioceptive sense in their fingers from the training phase to position the device. A push-button switch was used to confirm the subjects' inputs.

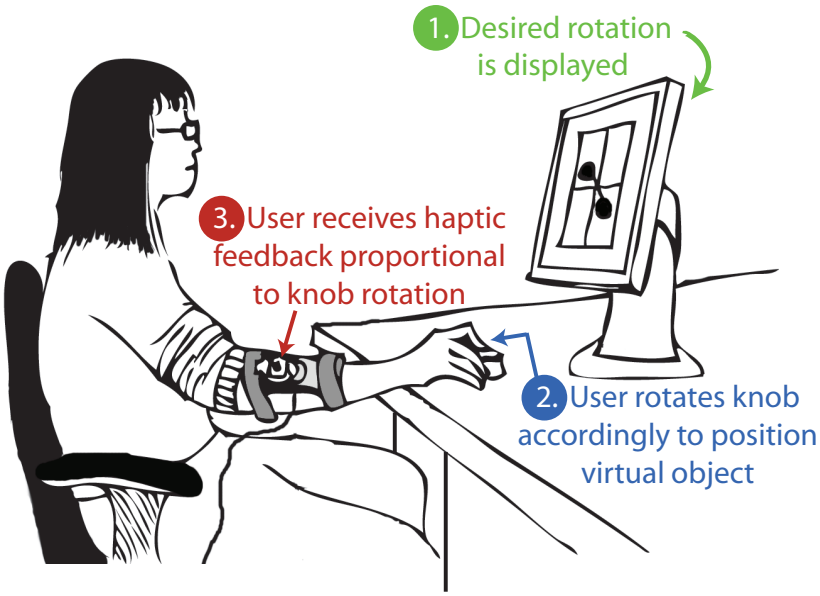

Figure 5.8: Depiction of the active positioning task.

Passive Perception Study

The second study is a perception experiment in which subjects no longer had control of the skin stretch device. In these trials, the device was moved from one quasi-random orientation to another at a random velocity and subjects were then asked to report the perceived orientation. Similar to the positioning study, the data set of commanded end effector orientations spanned the range of rotation set by the user in increments of 2 degrees. The device moved from one position to the next at a speed chosen randomly from [20,40,60,80,100] degrees per second and no visual feedback was provided. The subjects were asked to report the perceived orientation of the end effector by rotating the virtual end effector on the screen with the knob and confirmed the final position input by pressing a button.

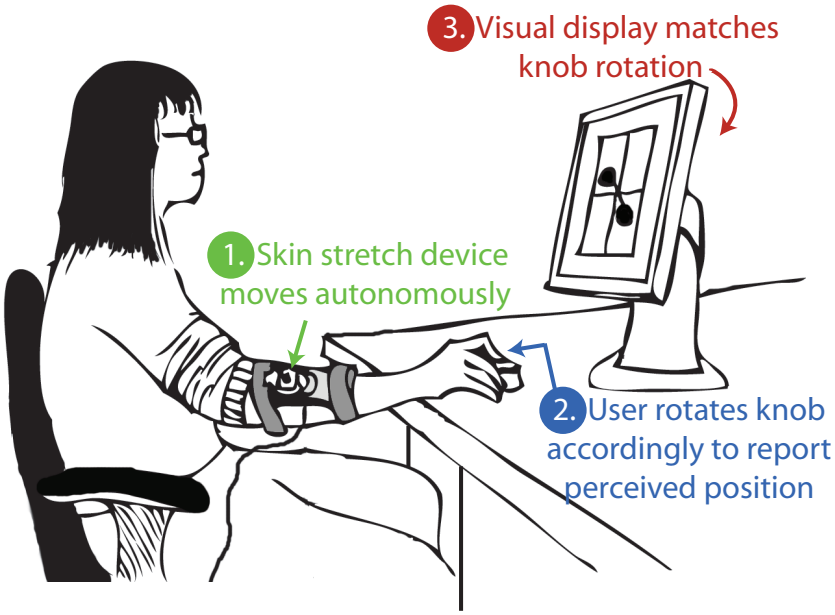

Figure 5.9: Depiction of the passive positioning task.

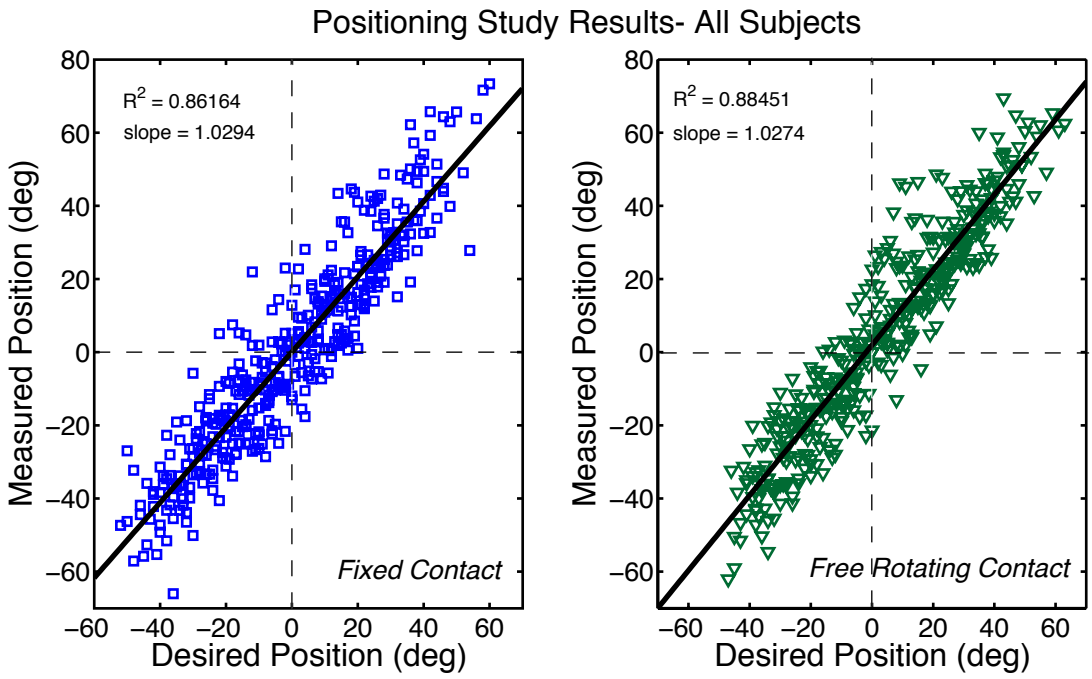

Figure 5.10: Data from all ten subjects in the positioning task.

5.3.2 Results

Active Positioning Study

Figure 5.10 shows the desired orientation versus the measured end effector orientation for all ten subjects, for both the fixed and free end effector configurations. A linear regression on the data is also shown as a measure of how well subjects could use the skin stretch feedback to correlate to end effector position. For both configurations, there is a linear trend to the results with fairly uniform scatter ($R^2 = 0.86$ fixed, $R^2 = 0.88$ free). A total of 393 trials were completed using the fixed end effector, and 407 trials for the free end effector.

Overall, subjects were able to map the skin stretch feedback linearly to the desired position using both end effector designs. The average residual for all ten subjects using the fixed end effector was 5.2 degrees with a standard deviation of 1.4 degrees,

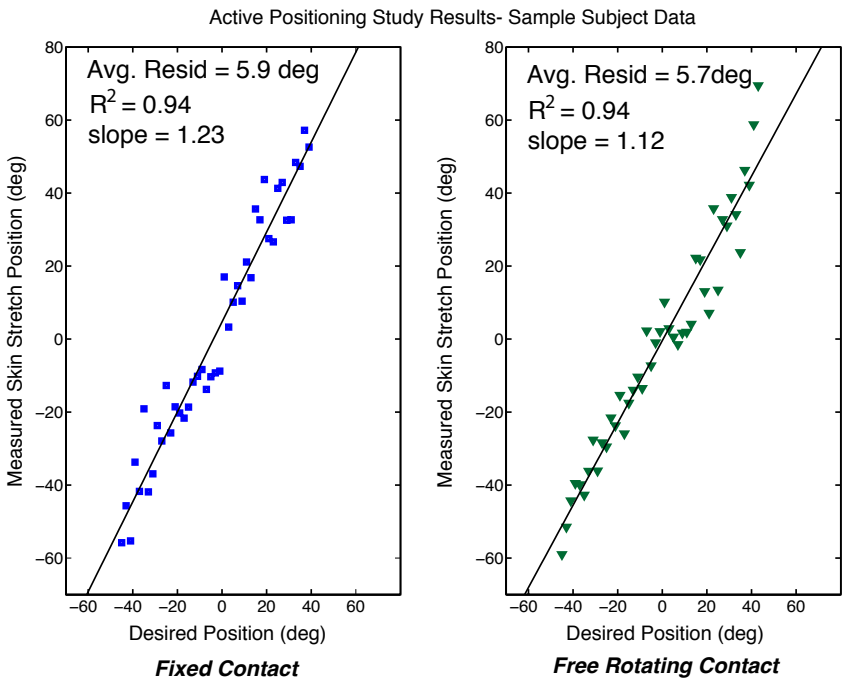

Figure 5.11: Data from one subject in the active positioning task. Residuals do not change for different end effector configurations and average residuals are close to 6 degrees.

and 4.8 degrees with a standard deviation of 2.1 degrees using the free end effector. There is no statistical difference in overall performance (residual or scatter) between the fixed and free end effectors across the ten subjects. Sample data from an individual subject is also provided in Figure 5.11, where it can be seen that individual data does not vary greatly from the overall data. The results of this study indicate that the accuracy with which subjects could position a virtual arm is approximately $\pm 6.5\%$ of their total range of motion when considering both end effector designs. The range of rotation varied between subjects and between end effector configurations, though there was no indication that one end effector design resulted in larger ranges of motion. However, when asked to indicate which of the two designs they preferred, seven of the ten subjects stated they preferred the free rotating contact pads due to the increased comfort. Two stated that there was no difference and only one

subject preferred the fixed configuration. Though it was hypothesized that subjects would have an increased range of motion using the free end effectors, the change in end effector design did not have a significant effect for most subjects. Of the ten subjects, six had a larger range of motion using the free end effector, three had a smaller range and one had an equal range. Linear regression slopes and R^2 values for individual subjects are presented in Table 5.1. Slopes greater than 1 indicate subjects were moving beyond the range of motion set in the training phase.

Table 5.1: Active Task Residuals and Regression Results for Individual Subjects

	Fixed End Effector			**Free End Effector**		
Subject	*Residual avg (deg)*	*Slope*	R^2	*Residual avg (deg)*	*Slope*	R^2
1	5.4	0.85	0.86	4.2	1.16	0.94
2	5.4	0.94	0.94	7.2	1.1	0.87
3	5.6	0.72	0.81	2.6	0.77	0.96
4	5.6	0.93	0.91	3.7	1.15	0.96
5	3.5	0.93	0.97	4.3	0.79	0.96
6	4.7	0.89	0.92	4.9	1.03	0.94
7	3.1	0.81	0.89	1.4	1.49	0.93
8	8.3	0.98	0.89	7.7	0.98	0.89
9	4.5	1.23	0.94	5.0	1.12	0.94
10	5.7	1.31	0.93	4.8	0.96	0.90

Passive Perception Study

Figure 5.12 shows the actual end effector orientation versus the reported end effector orientation for all ten subjects, for both the fixed and free end effector configurations. A weighted linear regression on the data is also shown. A total of 361 trials for the fixed end effector and 376 trials for the free end effector are represented in the plots. It is clear that subjects performed poorly in comparison to the positioning study. Specifically, subjects occasionally had trouble distinguishing which direction the skin stretch device was rotating. Data points located in quadrants II and IV represent

trials in which a direction error likely occurred.

Though most subjects performed comparatively poorly in this task, it was observed that a few subjects performed nearly as well as in the active positioning study. Of the ten subjects tested, three had prior experience with skin stretch feedback. The data from these subjects were grouped together and the results can be seen in Figure 5.13.

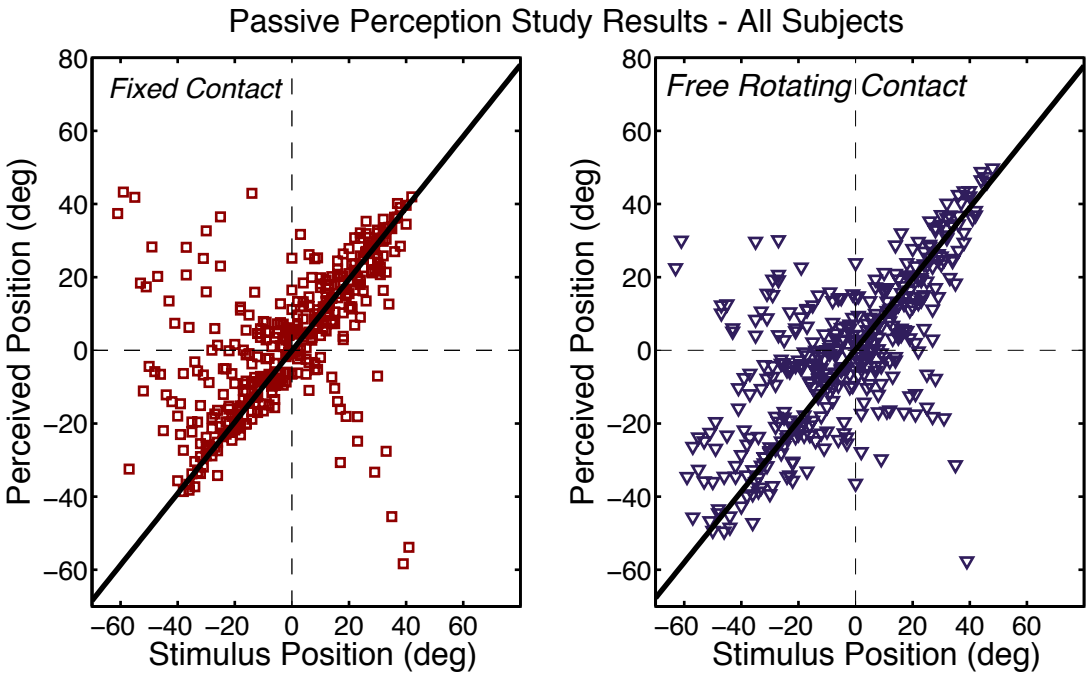

Figure 5.12: Data from all ten subjects in the perception study.

It is clear that subjects with prior experience using skin stretch feedback performed much better than subjects naive to the feedback. It can be inferred that with proper training and time, subjects can learn to use the feedback for an open loop task, when subjects receive information passively. However, the average residuals of the 3 experienced subjects differed between the two end effector designs, ±5.5 deg with the fixed end effector and ±8.1 deg for the free rotating contact. In fact,

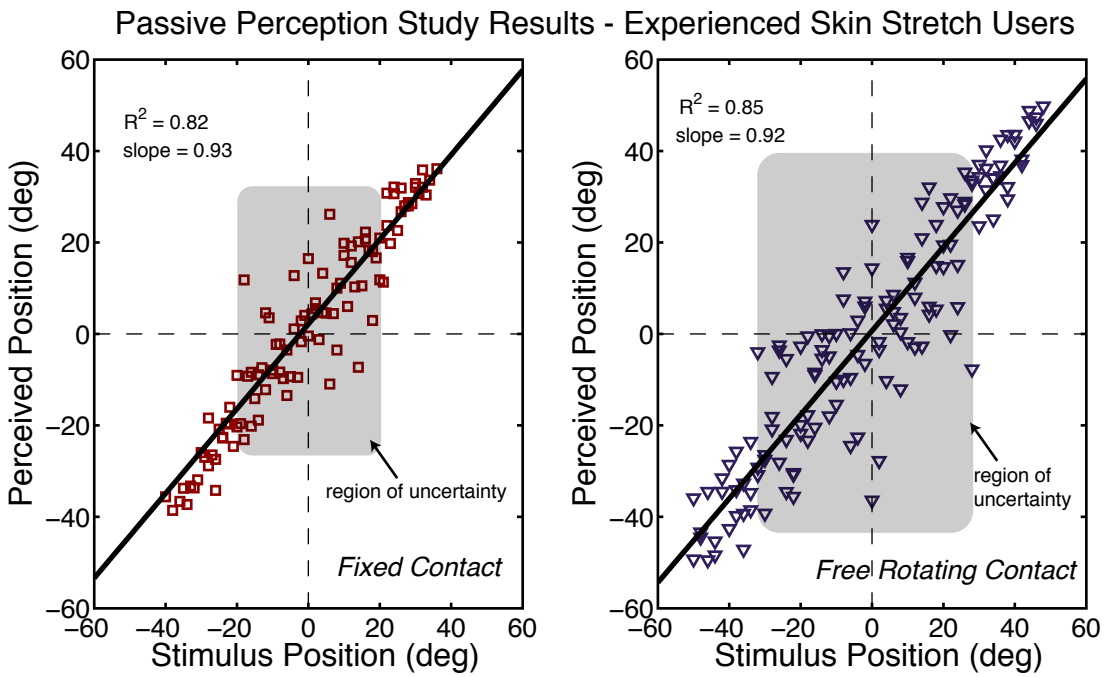

Figure 5.13: Scatter plot of actual end effector position vs. perceived position with regression line for three experienced subjects. Data with the fixed contact are on the left, free rotating on the right.

overall, subjects reported that they felt less confident in reporting the perceived position using the free end effector, particularly in regions of stretch near zero degrees. Looking at the data there does appear to be a region of uncertainty surrounding zero degrees, in which the residuals are larger, suggesting that subjects, on occasion, had difficulty perceiving the stimulus level in comparison to the outer limits of the stretch range. Qualitatively, if we estimate the region of uncertainty to be approximately between -20 and 20 degrees for the fixed end effector, there is indeed a difference between the average residuals within the region and outside (the region is marked in Figure 5.13). The average residual within the region of uncertainty is ± 6.4 deg while the average outside the region is ± 3.0 deg. Similarly for the free end effectors, we can estimate the region of uncertainty to be between -30 and 30 degrees, where the average residual is ± 9.6 deg and ± 5.6 deg otherwise. In both cases, there is a region

of uncertainty in which subjects are less accurate (though this effect is magnified with the free end effector) increasing the average residual.

5.3.3 Discussion

A new, wearable haptic device has been developed to provide users with skin stretch feedback. The relatively compact size and low weight of the device allow for unencumbered user movement and integration into a practical environment. Experiments have shown that the device is effective in closed-loop tasks where the feedback is correlated to user movements or commands. Minimal training is required for subjects to map the feedback linearly to movement of an external object, indicating the device could easily be used in applications to control movement or position. Examples of this type of use are display of kinesthetic or proprioceptive feedback of an arm such as a prosthetic device for an amputee, or motion training applications. Not surprisingly, when the feedback is not correlated to user input, it becomes comparatively difficult to interpret, though results indicate that with sufficient training, users are able to learn to use the device in a passive setting.

When in control of the device, subjects are able to use their own pre-determined methods to reach the desired position. Skin stretch feedback provides a complex combination of velocity, timing, and static force sense which subjects can use to map to a desired position. It is interesting to note that in the active positioning task, there are no direction error outliers as subjects trust that if they command the device to move in one direction, it will in fact, move in that direction. However, when subjects are not in control of the device and stimuli are presented passively, their perception of the direction of movement degrades, and they report that they require a higher level of concentration.

In evaluating end effector design, experimental and qualitative observations indicate that there are benefits and drawbacks to both fixed and free pads. Performance

with both designs was similar in the active studies, though more subjects qualitatively preferred using the freely rotating contact pads due to the increased comfort. In the passive studies, accuracy was measured for experienced users and it was determined that performance decreased using the free end effectors, resulting in larger residuals overall. In addition, the region of uncertainty near zero was found to be greater using the free end effectors compared to the fixed for the passive perception task with higher residuals. No such effect was identified in the active positioning study as subjects could use a variety of strategies to determine the position of the device.

We believe that the free end effector design reduces the shear strains applied near the contact pad, providing greater comfort but at the cost of reducing perceptual resolution. A hybrid design may provide the best combination of comfort at high rotations and increased resolution, with lower residuals, at low rotations in the region of uncertainty. The new design (Figures 5.14 and 5.15) incorporates a compliant mechanism that produces the desired effect. Each contact pad has torsional springs with a preload. For small angles of the device, the pads move as if they are fixed rigidly to the arms. However, as the torque at each pad increases, it overcomes the torsional preload so that the pads start to rotate, approximating the case of freely rotating pads (Figure 5.14). Studies to incorporate the hybrid design and test the device in a more practical setting are underway.

In summary, the foregoing results indicate that while rotational skin stretch feedback may be employed passively for long term applications in which users have significant time to become accustomed to the feedback and learn to utilize it, it is best suited for tasks such as those listed in the introduction, in which an afferent/efferent command loop exists so that users receive skin stretch feedback in response to motor commands. In addition, the discrimination threshold studies indicate that changes in velocity of skin stretch should not effect the ability of subjects to perceive the static position of the device. Experiments to evaluate the effectiveness of skin stretch for this type of application are discussed in the following chapter.

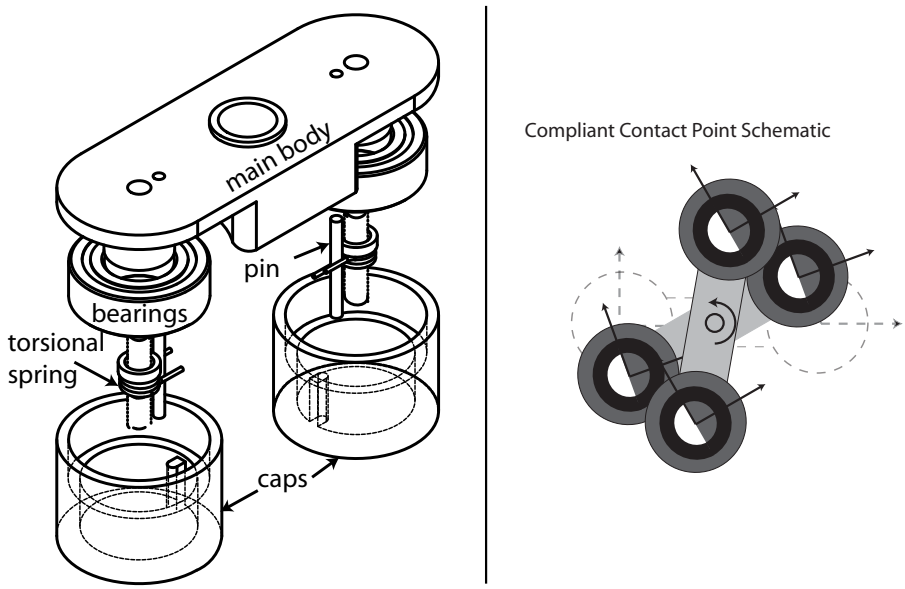

Figure 5.14: Hybrid end effector with torsional springs CAD (left) with schematic to describe achieved motion of contact points (right).

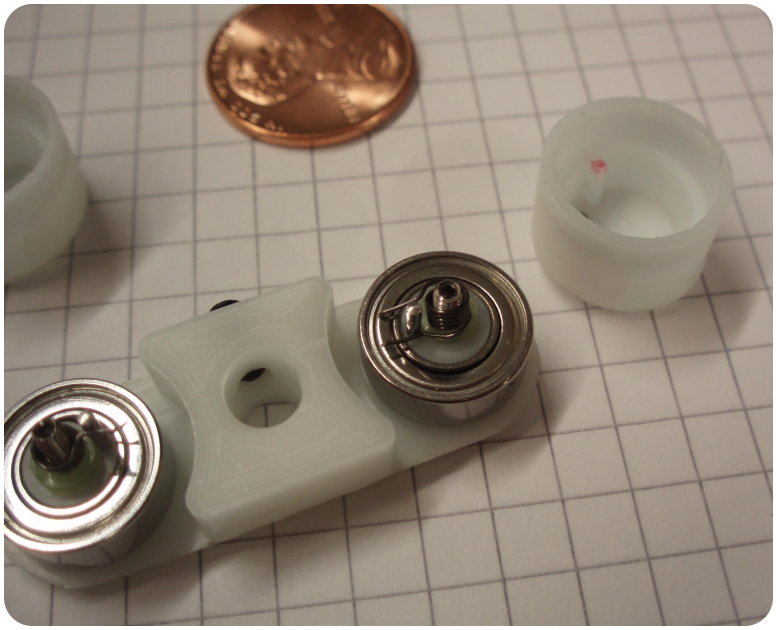

Figure 5.15: Hybrid end effector with torsional springs.

Chapter 6

Skin Stretch for Proprioceptive Feedback

There are many factors that contribute to our sense of proprioception, but one in particular is skin stretch [23, 31, 34]. This observation suggests that skin stretch display could be useful for small, body-worn devices used in motion training for sports, physical rehabilitation or therapy, and other applications where proprioceptive information is valuable. For example, upper-limb amputees are often given myoelectrically-controlled prosthetics in which joint movements are produced when the amputee flexes muscles adjacent to the prosthesis. No position or motion feedback, other than vision, is provided to the wearer and the amputee must visually concentrate on the device to perform precise movements. Other applications where proprioceptive feedback is deficient include people with certain neurological conditions (e.g. stroke, multiple sclerosis) where afferent function is sometimes distorted or largely absent.

In the following sections we describe an experiment in which we compared the ability of subjects to perform blind cursor movements without haptic feedback and with skin stretch feedback. To provide a baseline, simple vibration feedback was also tested. The task is roughly analogous to asking a person to move her hand specified

distances, such as 10 or 20 cm to the left or right, without looking. In the present case, subjects apply forces to a single-axis load-cell held between the fingers. The force input controls a cursor that is attached to a virtual object that, like a human or robotic arm, has position-dependent dynamics.

While there are a number of ways in which skin stretch and vibration could be used to convey information, this study focused on studying the merits of using skin stretch feedback in a more practical setting. It is difficult to make a fair comparison between vibration and skin stretch feedback as neither method was optimized for this study. Instead, the general area of tactile stimulation was kept comparable. Single actuators of comparable footprint on the skin (a few cm^2) and capable of being used continuously, varying the signal to represent position. More sophisticated approaches could be employed that utilize multiple actuators and add discrete event cues. However, in order to make as fair a comparison as possible between the modalities, we constrained the experiment to continuously varying signals with a single actuator in each case.

6.1 Background and Previous Work

6.1.1 Proprioception

As mentioned in Section 1.1, proprioception is the sense of position and movement of body segments not arising from vision [45]. A number of sensory receptors contribute to the proprioceptive sense. The muscle spindles and golgi tendon organs are sensitive to position and movement of muscles and sensors in the joints give a sense of flexion and extension [22, 23]. Mechanoreceptors in the skin, including ruffini endings and merkel cells, also contribute to the sense of motion and position [46, 131]. The brain integrates this afferent information to create a perception of the body segments' position and orientation. In addition, motor commands can create a perceived sensation of movement [44] even if the arm is in fact, stationary.

These phenomena can also be evidenced by the principle of extended physiological proprioception (EPP) as first described by Simpson [111]. EPP refers to the concept that the manner in which a mechanical device is controlled can lead to perceived static and dynamic movements through natural proprioceptive senses. A practical example of this concept is the way in which a tennis player uses his or her racquet as an extension of their arm. The dynamics of the racquet correspond to proprioceptive sensations the player feels through the grip and motion of the arm. As the player learns to interpret the proprioceptive sensations felt through the arm and hand, the player can control the racquet in the desired manner subconsciously [28]. Body controlled prostheses take advantage of this concept and have been largely popular within the prosthetic community [3, 16, 19, 55, 129].

In recent work, the value of proprioceptive feedback has been demonstrated in force-based targeting tasks, improving accuracy even when visual feedback is provided [69]. Methods to create illusory proprioceptive feedback to users have also been studied. Providing vibrotactile stimulation of about 75-100 Hz can create a sense of tendon lengthening [51], however more recent work has also shown that high frequency vibration may be unsuited for proprioceptive feedback as it can also impair acuity in movement detection [128]. Other potential drawbacks of using vibration are that on hairy skin, vibrotactile thresholds are much higher than on glabrous skin (5.1.1). Skin stretch near the joints also contributes to an illusory sense of motion. Collins et al. [23] found that skin stretch contributed to illusory movements at the index finger, elbow and knee and evaluated the relative magnitude of the perceived movements for various combinations of vibration and skin stretch.

6.2 Methods

In the following sections we describe two experiments used to assess the effectiveness of skin stretch feedback for proprioceptive feedback. We first describe a perception study that is used to validate the effectiveness of the stimulus mappings. We then

describe a closed-loop positioning task study in which subjects were asked to move a virtual object without vision under various feedback conditions, which utilized the stimuli from the perception study.

Subjects were asked to perform cursor movements using a single-axis load cell with two strain gauges in a half-bridge configuration, held between the fingers and thumb. The use of a force (versus position) input minimizes the use of the subject's own proprioceptive sense as the load cell replaces actual hand motion. The virtual dynamics of the cursor are described in Section 6.2.1 below. A virtual workspace with a range of motion from 0-10 units was displayed on a computer monitor (Figures 6.1, 6.2). For each task, the cursor appeared at a starting position that was randomly chosen from (3, 5, 7) and the subject was instructed to move 2, 4 or 6 units to the right or left. Movement commands were constrained so that the desired end location was always in the range of 1-9. Subjects could not see the cursor during trials but they were given post-trial visual feedback throughout the experiment (final cursor position and desired position shown on the workspace). Subjects were instructed to attempt to move the desired number of units, stop the cursor, and press a button when they thought the virtual object was brought to a stop. Each of twelve possible combinations of starting positions and movements was repeated three times, for a total of 36 trials.

The experiment described above was performed under four feedback conditions for each subject. First, subjects were tested with no haptic feedback. They were then tested with vibrotactile and skin stretch feedback. Then they repeated the no-feedback trial to evaluate training effects over the course of the experiment. Half of the subjects did the vibrotactile feedback trial before the skin stretch and the others did them in the opposite order. Before each trial, subjects were given training with visual feedback (cursor and workspace visible) for about one minute and then given ten practice trials with post-trial vision feedback, identical to the actual trials. For the no-feedback case, this practice allowed subjects to learn the position dependent cursor-dynamics. In the feedback cases, it allowed them to learn the haptic mapping

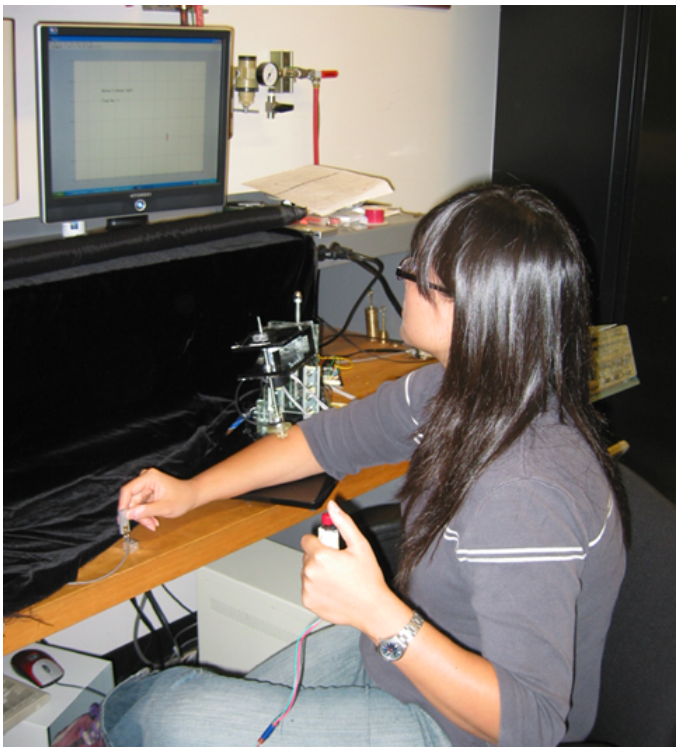

Figure 6.1: Subject completing the task with right arm controlling force sensor and left hand controlling button to end trial.

of the cursor position.

Ten subjects were tested (three female, seven male). Four had little or no experience with haptic devices; the other six had at least moderate experience. The experiment took about one hour to complete.

6.2.1 Cursor Dynamics

In pilot tests with four subjects we determined that if subjects are asked to move repeatedly to a single target, or one of a small number of targets, they often use feedback in a "pattern matching" mode. That is, they move until the vibration or skin stretch feels like it did previously when they were over the target, and then they stop. This way of using the feedback seems closer to an event-cue (event = target reached) than proprioception. Consequently, we revised the experiment to utilize

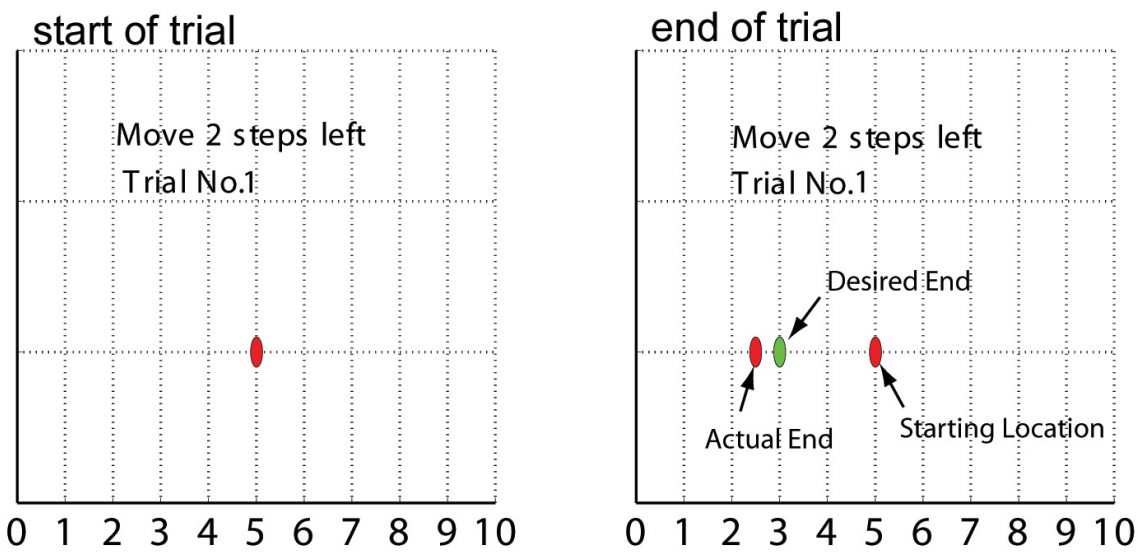

Figure 6.2: Screen shots of experiment task. The left graph shows the screen presented to the subject at the start of each trial. The right graph shows the screen presented to the subject at the end of each trial, showing desired cursor position and actual position to provide post-trial feedback.

varied starting locations and amounts of movement in the left or right direction, as described above.

We also discovered that the virtual object attached to the cursor should have non-trivial dynamics. If the virtual object has a fixed mass and damping, subjects quickly learn open-loop strategies such as pulsing the force applied to the sensor a certain number of times, or applying a steady force and counting "beats," to move the object a desired distance with accuracy. We hypothesize that analogous strategies do not work with human or prosthetic arms in part because the arm dynamics, and the mapping of muscle effort to movement, change continuously as a function of the arm configuration. Accordingly, we gave the cursor an inertia that varies somewhat like the endpoint inertia of a two-link robot arm whose end effector is constrained to move along a single direction in space. The endpoint inertia will be a polynomial involving sine and cosine functions of the position. A simplified approximation is a sinusoid, so that the cursor dynamics become:

$$m(x)\ddot{x} + b\dot{x} = F(t) \tag{6.1}$$

where b is the cursor damping, *F(t)* is the force applied to the force sensor which produces cursor motion, *x(t)*, and *m(x)* is the mass, which varies as

$$m(x) = 6 + 5sin(\frac{2\pi}{10}x) \tag{6.2}$$

The period of the mass variation matches the length of the visible workspace and the maximum and minimum mass are 11 and 1, respectively, with units such that a force magnitude of $F = 1$ and a mass of $m = 1$ result in an acceleration of 1 workspace unit/second^2. The damping was set to a constant value of $b = 10$. (The sinusoidal variation of the cursor mass can be seen superimposed on some of the subjects' data in Figure 6.15.)

A small deadband region was also added to reduce drift, such that the force applied to the cursor was related to the force from the sensor, F_j, by

$$F(s) = \begin{cases} 0 & |F_j| < 0.2 \\ F_j & |F_j| \geq 0.2 \end{cases} \tag{6.3}$$

Subjects removed their hands from the force sensor and the force was re-zeroed before each trial (which lasted approximately 15 seconds) to ensure that there was no drift or bias force.

Subjects were told that the behavior of the cursor was position dependent but they were not told the actual mapping. As described above, they were given time to practice moving the cursor while it was visible before the experiment.

6.2.2 Vibrotactile Feedback

The vibrotactile feedback in this study was provided by a C2 Tactor, from EAI Inc. This tactor consists of a linear electromagnetic actuator that produces relative

motion between two moving parts, a small mass in the center of the device and a larger mass surrounding it. The tactor was placed on the arm, just below the elbow joint using a Velcro strap as shown in Figure 6.3. The actuator was controlled with a computer running the Mathwork's xPC Target realtime operating system through a current amplifier, controlling the actuation force. The waveform sent to the actuator can be arbitrarily specified with this approach. A frequency domain characterization of the tactor attached to the skin was performed using an accelerometer placed directly above the actuator. A mechanical resonance was found near 250 Hz, near the peak sensitivity of pacinian corpuscles.

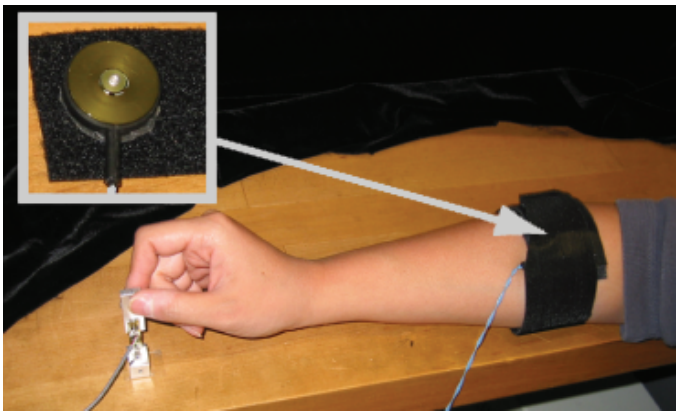

Figure 6.3: Vibrotactor strapped to test subject, placed on forearm below the elbow joint. The force sensor used to control cursor position is also pictured. Forces greater than 200 mN were needed to move the cursor.

Several position mappings were evaluated in pilot trials, including linear and nonlinear mappings of frequency, amplitude or both. Sine waves were used in all cases. Because of the dynamics of the actuator attached to the skin, varying the frequency also results in magnitude variations, though not linearly or even monotonically. This made a variable frequency mapping difficult to use. In addition, varying the frequency continuously results in Doppler effects when the cursor is moving rapidly, which cause the instantaneous frequency to be higher or lower depending on the direction of motion.

A pager motor was also used in pilot trials. This motor exhibited an approximately linear relationship between input voltage and magnitude and an approximately quadratic relationship between frequency and voltage input. However, the ranges of frequencies (from about 50 Hz to 175 Hz) and magnitudes that the motor was capable of producing were smaller than with the C2 Tactor.

Three subjects were tested with both the pager motor (input voltage varied as a function of cursor position) and the C2 Tactor (forcing amplitude varied as a function of cursor position at 250 Hz) and all three did better with the tactor. Based on these studies, we determined that varying the amplitude of the sine wave sent to the C2 Tactor at a constant frequency of 250 Hz provided the more effective position mapping. Pilot trials also showed that a logarithmic amplitude mapping was more effective than a linear one. This result is consistent with other findings in the literature that amplitude perception follows a logarithmic pattern [92].

The final mapping chosen obeyed the following relation:

$$A(x) = 0.5 \times 10^{0.06x} \tag{6.4}$$

where *A(x)* is the amplitude of the stimulus and x is the cursor position. This results in a small but perceivable stimulus level at $x = 0$ and a stimulus near the current limit of the actuator at $x = 10$ corresponding to $A(x) = 2$, which produces a peak acceleration of approximately 7.5 G as measured by an accelerometer on the tactor, in contact with skin. When the cursor moved outside the $0 \leq x \leq 10$ units workspace, the stimulus saturated at the values for 0 and 10, respectively. While more rigorous studies would be required to determine an optimal mapping of vibrotactile stimulation, this was the vibration mapping that our pilot subjects found most intuitive and performed best with.

6.2.3 Skin Stretch Feedback

The first benchtop skin stretch device (Figure 3.12) was used in these studies for controlled application of skin stretch. The skin stretch device was attached to the subject's arm, just below the elbow (Figure 6.4), in an area similar to where the vibration tactors were placed. The contact points were placed such that the line connecting them was perpendicular to the forearm.

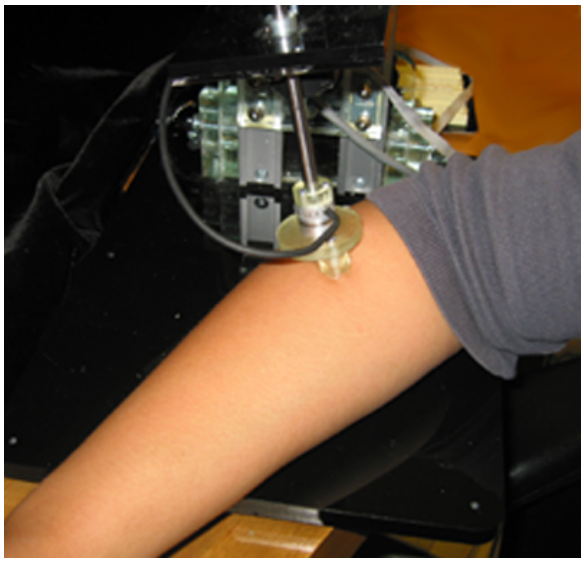

Figure 6.4: Skin stretch device attached to forearm below the elbow joint. Two contact points are attached using adhesive tape and rotate to apply skin stretch. Total contact area is approximately 2.5cm^2.

For these experiments, a range of ±45 degrees of rotation was mapped to the cursor position. This range of stretch was determined to produce sufficiently large, but comfortable, magnitudes of feedback in pilot studies.

One advantage of skin stretch feedback over vibration is the ability to convey direction. For these experiments, the rotation was set to 0 degrees when the cursor was in the middle of the workspace, at 5 units. The device subsequently rotated clockwise or counterclockwise according to the direction of the cursor movement.

Because there is relatively little information about perception of skin stretch applied to hairy skin, determining the optimal mapping of the cursor to magnitude of stretch is an open-ended problem. In pilot studies, a linear mapping of cursor position to degrees of skin stretch was first evaluated. Pilot subjects noted that there appeared to be a region of the cursor position surrounding $x = 5$ where it was difficult to detect rotation of the device. This region of uncertainty was also found in the studies described in Chapter 5. At higher levels of stretch, the skin stiffens nonlinearly (Chapter 4) so that linear increases in displacement produce more than linear increases in stress. Thus, when skin stiffness is low, at low rotations, a greater change in rotation is required to elicit sensations; at higher angles, near the saturation limits, smaller changes in angle are detectable. To account for these effects we used a slightly nonlinear monotonic, fifth order polynomial to map cursor position to rotation. A plot of the polynomial mapping is shown in Figure 6.5. The slope of the polynomial is also shown, which indicates the rate of change of skin stretch with respect to changes in cursor position. The varying slope reflects the hypothesized variation in skin compliance at low and high rotations, respectively.

Following the approach taken with vibration feedback, when the cursor left the region $0 \leq x \leq 10$ the skin stretch rotation was saturated at that the minimum or maximum angles (± 45 degrees). Although further testing is required to determine optimal mappings of skin stretch stimulation, the subjects in pilot tests found the slightly nonlinear mapping easy to interpret and they performed better with it than with a linear mapping.

6.2.4 Perception Study

To evaluate the effectiveness of the mappings used in the present study, a perception study of both vibration and skin stretch feedback was performed in which subjects were presented stimuli corresponding to five cursor positions and they were asked to report their perception of the stimulus. The five cursor positions corresponded to

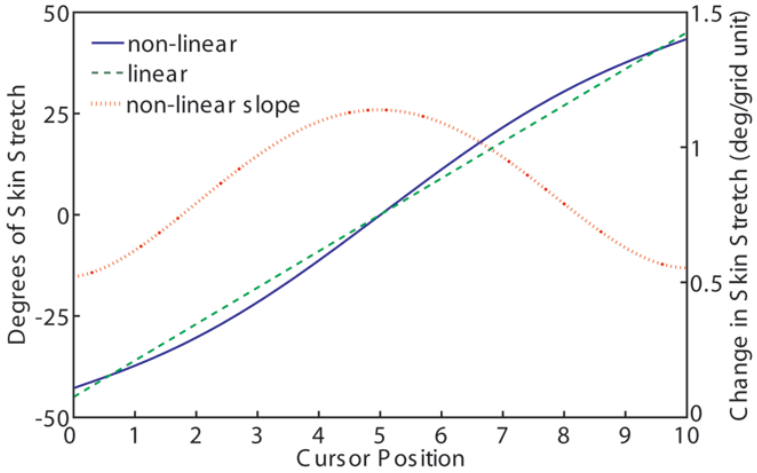

Figure 6.5: Skin stretch mapping relative to cursor position. Both the initial linear mapping as well as the non-linear method used are shown. Though the non-linear mapping is close to linear, at cursor locations near x=5 the increased change in stretch is great enough to overcome threshold limits to improve subject performance. The slope of the nonlinear mapping is also shown, reflecting the hypothesized variation in skin compliance.

the final locations in the cursor workspace subjects were asked to move towards in the targeting study. If the subjects could distinguish the different stimuli either by perceived magnitude or position, the use of our mapping could be validated.

One of the unique features of the skin stretch feedback is that it is inherently continuous and therefore, cannot be instantaneously changed in magnitude as vibration can be. Frequency and amplitude characteristics of a vibratory stimulus can be changed in software, prior to presenting the stimulus to the user. In contrast, skin stretch rotation must always ramp to the desired position. In order to apply 30 degrees of stretch, the rotation must pass through 10 and 20 degrees. Subjects can use not only the static position of stretch, but also the dynamic motion as the stretch applicator moves to distinguish between different stimuli. This makes a classical perception study like those typically used for vibration not practical. A more intuitive method of reporting perceived skin stretch with directional components was to think in terms of rotational displacement rather than magnitude, similar to the

studies in Chapter 5. Hence, subjects were asked to report their perception of the orientation of the skin stretch device, not simply the strength of the stimulus. For vibration, because it lacks a clear directional component, subjects were simply asked to report a perceived magnitude.

We also observed that subjects could use information about the motion of the device to detect the amount of static skin stretch by integrating the velocity sensation. In our closed-loop task, as described in Section 6.2, the dynamics of the cursor were position dependent which made it more difficult for subjects to use this open loop strategy. To prevent subjects from simply timing the duration of the stimulus, we presented stimuli (Skin Stretch and Vibration) that started at one of three easily distinguishable levels corresponding to the extremes and middle of the workspace (0, 5 and 10 units) and ramped the stimulus at a constant speed to the desired stimulus level (1,3,5,7 or 9 units). This followed the protocol outlined for the closed loop experiments. In this method, subjects were able to use a sense of static or dynamic information or both to estimate position. Vibration stimuli were applied in a similar manner to keep the experiment protocol consistent between feedback methods.

Prior to the experiment, subjects were presented with the three possible starting stimulus levels (min, max and zero) and they were asked to provide a numerical value on an absolute scale including integers or fractions [133] of their choosing corresponding to the minimum and maximum. For vibration, these numbers were constrained to be positive numbers. For skin stretch, one was positive and the other negative (for the opposite direction of rotation) but they did not need to be equal in value. Subjects were not told that the rotations were in fact symmetric. The center point, where no rotation was applied was constrained to be zero. After this initial calibration phase, subjects were given the changing stimuli as described above and were asked to report their perception on the scale that they had chosen by entering a numerical value into a spreadsheet. For each subject, 75 stimuli were presented (15 at each stimulus ending location) in random order. Five subjects were tested with each of the haptic feedback methods. To prevent subjects from using

audio cues to distinguish between stimuli, headphones were worn throughout the trials and subjects were instructed to look away from the skin stretch device when in use. Subjects were not told that there were only 5 different levels of stimuli and the stimuli were ramped to the desired levels at constant rates of change for both vibration and skin stretch. Vibrotactile trials were completed in 10 minutes while skin stretch trials lasted approximately 15 minutes.

6.3 Results

6.3.1 Perception Study Results

The results of the perception studies for vibration and skin stretch are shown in Figures 6.6 and 6.7 respectively. For each case, the results were independently normalized by dividing each of the subjects' responses by the mean of all of their responses for each point and then multiplying by the mean of all subjects' responses at that point [92] to account for subject to subject variation. The resulting means and standard deviations were then calculated and plotted.

For vibration, the perceived magnitudes were roughly linear on the average as a function of workspace location (recall that the actual mapping is logarithmic as given by equation 1). The standard deviations were smaller at low stimulus amplitudes. 5 subjects were tested using vibration feedback and a different set of 5 subjects were tested using skin stretch feedback. For data analysis, a one-way ANOVA comparison of means was conducted for each of the points and each of the adjacent points are statistically distinguishable ($p < 1 \cdot 10^{-5}$).

The skin stretch perception results were slightly less linear with more sensitivity near the extremes of the workspace. This indicates that a slightly more non-linear skin stretch mapping that the one chosen may have been more appropriate. Error bars were also quite large with skin stretch feedback, however upon further inspection of the data, we found that variances were generally low with the exception of a few

outliers. A total of eleven outliers out of 375 total data points were identified and two subjects had no outliers. For example, in one trial when the starting position was zero workspace units (about -45 degrees of skin stretch) and the stimulus ramped to 9 workspace units (about 40 degrees of skin stretch) the subject entered a negative number of appropriate magnitude but opposite sign based on their chosen scale. This could result from them making an error in detecting the direction of movement or, more likely, from them simply making a sign error. As this was an open loop perception study similar to the one completed in 5.3.2, these errors were expected. The red curve in Figure 6.7 shows the results if these points are corrected (sign reversed). As expected, sensitivity is improved and standard deviations reduced in this case. Even without correction all four sets of adjacent points are statistically different ($p < 0.001$) and with corrections the largest p-value was less than $1 \cdot 10^{-8}$.

Overall, the perception results seemed to indicate that the mappings used were satisfactory as users were able to statistically distinguish the various points from one another.

6.3.2 Targeting Study Results

The data collected from the experiments were analyzed to determine the effectiveness of providing haptic feedback in blind movement tasks. The main parameters of interest were the absolute and relative error (absolute error divided by desired movement length) in final cursor position and the instantaneous velocity of the cursor at the end of each trial. A repeated measures analysis of variance (ANOVA) comparison of means was conducted to determine if the means in position error were significantly different across the various feedback methods: no feedback (NF1), vibration (V), skin stretch (SS), and the final no feedback case (NF2). The ANOVA method used was a post hoc analysis conducted using the Bonferroni criterion [47]. The effects of varying step sizes and the starting/ending positions of the cursor were also studied. The data were grouped into several subcategories to identify patterns and trends.

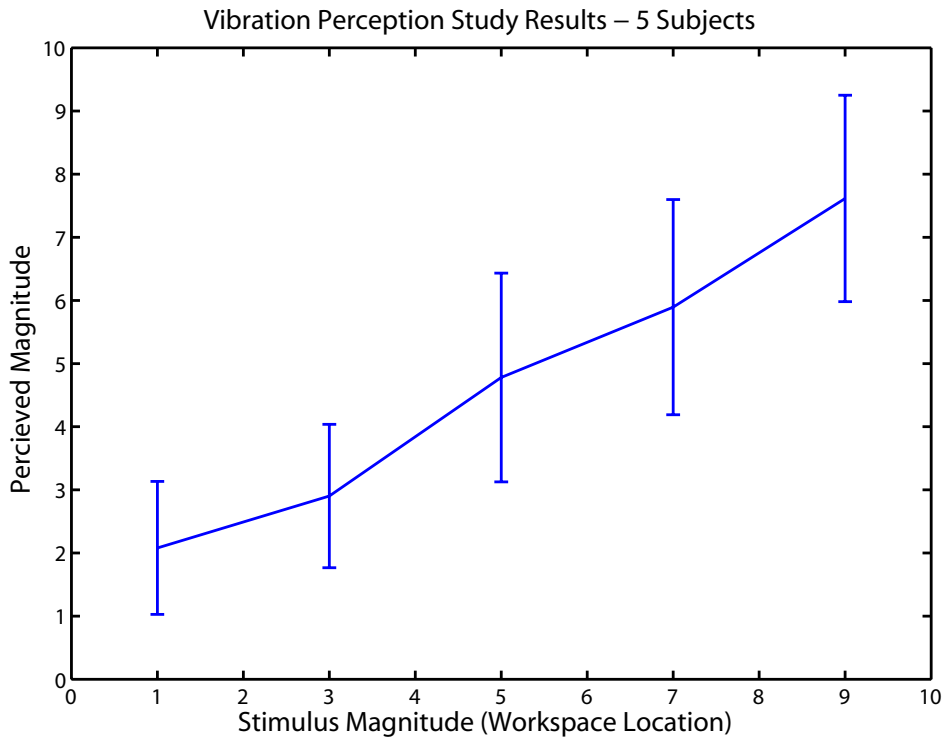

Figure 6.6: Perception curve for vibrotactile stimulation normalized over five subjects. The x-axis represents the workspace location that the stimulus corresponded to. The actual stimulus amplitude varied logarithmically with workspace location as given in equation 1. Error bars are plus and minus one standard deviation.

Error bars on the plots below indicate standard errors. In general, standard deviations were quite large relative to the means. This is largely due to the fact that the difficulty of the task caused standard deviations within subjects to be similar in magnitude to inter-subject standard deviations (such that normalization does not significantly decrease standard deviations). The task was designed to be comparably difficult to moving a real arm a specified distance without looking, which we expect would also result in relatively large variances. Quantitative results across all subjects as well as anecdotal observations of the most interesting cases are presented in the following sections.

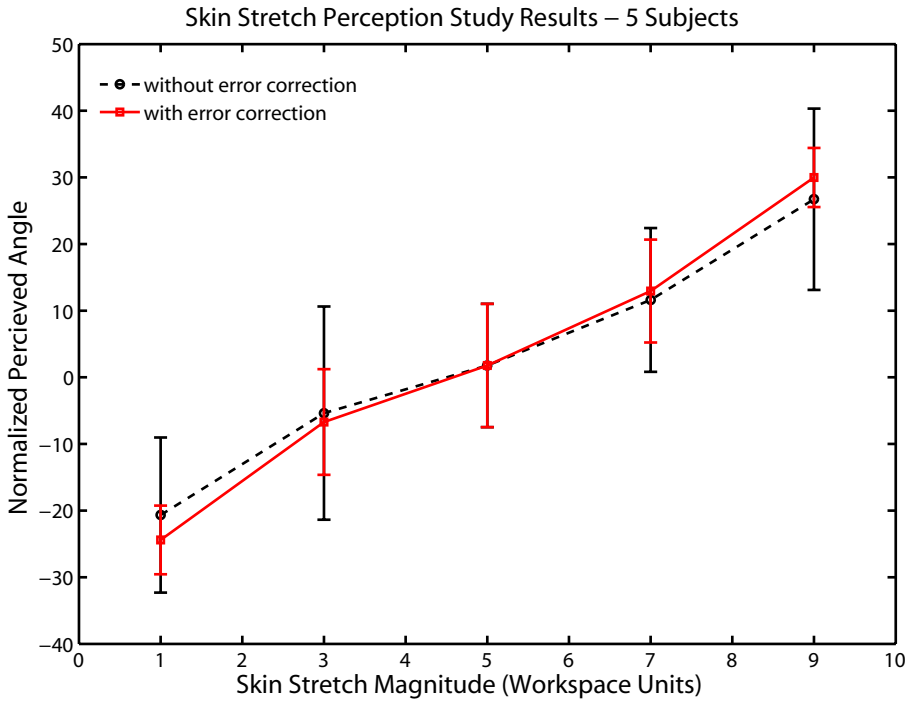

Figure 6.7: Perception curve for skin stretch normalized over five subjects with and without direction error correction. The x-axis represents the workspace location that the stimulus corresponded to. The actual amount of rotation applied is shown in Figure 6.5. Error bars are plus and minus one standard deviation.

6.3.3 Cursor Position

Overall Error

Repeated measures ANOVA applied to the absolute errors revealed signicant main effects due to the feedback method, $F(3, 10) = 7.848$, $p = 0.001$. For relative errors, main effects due to feedback method were also found, $F(3,10) = 9.415$, $p = 0.0001$. Post hoc paired t-test analysis was then applied to the data using Least Squared Differences, where Table 6.1 presents the p-values comparing the various feedback methods.

	NF	SS	VL	NF2
NF	x	**0.002**	**0.035**	0.214
SS	**.002**	x	**0.057**	**0.014**
VL	**.035**	**.057**	x	**0.088**
NF2	.214	**.014**	**.088**	x

bold denotes significance at $\alpha = 0.10$ level

Table 6.1: P-values for post hoc paired t-tests comparing absolute errors. Skin stretch and vibration feedback are significantly different than no feedback at the $\alpha = 0.10$ level. Skin stretch is also significantly different from vibration.

	NF	SS	VL	NF2
NF	x	**.0002**	**.027**	.228
SS	**.0002**	x	**.052**	**.008**
VL	**.027**	**.052**	x	.103
NF2	.228	**.008**	.103	x

bold denotes significance at $\alpha = 0.10$ level

Table 6.2: P-values for post hoc paired t-tests comparing relative errors. Skin stretch and vibration feedback are significantly different than no feedback at the $\alpha = 0.10$ level. Skin stretch is also significantly different from vibration.

As anticipated, the addition of skin stretch feedback improved movement accuracy. As seen in Figures 6.8 and 6.9, the relative and absolute position errors decreased with vibration and skin stretch feedback. Overall, in both absolute and relative error analysis, skin stretch produced statistically significant smaller error values (at the $\alpha = 0.10 level$) when compared to no feedback and vibrotactile feedback. The standard deviation of the errors was also lower with skin stretch than the other cases. Vibration feedback resulted in lower position errors as compared to receiving no feedback ($p < 0.10$). Of the 10 subjects tested, 9 performed best with skin stretch feedback (Figure 6.10).

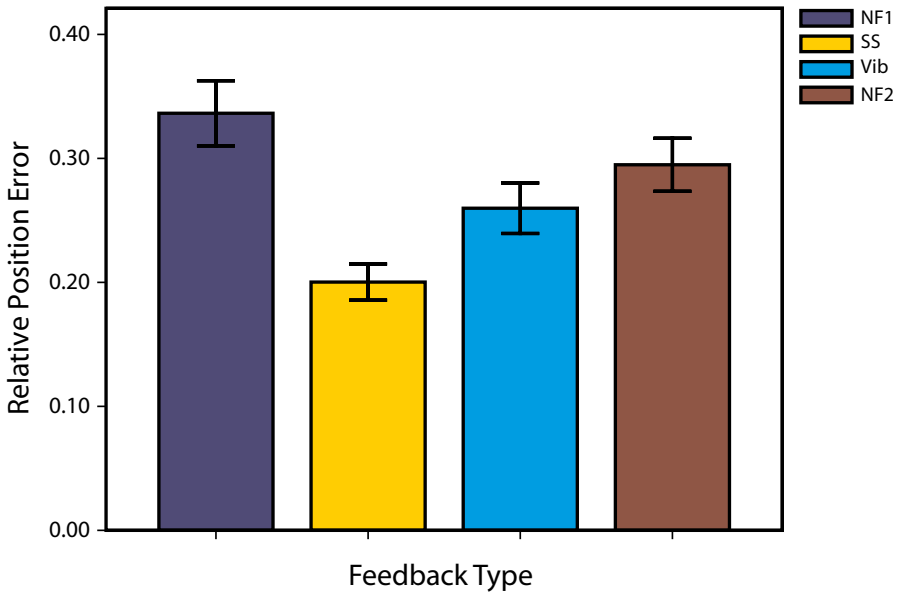

Figure 6.8: Average relative position errors for ten subjects. Error bars are plus one standard deviation. Skin stretch results in significantly smaller relative errors ($p < 0.05$) than no feedback.

Overall, subjects had significantly less error in the second no feedback case than the first, indicating that some improvement was taking place over the course of the experiment due to practice. However, this trend was not consistent across all subjects. Some did worse the second time and reported that they had become somewhat dependent on the feedback and had difficulty moving accurately when it was removed. We also performed a linear regression on the relative position errors across the 36 trials for each feedback case to see if significant improvement was occurring over the course of the trials. No significant trends were found in any of the feedback cases.

Error by Step Size

The position errors were sorted into various subcategories according to step size (the number of units the test subject was asked to move the cursor), and the desired

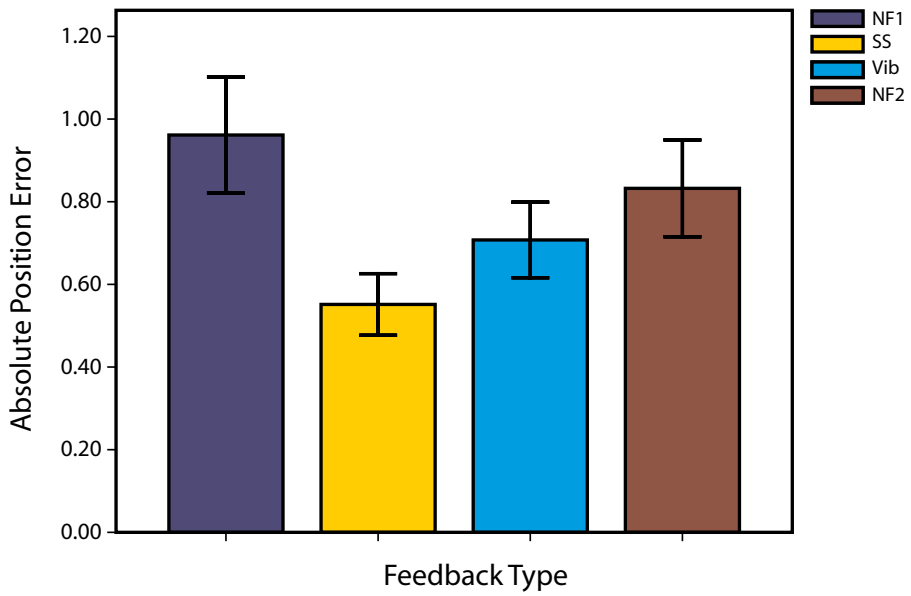

Figure 6.9: Average absolute position errors for ten subjects. Similar to relative error, skin stretch results in significantly smaller absolute errors ($p < 0.05$) than no feedback cases, though vibration does not.

ending position of the cursor. At first glance, when sorting the data by step size, it is clear that the addition of haptic feedback provides benefits over no feedback at each step magnitude (Figure 6.11). As expected, the absolute error increases as the desired step size increases, for all feedback modes. When no feedback is provided, the relative errors do not change significantly as a function of step size (Figure 6.12). However, for the two feedback modes, relative error decreases as step size increases from 2 to 6. This trend indicates that subjects seem to be getting a sense of absolute position when haptic feedback is provided. If a true sense of position were provided, we would expect to see uniform absolute errors at all step sizes, such that relative errors decrease for larger step sizes.

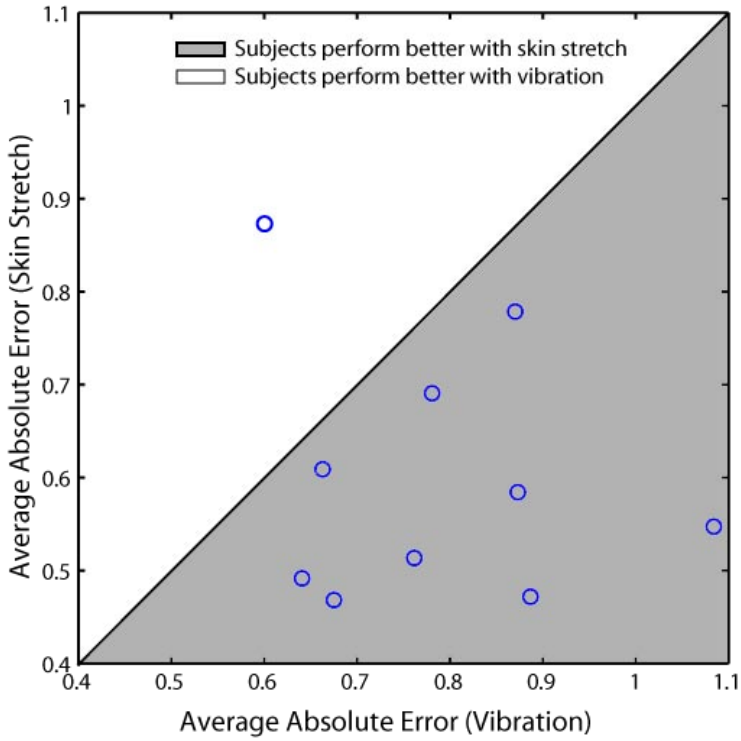

Figure 6.10: Average absolute position errors using vibration feedback and skin stretch feedback for each of the ten subjects. Each dot represents one subject. Dots in the shaded region indicates subjects who performed better with skin stretch feedback (9 of 10).

Error by Target Location

The overall error as a function of target location is shown in Figure 6.13. Skin stretch again resulted in the lowest errors at all targets. There are at least two position dependent factors that could influence these results. One is position dependent perception qualities of the haptic feedback, which are small (see perception study results below). The more dominant effect seems to be the cursor inertia. Errors were generally lowest near target location 7, which corresponds to a lower cursor inertia. The cursor was easier to stop in this location due to the low inertia.

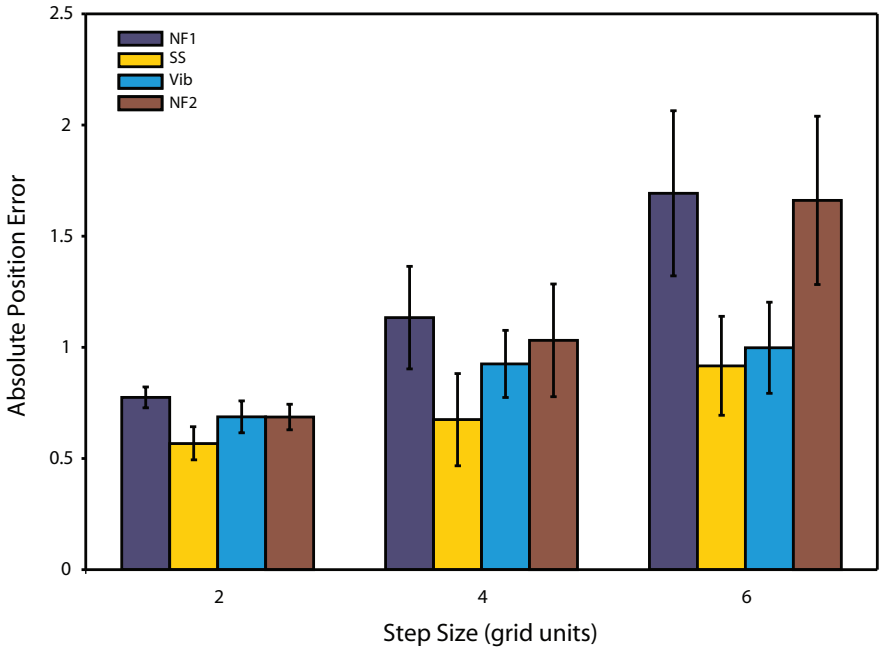

Figure 6.11: Average absolute position errors relative to step size. As expected, absolute errors tend to increase with increasing step sizes across all feedback modes. Both skin stretch and vibration feedback result in smaller errors at each step size, with skin stretch performing best, though not significantly.

6.3.4 Final Velocity

Overall Velocity

The cursor velocity was also calculated through differentiation (forward difference method) of the recorded cursor position throughout the experiment. No additional data filtering was needed since the cursor dynamics effectively act as a low-pass filter. The instantaneous velocity of the cursor when the subject pressed the button (i.e., when the subject believed the cursor had been brought to a stop) was determined for each trial. For velocity analysis, it was discovered that 2 of the 10 subjects recorded velocities that were up to 4 times larger than the velocities measured during their first

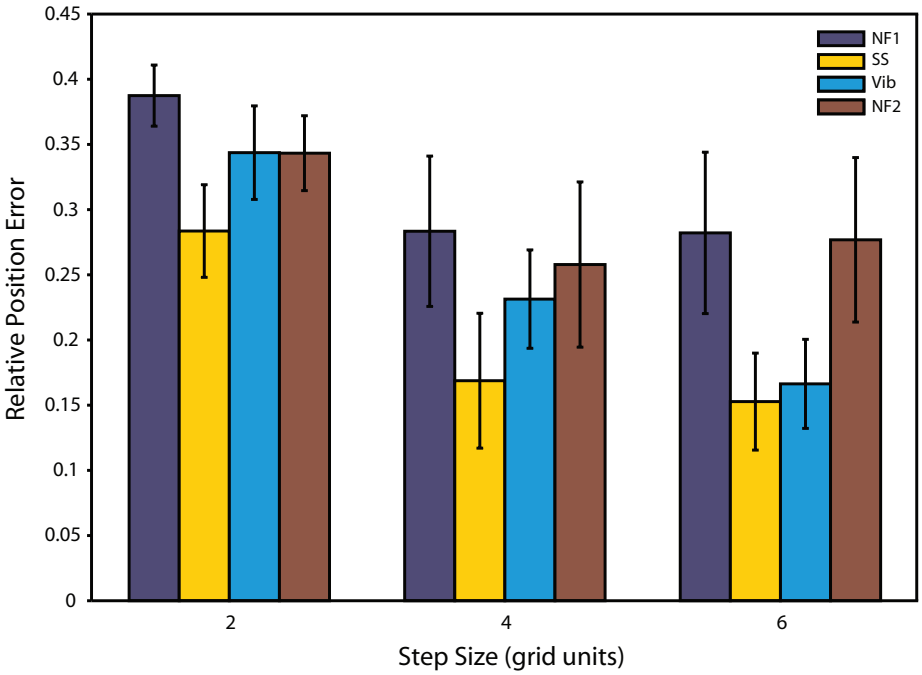

Figure 6.12: Average relative position errors by step size. The general trend is that relative errors decrease with increasing step sizes with feedback. At large step sizes (6), subjects perform better with feedback than without, though there is no significant difference between skin stretch and vibration. In addition, relative error decreases as step size increases from 2 to 6 when feedback is provided

no feedback trial. These subjects were considered to be outliers as it was apparent they made no attempt to stop the cursor from moving before pushing the button in subsequent trials, though position errors were not large in comparison. The average cursor velocity for the remaining 8 subjects is seen in Figure 6.14.

Here, it is abundantly clear that skin stretch provided users with a sense of motion, allowing them to consistently stop the cursor. Velocities measured with skin stretch feedback are significantly lower than all other feedback modes with p-values less than 0.05.

It appears that the subjects were only able to easily detect velocity when skin stretch feedback was provided. However, we also note that the average velocities

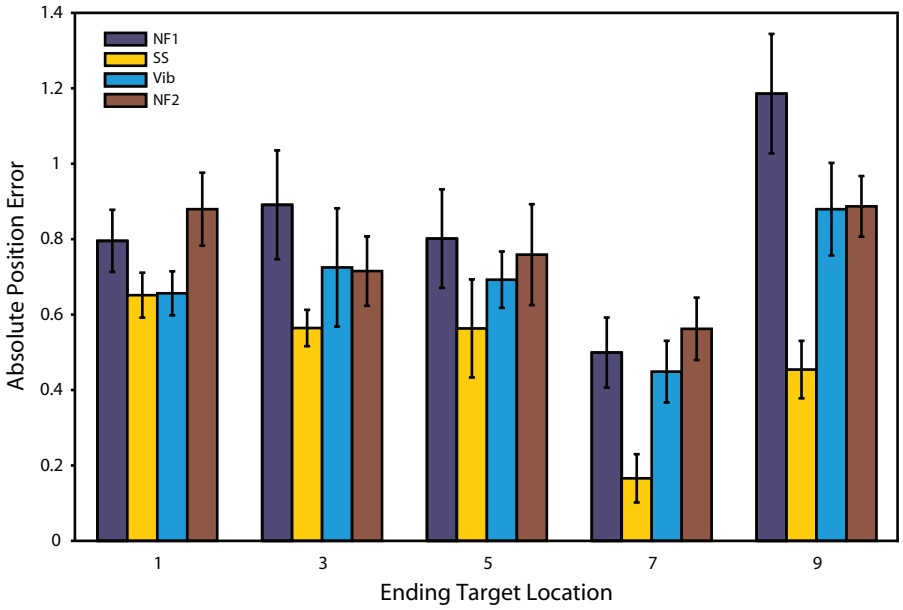

Figure 6.13: Average absolute position error versus desired target location. Skin stretch produced the lowest error at all targets. Lower errors are found where the cursor inertia is low (i.e. near point 7).

at which the subjects moved the cursor were lower with skin stretch than in the vibration or no feedback modes. It appears that because skin stretch provided a better qualitative sense of velocity, subjects moved more slowly in this case. In the other cases, there was little sense of cursor velocity and no motivation to limit speed.

Velocity by Cursor End Position

A point of interest when examining the final velocities is the correlation with cursor position and inertia. As the cursor inertia increases, while damping remains constant, more effort is required to bring the cursor to a stop. In all feedback methods, the average ending velocity of the cursor relative to the desired ending position closely matches the pattern of the inertial changes (Figure 6.15). A cursor position of 7 corresponds to a low cursor inertia, and correspondingly, the measured ending

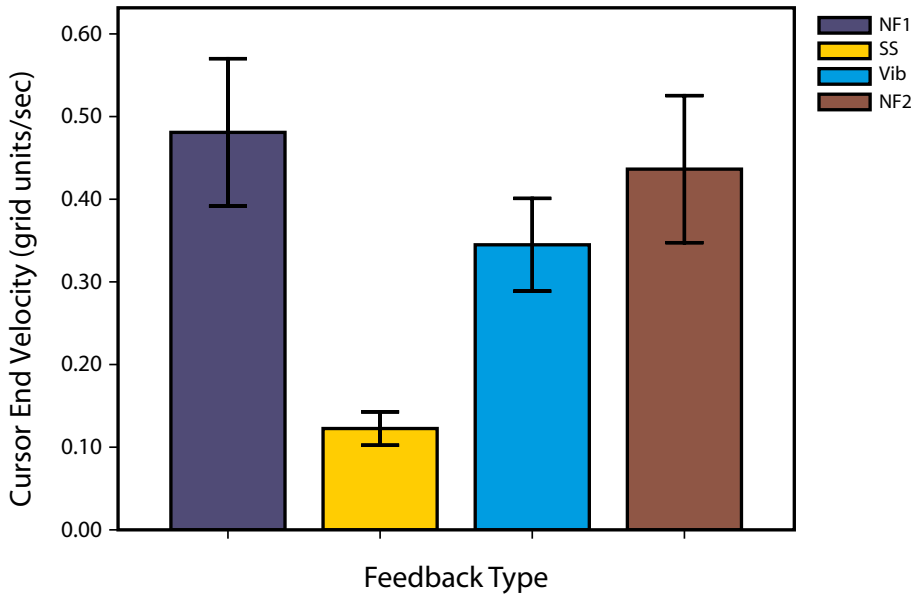

Figure 6.14: Overall average ending velocities. Skin stretch is far superior to all other feedback modes in maintaining low end velocities ($p < 0.05$).

velocities of the cursor are lowest at that location. This suggests that subjects were indeed experiencing the challenges of controlling the varying cursor dynamics. However, the errors are consistently lower with skin stretch and the variation with cursor position is generally lower than with other feedback modes.

6.4 Discussion

The results of the present study indicate that skin stretch may be an effective method for providing proprioceptive feedback in wearable displays. Skin stretch is an important part of the proprioceptive sense and provides a useful mapping for position information. In particular, skin stretch gives a realistic sense of dynamic motion in addition to static position using just a single stimulus, which could provide benefits for many applications. As observed in previous studies, this feedback is effective for closed loop control, providing a better sense of location and position when vision is

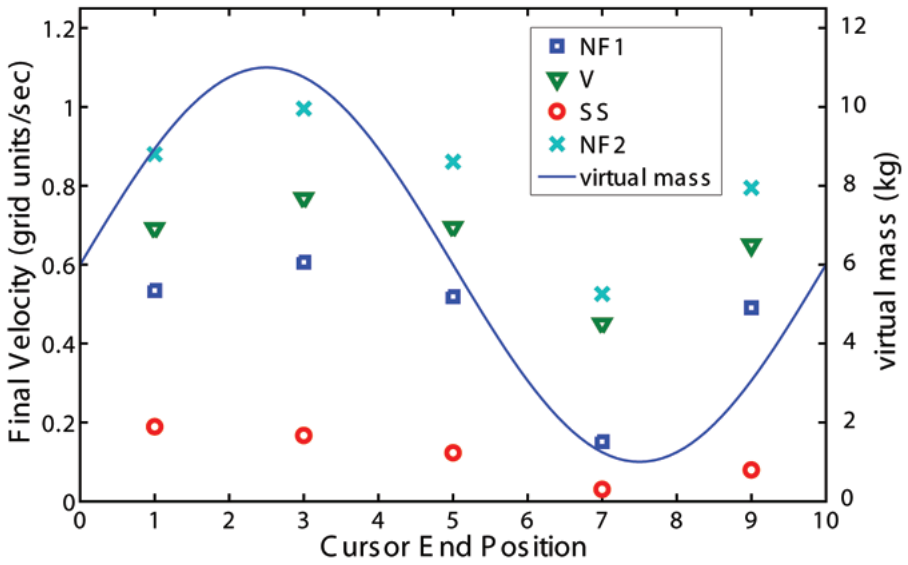

Figure 6.15: Average ending velocities with respect to desired ending cursor position. Average ending velocities from each feedback mode follow the sinusoidal characteristics of the varying inertial properties of the cursor with respect to cursor position.

not present. Though subjects were able to position the cursor with smaller errors using skin stretch feedback, the true value of skin stretch feedback lies in its' ability to convey a sense of motion. Subjects could easily detect whether the cursor was moving or had stopped and in combination with the motor commands through the force sensor input, users had a clear idea of the cursor direction. This perception of motion becomes even more important when control channels or dynamics of a system are complex. In this study, the dynamics of the system were complex to prevent users from simply using open-loop strategies to position the cursor. In systems where the dynamics are simple, skin stretch feedback may not provide a good cost to benefit ratio. However, in systems such as a prosthetic arm, the dynamics can be difficult to predict and the control channels can be noisy. Myoelectrically controlled prostheses, which use electrical impulses produced from muscle contractions to control high-impedance prosthetic joint actuators, may contain noisy signals. Coupled with friction and the changing inertia and dynamics of the arm itself make it a difficult

system to control. It is this type of application in which skin stretch may provide to be a very effective method of feedback. Studies to validate this are underway.

Although vibrotactile feedback was provided in these experiments and found to be less effective in positioning accuracy than skin stretch, it must be noted that it still remains an attractive choice for wearable haptic applications due to its size and power characteristics. In the present study, the amplitude of the vibration was continuously varied according to cursor position as this was found to be the most effective continuous mapping. However, other strategies could be employed where discrete changes in amplitude or frequency occur at specific intervals. This would require the subject to "count" to some extent to perform movements and the inherent resolution of the feedback channel would be limited. In any case, when vibration is used, it is desirable only to turn on the stimulation when a movement is being made as many subjects reported that continuous vibration was annoying. In addition, neural adaptation causes desensitization over time [5, 57]. Multiple vibration stimulators could also convey a sense of motion if they are appropriately sequenced [117]. However the stimulators must be spaced relatively far apart due to the large receptive fields of the deep pacinian corpuscles. Because skin stretch activates primarily superficial, slow acting receptors, it is less susceptible to these issues. A constant stimulation is not annoying and can be effectively ignored if desired.

Although these initial studies indicate there are unexplored benefits to using skin stretch for tactile feedback, there are a few practical issues that must be addressed when attempting to implement skin stretch. Particularly if the skin contact area is relatively small, as with the device used in this study, care must be taken so that the device does not slip on the skin. How well the device works is highly dependent on the where it is placed on the skin and on the subject. The device tends to slip more if there is a lot of hair on the skin or in areas where skin curvature is high. Though the Red-E-Tape was found to adhere adequately to the skin, it is assumed that some amount of slip occurred throughout the skin stretch trials.

The varying stiffness of skin on different parts of the body, as well as subject-to-subject variation of skin properties, present significant design and control challenges. Some individual calibration may be required when the device is attached. Because skin stiffness properties also depend on the configuration of the body or limbs, the perceived magnitude of stretch also appears to change. In early pilot experiments, we attempted to place the skin stretch applicator near the elbow joint to provide something closer to an illusory sense of joint movement. However, we observed that as the trials progressed, subjects would move and bend their elbows slightly to re-adjust their seating configuration. Using the wearable device would be more comfortable for users and we can infer from these results and previous studies that the results from a study such as this would be similar with the wearable device.

The present study did not fully assess the effects of training on movement accuracy. Because subjects were given post-trial vision feedback throughout the experiment, some improvement over time was expected. In fact, most subjects had lower errors in the second no feedback trial than the first but no significant improvement was found across the 36 trials for a given feedback case. All subjects were given uniform training in this study. To fully assess learning effects, a future study should be done where the training method is a controlled variable.

Overall, skin stretch feedback was found to provide effective feedback. It should not be used to replace vision, yet it can be used to reduce the dependence on vision by providing a relative sense of position and motion.

Chapter 7

Conclusions

In conclusion, this work has initiated the study of skin stretch on the body for haptic feedback of proprioception and related phenomena. It should not be considered a replacement for other modes of feedback such as vibration or force. It is a new mode of tactile communication in its own right with its own characteristics and benefits. This final chapter summarizes the work obtained in the preceding chapters as well as suggestions for possible extensions and future work are also presented. A description of the major contributions can be found in Section 1.3.

7.1 Summary of Results

The most significant result produced by this research is a new method for providing tactile feedback in the form of rotational skin stretch. Though there are a variety of methods in which to induce skin stretch, the two point rotational stretch developed here provides a useful range and resolution of perceived feedback. There are distinct mechanical advantages to choosing rotational motion as well as perceptual benefits. For portable wearable devices, size, weight and power consumption are critical design requirements. The haptic device described in this thesis uses a novel actuator that allows large torques to be applied at low speeds with minimal gear reduction. While

in many haptic devices it is desirable to have low-impedance actuators, in cases where position control is needed, a non-backdriveable motor like the piezo-motor used in this device also requires much less power as it can hold its position without a current. The rotational, two point method also allows for some leeway when grounding the device to the user to provide the appropriate torques. As the two points move in opposing directions, the device does not have to be firmly grounded to the user's body, as would be necessary for a single contact pad. In addition, the rotational motion produces increased amounts of strain to provide a stronger stimulus. In particular, compressive and shear strains are higher, producing a higher perceived magnitude, though there is danger in producing too much strain, causing discomfort to the user.

One of the unique attributes of skin stretch feedback is that it can provide a sense of position and velocity within a single stimulus. One may argue that a display designed to move across the surface of the skin could also provide a sense of motion, combining a sense of velocity and position with a single stimulus. However, what makes skin stretch unique is that it also provides a sense of intensity due to the increasing strain with higher rotations. Therefore, not only does skin stretch stimuli contain dynamic and static components, with the ability to convey directions, but it also imparts a sense of magnitude to a user through the changes in intensity. If necessary, users can use the static position of the skin stretch for static information as evidenced by the difference threshold tests. The changes in velocity of stretch had little to no affect on a subject's ability to distinguish between different positions. However, subjects can also use the dynamic sense of motion from skin stretch to interpret the relative changes in the feedback. In fact, users are quite adept at integrating the motion to obtain a relative position. Given the correct application and interface, users can quickly learn to use skin stretch feedback with minimal training. However, for applications in which skin stretch feedback is not directly correlated to the user's commands, more training and experience are necessary.

The applications in which skin stretch feedback is most useful are when the

feedback is directly correlated to a user's input. When it is not, users have a difficult time determining the direction of movement. However, humans are remarkably adept at developing internal models of simple systems, as evidenced by the proprioception study in which the cursor was given complex dynamics to discourage users from using open loop strategies. Therefore, applications in which the control channel is unpredictable or noisy, are those for which skin stretch will provide significant benefit. One such application is proprioceptive feedback for amputees. Amputees have difficulty in controlling their prosthetic limbs and grips, with the result that although they command the prosthetic to move in a certain manner, they cannot be sure that it moves as intended. A skin stretch feedback device would provide a sense of movement and static position, allowing them to reduce the amount of visual attention necessary to control their prosthetic.

7.2 Future Work

Because of the novelty of using skin stretch for haptic feedback, there is a wide range of avenues that can be explored to improve upon this work. Three paths that can be followed include exploring other practical applications and settings for which skin stretch would be particularly useful, improving the design of the skin stretch device and method, and developing a clearer understanding of how users perceive and interpret skin stretch feedback.

Studies to quantify the benefits of using skin stretch feedback in more practical applications should be undertaken. Though the experiment in Chapter 6 provided evidence that skin stretch can be used for proprioceptive feedback, a clinical study with amputees is necessary. Significant differences between the studies presented here and amputee performance exist. First, an amputee's feedback properties will mostly likely differ from those of unimpaired users, with different muscle and nerve configurations. Also, conformal changes to an amputee's residual limb could affect the performance of skin stretch for some subjects. Long term effects of using skin

stretch feedback are also largely unknown. Though proprioceptive feedback seems to be a good fit for skin stretch feedback, there are possibly other applications in which skin stretch could be useful. As skin is stretched, it can be used for position information, but it is also clear that users obtain a sense of torque/force as the rotation increases. It is possible that a clever interface would allow humans to use skin stretch for force feedback.

While the design parameters used for this device have proven to be useful, the device has been specialized for use on the forearm. Skin stretch can be applied on virtually any location of the body, yet it is unknown how well users would interpret skin stretch on locations other than the arm or fingerpad. As it is well known that our sensitivity to touch varies with body location, as do our skin properties. It can be assumed that our abilities to sense skin stretch will also vary as it is applied on our shoulders, legs, or torso- locations which may be more desirable or intuitive for different applications. The size and number of contact pads, as well as the spacing between the pads should be optimized for different areas of the body, as well as for different practical applications. Furthermore, though the method chosen for this work was rotational skin stretch, it is quite plausible that for other applications, linear stretch or even different patterns of stretch would provide useful information to a user. For example, in navigational purposes, it may be much more intuitive to use a linear motion for directional information. For communicating codes, different patterns of stretch may prove to be useful. A method to adhere to the skin without the use of double sided tape would also be immensely beneficial to the design of the device. Work to develop dry adhesives, such as those used in climbing robotics [67] may provide inspiration for developing a skin safe dry adhesive that can withstand the forces and torques necessary for skin stretch. Finally, though the device presented here is wearable, it is not yet portable. Work to convert this device to a truly wireless, portable device would expand the realm of applications.

Finally, although we discovered that our perception of skin stretch relies on both the static and dynamic portions of the stimulus, it is unknown to what extent users

rely on the dynamic sense to determine the static position of the skin stretch feedback. In other words, our ability to integrate the velocity of skin stretch to obtain a static position of stretch is unknown. The perception studies presented here, in particular the difference threshold study, made little attempt to account for a user's sense of timing and velocity to estimate a position. We hypothesize that a user's true static sense of skin stretch position would degrade significantly if the dynamic sensation was removed. One possible way to test this is to repeat the difference threshold test by applying skin stretch at an extremely slow rate (0.5 deg/s). This would provide a more accurate view of what our static resolution of skin stretch is and possibly shed some light on the region of uncertainty that was found in Chapter 5. Do users primarily depend on the dynamic sense within this range to determine the position? The dynamic portion of the stimulus is hypothesized to be quite important, yet there is no perceptual data on our abilities to distinguish between different velocities of stretch. The psychophysical studies carried out in this work were designed for more practical applications, yet for more scientific purposes, psychophysical studies to better characterize our sense of skin stretch could provide better insights on how to optimize this type of haptic feedback.

Appendix A

Preliminary Strain Analysis

This section describes the calculations and assumptions used to estimate strains to compare linear and rotational stretch, as described in Section 3.2.2.

A.1 Curvature Correction

The images taken from the camera are 2D. The curvature of the arm is not accounted for in the absolute location of points from the 2D images. To capture the true movement or strain on the surface of the skin, a curvature correction factor was applied to all the points.

As this experiment was only for estimation purposes, several assumptions were made to simplify calculations:

- The arm is assumed to be a perfectly shaped tapered cylinder. At each cross section, the arm is assumed to be circular, not elliptical. The maximum and minimum radii for the arm are estimated to be 4 cm and 3.5 cm respectively (see Figure A.1).
- The central axis of the forearm is parallel to the x-axis of the general coordinate frame. Images were rotated to align the arm to the axis.

- There is no movement of the skin in the z-axis (indentation).

The strategy used here to calculate the curvature correction was to simply estimate the arc-length of the point from the top of the arm along the y-axis of the coordinate frame. The arc-length then served as the corrected y coordinate of the point for analysis.

The radius of the arm at the location of each point is estimated by assuming that the radius of the arm changes linearly. The absolute distance of the point from the central axis of the arm in the y-axis is then calculated.

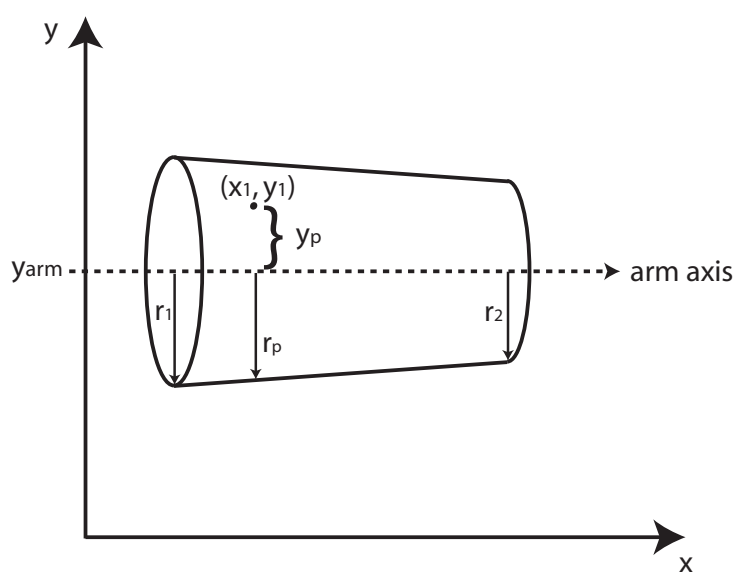

Figure A.1: Showing coordinate conventions for computing strains. These dimensions were used to transform the grid points to a 2D planar surface.

- (x_1, y_1) are the x and y coordinates of a point on the skin
- $r_1 = 4$ cm
- $r_2 = 3.5$ cm
- $r_p =$ the estimated radius of the arm at point (x_1, y_1), assuming a linearly changing radius

- $y_p = y_1 - y_{arm}$, the distance of the point from the x-axis of the forearm

To estimate the arc-length, the estimated radius, r_p and the distance y_p can be used with the following relationship (Figure A.2).

$$arc_p = r_p[asin(\frac{y_p}{r_p})] \tag{A.1}$$

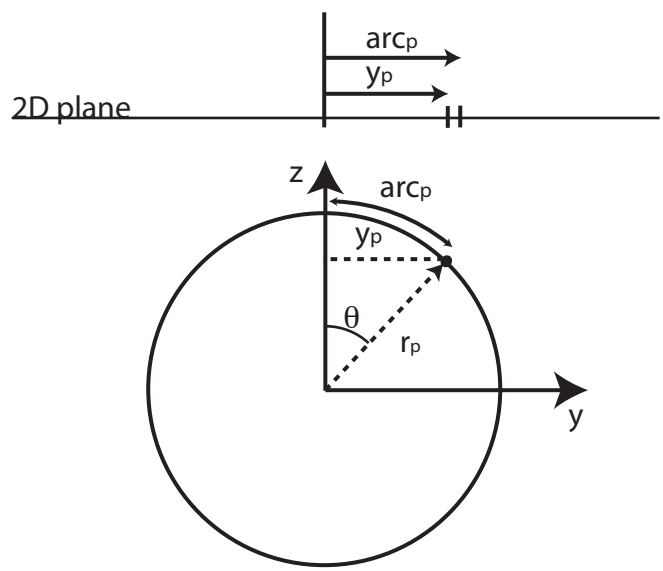

Figure A.2: Cross sectional view of arm, displaying arc length measurements used to re-map grid point to 2D plane.

A.2 2D Strain Estimate

Once the points were transformed to fit a 2D plane, a simple strain analysis was conducted. To estimate the strains, it was assumed that there were no rigid-body displacements of the arm. Each grid point, $p_{i,j}$ was then assumed to be a point on a small element, dx, dy of an elastic body. If the body undergoes a deformation and

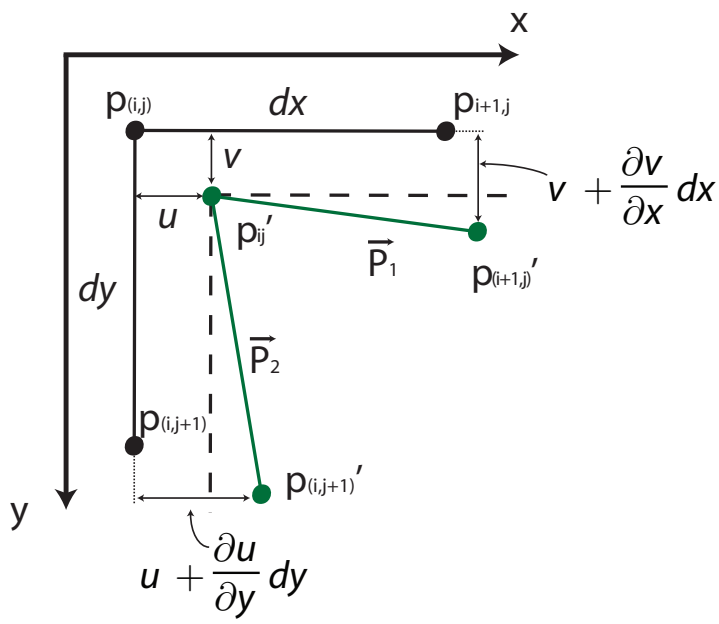

Figure A.3: Strain calculations.

point $p_{i,j}$ is displaced by u and v in the x and y axes respectively, the displacement in the x-direction of an adjacent point, $p_{(i+1,j)}$ on the x axis is

$$u + \frac{\partial u}{\partial x} dx \tag{A.2}$$

The increase in length of the element in the x-direction is then $\frac{\partial u}{\partial x} dx$. The unit elongation at point $p_{i,j}$ is then simply the strain, ϵ_x, given by Equation A.3. Similarly, unit elongation of the segment between points $p_{(i,j)}$ and $p_{(i,j+1)}$ in the y-direction is then given by Equation A.4. The shear strain, ϵ_{xy}, is given by Equation A.5.

$$\epsilon_x = \frac{\partial u}{\partial x} \tag{A.3}$$

$$\epsilon_y = \frac{\partial v}{\partial y} \tag{A.4}$$

$$\epsilon_{xy} = \frac{\partial u}{\partial y} + \frac{\partial v}{\partial x} \tag{A.5}$$

For each grid point, a two dimensional coordinate system was assumed and using the adjacent gridpoints, four quadrants were formed (see Figure A.4. The next set of images at a new displacement created new grid points, $p'_{i,j}$, etc, and the above strain analysis was completed to estimate transverse and longitudinal strains in the x and y directions respectively. The shear strains for each quadrant were also estimated. The overall strain was calculated by taking the average of the strains estimated in each quadrant (Equations A.6 - A.8). This only represented incremental strains at each moment an image was captured, h. To obtain the overall strain, the values were summed (Equations A.9 - A.11).

$$\epsilon_x(h) = \frac{\epsilon_{x,I} + \epsilon_{x,II} + \epsilon_{x,III} + \epsilon_{x,IV}}{4} \tag{A.6}$$

$$\epsilon_y(h) = \frac{\epsilon_{y,I} + \epsilon_{y,II} + \epsilon_{y,III} + \epsilon_{y,IV}}{4} \tag{A.7}$$

$$\epsilon_{xy}(h) = \frac{\epsilon_{xy,I} + \epsilon_{xy,II} + \epsilon_{xy,III} + \epsilon_{xy,IV}}{4} \tag{A.8}$$

$$\epsilon_{xTotal} = \sum_{h=0}^{n} \epsilon_x(h) \tag{A.9}$$

$$\epsilon_{yTotal} = \sum_{h=0}^{n} \epsilon_y(h) \tag{A.10}$$

$$\epsilon_{xyTotal} = \sum_{h=0}^{n} \epsilon_{xy}(h) \tag{A.11}$$

Principal strains were estimated using the relationship in Equation A.12 . The direction of the principal stresses were found using Equation A.13, where θ_p gives

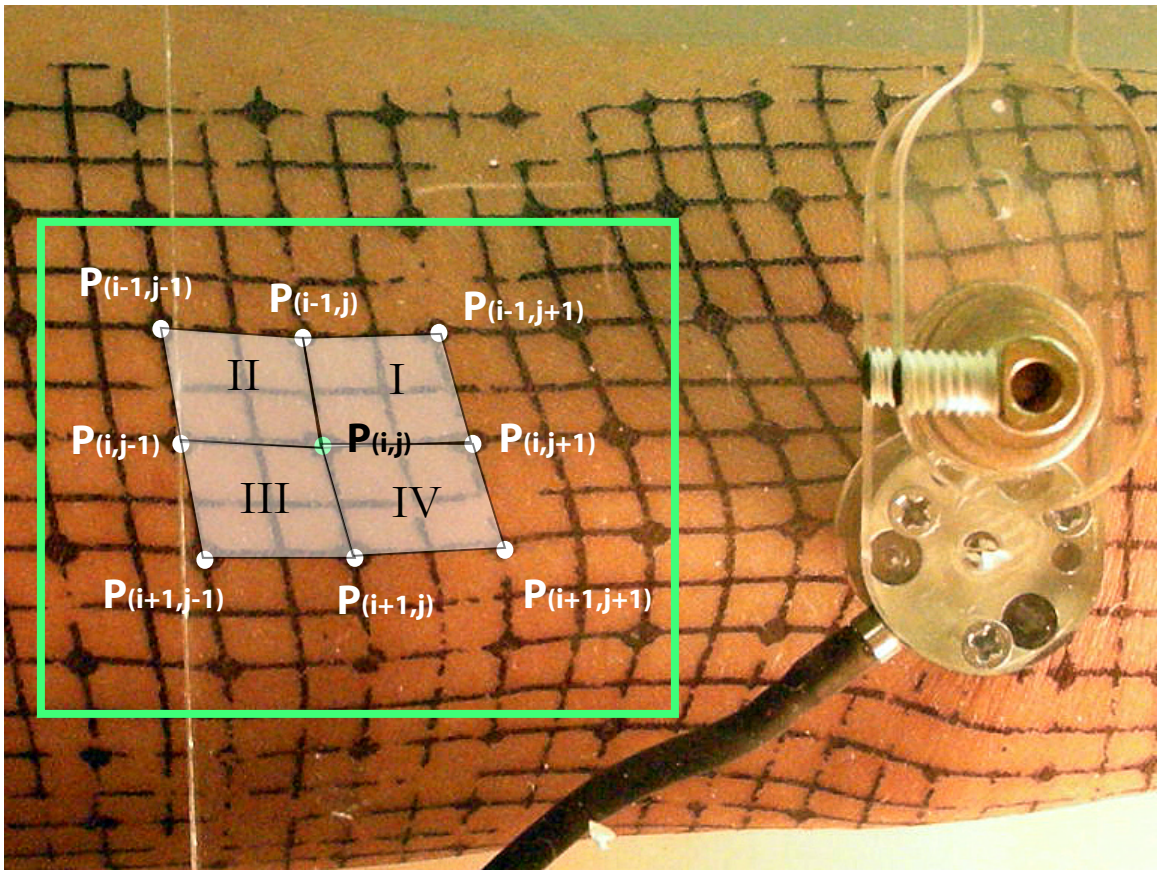

Figure A.4: Quadrants formed to estimate the strain at the point of interest, $p(i, j)$ using adjacent points.

the orientation of the principal planes of strain.

$$\epsilon_{1,2} = \frac{\epsilon_x + \epsilon_y}{2} \pm \sqrt{(\frac{\epsilon_x - \epsilon_y}{2})^2 + (\frac{\gamma_{xy}}{2})^2} \tag{A.12}$$

$$tan(2\theta_p) = \frac{\gamma_{xy}}{\epsilon_x - \epsilon_y} \tag{A.13}$$

Appendix B

Surface Strain Estimation

The data collected from the motion capture studies presented in Chapter 4 represented the displacement of 63 markers in a 9 x 7 grid. The analysis to estimate the surface strains is taken from similar analysis in [6].

B.1 Nomenclature

Each marker used in the analysis is defined by it's row and column location specified by i and j indices. For analysis, we used 9 rows of markers and 7 columns as indicated in Figure B.1. The remaining makers were not used in any other analysis. The rows i = 1, 2, 3,...,9 were labeled from top to bottom as oriented in the figure, and the columns were labeled j = 1,2,3,...,7 from elbow to wrist.

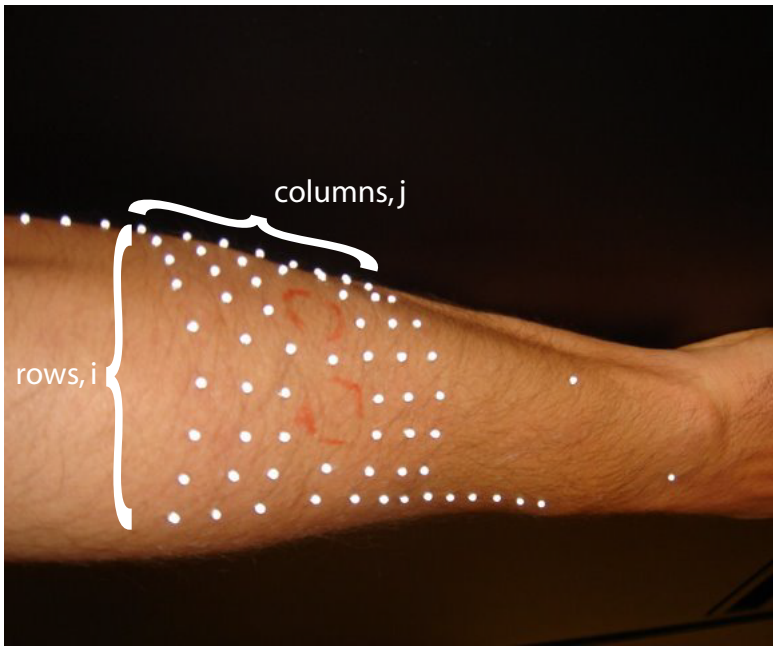

Figure B.1: The grid points used in strain analysis that track displacement of skin as stretch is applied. Four additional markers were placed on the end effector (not shown) to fill out a 9 x 7 grid of points. the rows increase top to bottom and the columns increase from elbow to wrist.

We let $\overrightarrow{X}_{i,j}$ be the initial configuration of the forearm skin surface at rest of a material point in the ith row and j^{th} column of the grid of markers. $\overrightarrow{x}_{i,j}$ is then the deformed configuration of the same point at the next instant of time or following data set (Figure B.2).

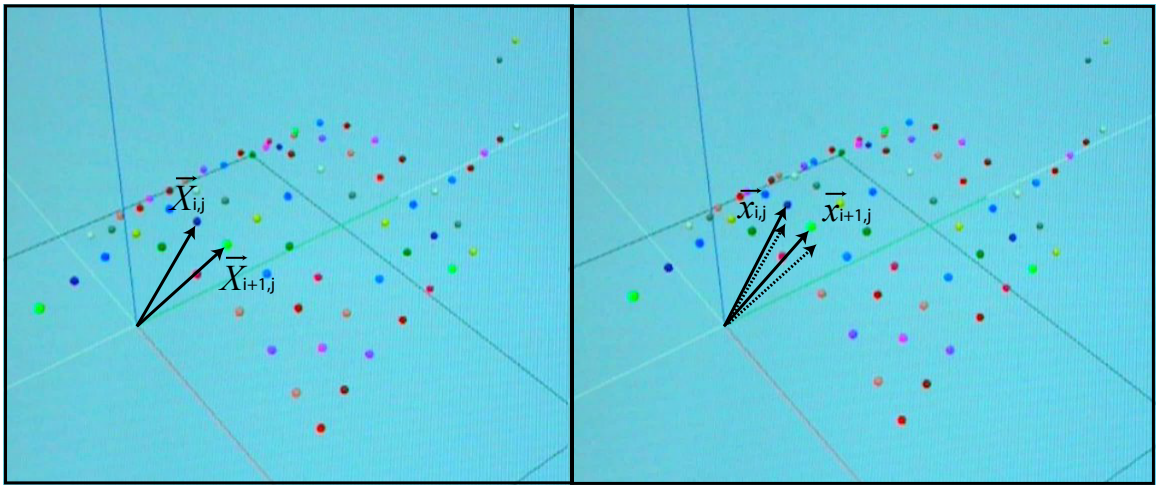

Figure B.2: Defining local reference frames. The markers in their original position at rest are on the left. A sample reference point $X_{i,j}$ and a point adjacent to it, $X_{i+1,j}$ are indicated in the figure. On the left is the same set of markers at a different point in time, in a deformed state. The dotted lines represent the original vectors $X_{i,j}$ and $X_{i+1,j}$ and the new lines show the deformed vectors $x_{i,j}$ and $x_{i+1,j}$.

The vectors describing the separation between a point at location *(i,j)* and its neighboring points are defined as shown in the Figure B.3. The vector $\overrightarrow{D}_{i+m,j+n}$ is the full three dimensional vector at rest where m = -1,0,1 and n = -1,0,1. Similarly, a set of eight vectors $\overrightarrow{d}_{i+m,j+n}$ can also be defined as the separation vectors in the deformed configuration of the arm. The magnitude of the vectors are given by $d_{i+m,j+n} = \mid \overrightarrow{d}_{i+m,j+n} \mid$.

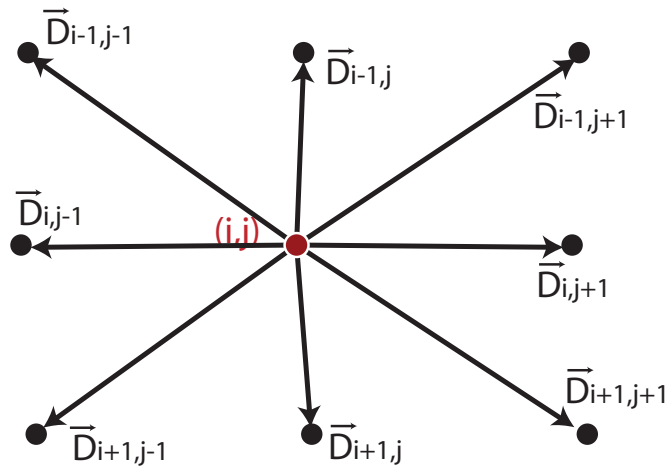

Figure B.3: Illustrating the nearest-neighbor separation vectors for a point *i,j*.

B.2 Strains

B.2.1 Normal Strain

The method used in this analysis to estimate longitudinal and transverse strains along the surface of the skin was strain gage rosette theory in which a pattern of normal strains in a rosette configuration allows for orthogonal normal strains and shear strains can be computed (see Figure B.4). The normal strains in the direction of each adjacent grid point form a series of rosettes. These normal strains were approximated using Equation B.1, where m = -1,0,1; n=-1,0,1. For example, $\epsilon_{i+1,j+1}$ is the normal strain for a grid point, (i, j) in the initial direction of the $(i+1, j+1)$ neighbor. Using equations B.2 - B.4, the strains, ϵ_x, ϵ_y, and γ_{xy} can be determined, solving the three equations for the three unknowns.

$$\epsilon_{i+m,j+n} = \frac{d_{i+m,j+n} - D_{i+m,j+n}}{D_{i+m,j+n}} \tag{B.1}$$

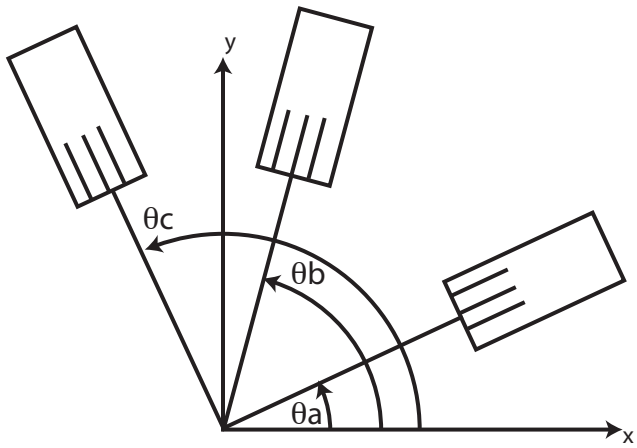

Figure B.4: Strain gage rosette configuration.

$$\epsilon_a = \epsilon_x cos^2\theta_a + \epsilon_y sin^2\theta_a + \gamma_{xy} sin\theta_a cos\theta_a \tag{B.2}$$

$$\epsilon_b = \epsilon_x cos^2\theta_b + \epsilon_y sin^2\theta_b + \gamma_{xy} sin\theta_b cos\theta_b \tag{B.3}$$

$$\epsilon_c = \epsilon_x cos^2\theta_c + \epsilon_y sin^2\theta_c + \gamma_{xy} sin\theta_b cos\theta_c \tag{B.4}$$

B.2.2 Local Reference Frame

To estimate the strains at each point, a local reference frame approximately tangent to the surface of the arm was constructed in each of the four quadrants. The normal strain components computed above are then transformed from the global reference frame to the local frame in each quadrant. The longitudinal axis was always assumed to be along the long axis of the forearm, pointing from elbow to wrist, while the transverse axis changed depending on the surface of the quadrant. Let $\overrightarrow{e}_1$ and $\overrightarrow{e}_2$ be the unit vectors that define the local axes on the surface of a quadrant. $\overrightarrow{e}_1$ points along the circumference of the arm while $\overrightarrow{e}_2$ points in the longitudinal direction.

If $\overrightarrow{n}$ is the unit vector normal to the surface of the point on the arm and the first quadrant of points consists of points directly to the right and above the point of interest, $\overrightarrow{n}^I$ within the first quadrant can be computed as follows:

$$\overrightarrow{n}^I = \frac{\overrightarrow{D}_{i-1,j+1} \times \overrightarrow{D}_{i-1,j}}{\mid \overrightarrow{D}_{i-1,j+1} \times \overrightarrow{D}_{i-1,j} \mid} \tag{B.5}$$

If $\overrightarrow{e}_2{}^I$ is the vector in the longitudinal direction, always assumed to be parallel to the vector pointing from elbow to wrist, along the longitudinal axis of the forearm and $\overrightarrow{e}_1{}^I$ the x-axis, $\overrightarrow{e}_1{}^I$ is the vector normal to both $\overrightarrow{n}^I$ and $\overrightarrow{e}_2{}^I$. An illustration of the local reference frames can be seen in Figure B.5.

$$\overrightarrow{e}_1{}^I = \overrightarrow{e}_2{}^I \times \overrightarrow{n}^I \tag{B.6}$$

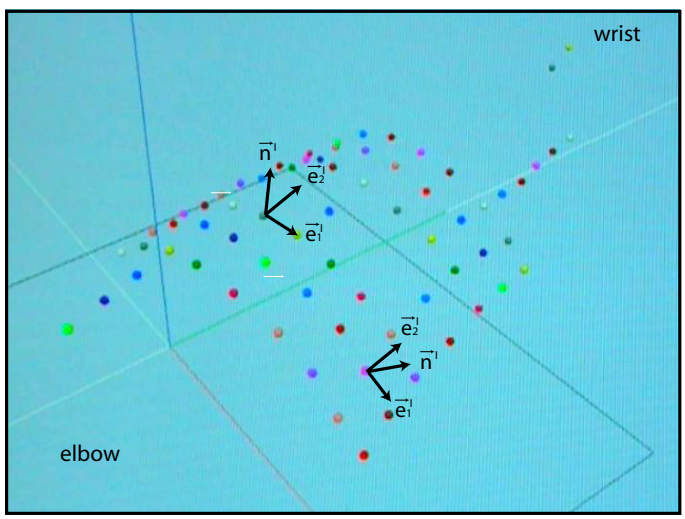

Figure B.5: Illustrating the local reference frame construction for various points.

B.2.3 Transformation to local reference frame

In equations B.2 - B.4, θ_a, θ_b, and θ_c can be re-written in terms of the adjacent grid point nomenclature, where in the first quadrant of points, $\theta_a = \theta_{i,j+1}{}^I$, $\theta_b = \theta_{i-1,j+1}{}^I$,

and $\theta_c = \theta_{i-1,j}{}^{I}$. These angles can be deterimined by equations B.7 - B.9. Then, substituting the known values into Equations B.2 - B.4, gives the desired strains in the local reference frame for each grid point.

$$\theta_{i,j+1} = cos^{-1}\left(\frac{\overrightarrow{D}_{i,j+1} \cdot \overrightarrow{e}_1{}^{I}}{\mid \overrightarrow{D}_{i,j+1} \mid\mid \overrightarrow{e}_1{}^{I} \mid}\right) \tag{B.7}$$

$$\theta_{i-1,j+1} = cos^{-1}\left(\frac{\overrightarrow{D}_{i-1,j+1} \cdot \overrightarrow{e}_1{}^{I}}{\mid \overrightarrow{D}_{i-1,j+1} \mid\mid \overrightarrow{e}_1{}^{I} \mid}\right) \tag{B.8}$$

$$\theta_{i-1,j} = cos^{-1}\left(\frac{\overrightarrow{D}_{i-1,j} \cdot \overrightarrow{e}_1{}^{I}}{\mid \overrightarrow{D}_{i-1,j} \mid\mid \overrightarrow{e}_1{}^{I} \mid}\right) \tag{B.9}$$

B.2.4 Overall strain

This analysis is repeated for each of the four quadrants for a given grid point. Four local reference frames are determined and four estimations of local strains are calculated. $\overrightarrow{e}_2^{I-IV}$ is still given by determining the vector parallel to the longitudinal axis of the forearm each of the four surface planes. The average of these four strain values estimates the longitudinal and transverse strains at each grid point, given by equations B.13 to B.15. Principal strains and directions are determined using equations A.12 and A.13.

$$\overrightarrow{n}^{II} = \frac{\overrightarrow{D}_{i-1,j} \times \overrightarrow{D}_{i-1,j-1}}{\mid \overrightarrow{D}_{i-1,j} \times \overrightarrow{D}_{i-1,j-1} \mid} \tag{B.10}$$

$$\overrightarrow{n}^{III} = \frac{\overrightarrow{D}_{i+1,j-1} \times \overrightarrow{D}_{i+1,j}}{\mid \overrightarrow{D}_{i+1,j-1} \times \overrightarrow{D}_{i+1,j} \mid} \tag{B.11}$$

$$\overrightarrow{n}^{IV} = \frac{\overrightarrow{D}_{i+1,j} \times \overrightarrow{D}_{i+1,j+1}}{\mid \overrightarrow{D}_{i+1,j} \times \overrightarrow{D}_{i+1,j+1} \mid} \tag{B.12}$$

$$\epsilon_x{}^{avg} = \frac{\epsilon_x{}^{I} + \epsilon_x{}^{II} + \epsilon_x{}^{III} + \epsilon_x{}^{IV}}{4} \tag{B.13}$$

$$\epsilon_y{}^{avg} = \frac{\epsilon_y{}^{I} + \epsilon_y{}^{II} + \epsilon_y{}^{III} + \epsilon_y{}^{IV}}{4} \tag{B.14}$$

$$\epsilon_{xy}{}^{avg} = \frac{\epsilon_{xy}{}^{I} + \epsilon_{xy}{}^{II} + \epsilon_{xy}{}^{III} + \epsilon_{xy}{}^{IV}}{4} \tag{B.15}$$

Bibliography

[1] S Adee. Dean Kamen's "Luke Arm" prosthesis readies for clinical trials. *IEEE Spectrum*, Feb 2008.

[2] P Agache, C Monneur, J Leveque, and J Rigal. Mechanical properties and young's modulus of human skin in vivo. *Archives of Dermatological Research*, 269:221–232, Jan 1980.

[3] HM Al-angari, R ff Weir, CW Heckathorne, and DS Childress. A two degree-of-freedom microprocessor based extended physiological proprioception (EPP) controller for upper limb prostheses. *Technology and Disability*, 15(2):113–127, 2003.

[4] R Archer, SH Crandall, NC Dahl, and TJ Lardner. *An Introduction to the mechanics of solids*, chapter 5, pages 287–317. McGraw Hill, second edition, 1978.

[5] U Berglund and B Berglund. Adaptation and Recovery in Vibrotactile Perception. *Perceptual and Motor Skills*, 30(3):843–&, 1970.

[6] K Bethke. The second skin approach: Skin strain field analysis and mechanical counter pressure prototyping for advanced spacesuit design. *Master's Thesis, MIT*, Jun 2005.

[7] J Biggs and M Srinivasan. Tangential versus normal displacements of skin: Relative effectiveness for producing tactile sensations. *Proceedings of the 10th*

Symp. On Haptic Interfaces For Virtual Envir. & Teleoperator Systems, Mar 2002.

[8] M Binnard and M Cutkosky. Design by composition for layered manufacturing. *Journal of Mechanical Design*, 122:91–101, Jan 2000.

[9] I Birznieks, P Jenmalm, AW Goodwin, and RS Johansson. Encoding of direction of finger tip forces by human tactile afferents. *The Journal of Neuroscience*, 21:8222–8237, Oct 2001.

[10] A Bloomfield and N Badler. Virtual training via vibrotactile arrays. *Presence: Teleoperators and Virtual Environments*, 17(2):103–120, Apr 2008.

[11] L Bonanni, C Vaucelle, J Lieberman, and O Zuckerman. Taptap: a haptic wearable for asynchronous distributed touch therapy. *Conference on Human Factors in Computing Systems*, Jan 2006.

[12] A Brisben, S Hsiao, and K Johnson. Detection of vibration transmitted through an object grasped in the hand. *Journal of Neurophysiology*, 81:1548–1558, Jan 1999.

[13] L Brown, S Brewster, and H Purchase. A first investigation into the effectiveness of tactons. *Eurohaptics Conference, 2005 and Symposium on Haptic Interfaces for Virtual Environment and Teleoperator Systems.*, pages 167 – 176, Feb 2005.

[14] D Caldwell and C Gosney. Enhanced tactile feedback (tele-taction) using a multi-functional sensory system. *1993 IEEE International Conference on Robotics and Automation*, pages 3215–3221, Jan 1993.

[15] D Caldwell, N Tsagarakis, and C Giesler. An integrated tactile/shear feedback array for stimulation of finger mechanoreceptor. *Proceedings of the 1999 IEEE International Conference on Robotics & Automation*, 1:287 – 292, Apr 1999.

[16] LE Carlson. Control of powered arm prosthesis with extended physiological proprioception. In *Proceedings of the 7th World Congress of the International Society for Prosthetics and Orthotics*, 1992.

[17] M Chambers, K Andres, M Duering, and A Iggo. The structure and function of the slowly adapting type II mechanoreceptor in hairy skin. *Experimental Physiology*, Jan 1972.

[18] A Chatterjee, P Chaubey, J Martin, and NV Thakor. Quantifying prosthesis control improvements using a vibrotactile representation of grip force. *Region 5 Conference, 2008 IEEE*, pages 1–5, April 2008.

[19] DS Childress, EC Grahn, RF ff Weir, CW Heckathorne, and JE Uellendahl. Modification of a bock hand for e.p.p. control by exteriorized tendons. In *Proceedings of the 19th Annual Meeting of American Academy of Orthotics and Prosthetics*, page 13, 1993.

[20] T Chu, WF Ranson, MA Sutton, and WH Peters. Applications of digital-image-correlation techniques to experimental mechanics. *Experimental Mechanics*, 25(3):232–244, Sep 1985.

[21] C Cipriani, F Zaccone, S Micera, and M Carrozza. On the shared control of an emg-controlled prosthetic hand: Analysis of user–prosthesis interaction. *Robotics*, 24(1):170–184, Feb 2008.

[22] D Collins and A Prochazka. Movement illusions evoked by ensemble cutaneous input from the dorsum of the human hand. *Journal of Physiology*, 496.3:857–871, Jan 1996.

[23] D Collins, K Refshauge, G Todd, and S Gandevia. Cutaneous receptors contribute to kinesthesia at the index finger, elbow, and knee. *Journal of Neurophysiology*, 94:1699–1706, May 2005.

[24] CuteCircuit. The hug shirt. Website, 2006. `http://www.cutecircuit.com/projects/wearables/thehugshirt/`.

[25] C Daly and G Odland. Age-related changes in the mechanical properties of human skin. *Journal of Investigative Dermatology*, 73(1):84–87, Jan 1979.

[26] K Dandekar and M A Srinivasan. Role of mechanics in tactile sensing of shape. touch lab report 2. rle tr-604. mit. cambridge. *Touch Lab Report 2*, RLE TR-604, Jan 1997.

[27] G Dhillon and K Horch. Direct neural sensory feedback and control of a prosthetic arm. *Neural Systems and Rehabilitation Engineering*, Jan 2005.

[28] JA Doeringer and N Hogan. Performance of above elbow body-powered prostheses in visually guided unconstrained motion tasks. *Biomedical Engineering, IEEE Transactions on*, 42(6):621–631, June 1995.

[29] L Douven, R Meijer, and C Oomens. Characterization of mechanical behavior of human skin in vivo. *Laser-Tissue InteractionXI: Photochemical, Photothermal, and Photomechanical*, 3914:618–629, Jan 2000.

[30] B Edin. Quantitative analysis of static strain sensitivity in human mechanoreceptors from hairy skin. *Journal of Neurophysiology*, 67(5), May 1992.

[31] B Edin. Cutaneous afferents provide information about knee joint movements in humans. *J Physiol (Lond)*, 531(1):289–297, Nov 2001.

[32] B Edin. Quantitative analyses of dynamic strain sensitivity in human skin mechanoreceptors. *Journal of Neurophysiology*, 92:3233–3243, Jul 2004.

[33] B Edin, L Beccai, L Ascari, and S Roccella. A bio-inspired approach for the design and characterization of a tactile sensory system for a cybernetic prosthetic hand. *Proceedings of the IEEE International Conference on Robotics and Automation*, Jan 2006.

[34] B Edin and N Johansson. Skin strain patterns provide kinaesthetic information to the human central nervous system. *J Physiol (Lond)*, 487:242–251, Jan 1995.

[35] K Englehart and B Hudgins. A robust, real-time control scheme for multifunction myoelectric control. *Biomedical Engineering*, 50(7):848–854, Jul 2003.

[36] A Faga. A new method to visualize langer's lines. *The Journal of Dermatologic Surgery and Oncology.*, 7(1):53–55, Feb 1981.

[37] R.E. Fan, M.O. Culjat, Chih-Hung King, M.L. Franco, R. Boryk, J.W. Bisley, E. Dutson, and W.S. Grundfest. A haptic feedback system for lower-limb prostheses. *Neural Systems and Rehabilitation Engineering, IEEE Transactions on*, 16(3):270–277, June 2008.

[38] B Finlay. Dynamic mechanical testing of human skin "in vivo". *J Biomech*, 3:557–568, Jan 1970.

[39] O Franzen and J Nordmark. Vibrotactile frequency discrimination. *Perception and Psychophysics*, 17(5):480–484, Feb 1975.

[40] A Frisoli, F Rocchi, S Marcheschi, and A Dettori. A new force-feedback arm exoskeleton for haptic interaction in virtual environments. *Proceedings of the First Joint Eurohaptics Conference and Symposium on Haptic Interfaces for Virtual Environment and Teleoperator Systems*, pages 195– 201, Jan 2005.

[41] M Fritschi, W LSC, and C Public. Design of a tactile shear force prototype display. touch-hapsys.org, 2003. `http://www.touch-hapsys.org/data/paper/TH-D6_1.pdf`.

[42] Y.C. Fung. *A First Course in Continuum Mechanics*. Prentice Hall, Inc., second edition, 1977.

[43] A Gallace, H Tan, and C Spence. Tactile change detection. *First Joint Eurohaptics Conference and Symposium on Haptic Interfaces for Virtual Environment and Teleoperator Systems (WHC'05), 2005*, pages 12 – 16, Feb 2005.

[44] S Gandevia, J Smith, M Crawford, and U Proske. Motor commands contribute to human position sense. *Journal of Physiology*, 571.3:703–710, Jan 2006.

[45] E Gardner and J Martin. *Coding of Sensory Information*. Principles of Neural Science. McGraw-Hill, fourth edition, 2000.

[46] E. Gardner, J. Martin, and T. Jessell. *The Bodily Senses*. Principles Of Neural Science. McGraw Hill, fourth edition, 2000.

[47] GD Garson. Univariate glm, anova, and ancova from statnotes: Topics in multivariabe analysis. Website, 2007. `http://www2.chass.ncsu.edu/garson/pa765/anova.htm`.

[48] G Gescheider. Psychophysics: The fundamentals. *3rd ed: Lawrence Erlbaum Associates*, 1997.

[49] S Gilman. Joint position sense and vibration sense: anatomical organisation and assessment. *Journal of Neurology, Nerosurgery, and Psychiatry*, 73:473–477, Jan 2002.

[50] G Goff. Differential discrimination of frequency of cutaneous mechanical vibration. *Journal of Experimental Psychology*, 74(2):294–299, Jun 1967.

[51] G Goodwin, D McCloskey, and P Matthews. The contribution of muscle afferents to kinaesthesia shown by vibration induced illusions of movement and by the effects of paralysing joint afferents. *Brain*, 95:705–748, Jan 1972.

[52] P Grigg. Stretch sensitivity of mechanoreceptor neurons in rat hairy skin. *Journal of Neurophysiology*, 76(5), Jan 1996.

[53] J Harris, E Arabzadeh, C Moore, and C Clifford. Noninformative vision causes adaptive changes in tactile sensitivity. *Journal of Neuroscience*, 27(27):7136–7140, Jul 2007.

[54] V Hayward and M Cruz-Hernandez. Tactile display device using distributed lateral skin stretch. *Proceedings of the Haptic Interfaces for Virtual Environment and Teleoperator Systems*, Jan 2000.

[55] CW Heckathorne, DS Childress, EC Grahn, J Strysik, and J Uellendahl. E.p.p. control of an electric hand by exteriorized forearm tendons. In *Proceedings of the 8th World Conference of the International Society of Prosthetics and Orthotics)*,, 1995.

[56] F. M. Hendriks. Mechanical behaviour of human skin in vivo - a literature review. In *Nat.Lab. Unclassified Report 820. Philips Research Laboratories*, 2001.

[57] M Hollins, AK Goble, BL Whitsel, and M Tommerdahl. Time Course and Action Spectrum of Vibrotactile Adaptation. *Somatosensory and Motor Research*, 7(2):205–221, 1990.

[58] RD Howe and MR Cutkosky. Sensing skin acceleration for slip and texture perception. *1989 IEEE International Conference on Robotics and Automation*, 1:145–150, May 1989.

[59] A Israr, H Tan, and C Reed. Frequency and amplitude discrimination along the kinesthetic-cutaneous continuum in the presence of masking stimuli. *The Journal of the Acoustical Society of America*, 120(5):2789–2800, Nov 2006.

[60] L Jiang, R Girotra, M Cutkosky, and C Ullrich. Reducing error rates with low-cost haptic feedback in virtual reality-based training applications. *Proceedings of the First Joint Eurohaptics Conference and Symposium on Haptic Interfaces for Virtual Environment and Teleoperator Systems*, pages 420 – 425, Feb 2005.

[61] L Jones, B Lockyer, and E Piateski. Tactile display and vibrotactile pattern recognition on the torso. *Advanced Robotics*, 20(12):1369–1374(16), 2006.

[62] L Jones and N Sarter. Tactile displays: Guidance for their design and application. *Human Factors: The Journal of the Human Factors and Ergonomics Society*, 50(1):90–111, Feb 2008.

[63] LA Jones and K Ray. Localization and pattern recognition with tactile displays. *Symposium on Haptic Interfaces for Virtual Environments and Teleoperator Systems 2008*, pages 33–39, March 2008.

[64] R Voyles Jr, G Fedder, and P Khosla. Design of a modular tactile sensor and actuator based on an electrorheological gel. *1996 IEEE International Conference on Robotics and Automoation*, pages 13–17, Apr 1996.

[65] P Khalsa, A Hoffman, and P Grigg. Mechanical states encoded by stretch-sensitive neurons in feline joint capsule. *Journal of Neurophysiology*, 76(1), Jul 1996.

[66] F Khatyr, C Imberdis, P Vescovo, and D Varchon. Model of the viscoelastic behaviour of skin in vivo and study of anisotropy. *Skin Research and Technology*, 10:96–103, Jan 2004.

[67] S Kim, M Spenko, S Trujillo, B Heyneman, D Santos, and MR Cutkosky. Smooth vertical surface climbing with directional adhesion. *Robotics, IEEE Transactions on*, 24(1):65–74, Feb. 2008.

[68] B Kollmeier, R Gilkey, and U Sieben. Adaptive staircase techniques in psychoacoustics: A comparison of human data and a mathematical model. *The Journal of the Acoustical Society of America*, 83(5):1852–1862, May 1988.

[69] KJ Kuchenbecker, N Gurari, and AM Okamura. Effects of visual and proprioceptive motion feedback on human control of targeted movement. *Proceedings*

of the 2007 IEEE 10th International Conference on Rehabilitation Robotics,, pages 513–524, June 2007.

[70] T Kuiken, G Li, B Lock, R Lipschutz, and L Miller. Targeted muscle reinnervation for real-time myoelectric control of multifunction artificial arms. *JAMA*, 301(6):619–628, Feb 2009.

[71] K Langer. On the anatomy and physiology of the skin. I. the cleavability of the cutis. *British Journal of Plastic Surgery*, 31(1):3–8, 1978.

[72] K Langer. On the anatomy and physiology of the skin. II. skin tension. *British Journal of Plastic Surgery*, 31(2):93–106, 1978.

[73] C Layne. Pep 6397 introduction to neuroscience. Website, 2009. `http://grants.hhp.coe.uh.edu/clayne/6397/Unit4a.htm`.

[74] M Leek. Adaptive procedures in psychophysical research. *Perception & Psychophysics*, 63(8):1279–1292, 2001.

[75] V Levesque, J Pasquero, and V Hayward. Braille display by lateral skin deformation with the stress 2 tactile transducer. *Proc. World Haptics Conference*, Jan 2007.

[76] H Levitt. Transformed up and down methods in psychoacoustics. *The Journal of the Acoustical Society of America*, Jan 1971.

[77] J Lieberman and C Breazeal. Tikl: Development of a wearable vibrotactile feedback suit for improved human motor learning. *Robotics, IEEE Transactions on*, 23(5):919–926, Oct. 2007.

[78] J Loomis and S Lederman. Tactual perception. *In Boff, K.R., Kaufman, L., and Thomas, J.P. (Eds.), Handbook of perception and human performance: Vol. 2. Cong- nitive processes and performance. New York: Wiley, 1986, pp. 31.1-31.41*, 1986.

[79] H Maekawa and J Hollerbach. Haptic display for object grasping and manipulating in virtual environment. *Robotics and Automation, 1998. Proceedings. 1998 IEEE International Conference on*, 3:2566 – 2573, Apr 1998.

[80] D Mahns, N Perkins, V Sahai, L Robinson, and M Rowe. Vibrotactile frequency discrimination in human hairy skin. *Journal of Neurophysiology*, 95:1442–1450, Nov 2006.

[81] Y Makino and H Shinoda. Selective stimulation to superficial mechanoreceptors by temporal control of suction pressure. *Proceedings of the First Joint Eurohaptics Conference and Symposium on Haptic Interfaces for Virtual Environment and Teleoperator Systems*, Jan 2005.

[82] J Manschot and A Brakkee. The measurement and modeling of the mechanical properties of human skin in vivo - II. the model. *Journal of Biomechanics*, 19(7):517–521, Nov 1986.

[83] J Manschot and A Brakkee. The measurement and modelling of the mechanical properties of human skin in vivo–I. the measurement. *Journal of Biomechanics*, 19(7):511–515, Jan 1986.

[84] H Marcellier, P Vescovo, D Varchon, P Vacher, and P Humbert. Optical analysis of displacement and strain fields on human skin. *Skin Research and Technology*, 7(4):246–253, May 2001.

[85] D McFarland and J Wolpaw. Brain-computer interface operation of robotic and prosthetic devices. *Computer*, 41(10):52–56, Oct 2008.

[86] R Meijer, L Douven, and C Oomens. Characterisation of anisotropic and nonlinear behaviour of human skin in vivo. *Computer Methods in Biomechanics and Biomedical Engineering*, 1:13–27, May 1999.

[87] Takashi Mitsuda, Sachiko Kuge, Masato Wakabayashi, and Sadao Kawamura. Wearable force display using a particle mechanical constraint. *Presence: Teleoperators and Virtual Environments*, 11(6):569–577, 2002.

[88] J Morley and M Rowe. Perceived pitch of vibrotactile stimuli: effects of vibration amplitude, and implications for vibration frequency coding. *Journal of Physiology*, 431:403–416, May 1990.

[89] Shinsei Motors. Ultrasonicmotor general catalogue. Website, 2007. `http://www.shinsei-motor.com/downloads/Catalog\_E\_2005\_09.pdf`.

[90] G Mowbray and J Gebhard. Sensitivity of the skin to changes in rate of intermittent mechanical stimuli. *Science*, 125:1297–1298, Jun 1957.

[91] G Moy and RS Fearing. Effects of shear stress in teletaction and human perception. In *Proc. ASME Dyn. Systems and Control Division, DSC-Vol 64*, pages 265–272, 1998.

[92] AM Murray, RL Klatzky, and P Khosla. Psychophysical characterization and testbed validation of a wearable vibrotactile glove for telemanipulation. *MIT Press: Presence*, 12(2):156–182, 2003.

[93] SK Nagel, C Carl, T Kringe, T Martin, and P Konig. Beyond sensory substitution—learning the sixth sense. *Journal of Neural Engineering*, 2(4):R13–R26, 2005.

[94] U Norrsell and H Olausson. Human, tactile, directional sensibility and its peripheral origins. *Acta physiologica scandinavica*, 144(2):155–161, Jan 1992.

[95] U Norrsell and H Olausson. Spatial cues serving the tactile directional sensibility of the human forearm. *J Physiol (Lond)*, 478 Pt 3:533–40, Aug 1994.

[96] H Olausson. Tactile directional sensibility: peripheral neural mechanisms in man. *Brain Research*, 866(1-2):178–187, Jun 2000.

[97] H Olausson, I Hamadeh, P Pakdel, and U Norrsell. Remarkable capacity for perception of the direction of skin pull in man. *Brain Research*, 808(1):120–3, Oct 1998.

[98] H Olausson and U Norrsell. Observations on human tactile directional sensibility. *J Physiol (Lond)*, Jan 1993.

[99] T Pakkanen, J Lylykangas, J Raisamo, R Raisamo, K Salminen, J Rantala, and V Surakka. Perception of low-amplitude haptic stimuli when biking. *International Conference on Multimodal Interfaces*, 2008.

[100] Panasonic. Panasonic stroke rehabilitation suit. Website, 2006. `http://panasonic.co.jp/corp/news/official.data/data.dir/en060925-6/en060925-6.html`.

[101] M Paré, H Carnahan, and A Smith. Magnitude estimation of tangential force applied to the fingerpad. *Experimental Brain Research*, 142:342–348, Jan 2002.

[102] J Pasquero, J Luk, V Levesque, Q Wang, and V Hayward. Haptically enabled handheld information display with distributed tactile transducer. *IEEE Transactions on Multimedia*, 9(4):746–753, Jan 2007.

[103] J Phillips and K Johnson. Tactile spatial resolution. iii. a continuum mechanics model of skin predicting mechanoreceptor responses to bars, edges, and gratings. *Journal of Neurophysiology*, 46(6):1204–1225, Dec 1981.

[104] E Piateski and L Jones. Vibrotactile pattern recognition on the arm and torso. *Proceedings of the First Joint Eurohaptics Conference and Symposium on Haptic Interfaces for Virtual Environment and Teleoperator Systems*, Jan 2005.

[105] W Provancher, B Erickson, F Barbagli, and H Tan. Tactile perception of rotational sliding. *Proceedings of the Second Joint EuroHaptics Conference*

and Symposium on Haptic Interfaces for Virtual Environment and Teleoperator Systems, pages 127–132, Mar 2007.

[106] R Reihsner, B Balogh, and E J Menzel. Two-dimensional elastic properties of human skin in terms of an incremental model at the in vivo configuration. *Medical engineering & physics*, 17(4):304–13, Jun 1995.

[107] M Rothenberg, R Verrillo, Stephen A Zahorian, Michael L Brachman, and Stanley J Bolanowski. Vibrotactile frequency for encoding speech parameters. *The Journal of the Acoustical Society of America*, 62:1003–1012, Jun 1977.

[108] D Ryu, K Moon, S Kang, M Kim, and JB Song. Development of wearable haptic system for tangible studio to experience a virtual heritage alive. *2006 IEEE/RSJ International Conference on Intelligent Robots and Systems*, pages 466–471, Oct. 2006.

[109] R Sanders. Torsional elasticity of human skin in vivo. *Pflügers Archiv European Journal of Physiology*, 342:255–260, Jan 1973.

[110] B Shelton and I Scarrow. Two-alternative versus three-alternative procedures for threshold estimation. *Perception and Psychophysics*, 35(4):385–392, Jan 1984.

[111] D Simpson. The choice of control system for the multimovement prosthesis: extended physiological proprioception (e.p.p). *The Control of Upper-Extremity Prostheses and Orthoses*, Jan 1973.

[112] R Skalak and S Chien. *Handbook of Bioengineering*. McGraw Hill Book Company, 1987.

[113] K Spanner. Survey of the various operating principles of ultrasonic piezomotors. *Proceedings of the 10th International Conference on New Actuators*, 2006.

[114] H Tan, F Barbagli, K Salisbury, C Ho, and C Spence. Force-direction discrimination is not influenced by reference force direction. *Haptics-e*, Jan 2006.

[115] H Tan, R Gray, J Young, and P Irawan. Haptic cueing of a visual change-detection task: Implications for multimodal interfaces. *Proceedings of the 9th International Conference on Human-Computer Interaction*, pages 678–682, 2001.

[116] H Tan, R Gray, J Young, and R Traylor. A haptic back display for attentional and directional cueing. *Haptics-e*, Jan 2003.

[117] H Tan, A Lim, and R Traylor. A psychophysical study of sensory saltation with an open response paradigm. *Proceedings of the ASME Dynamic Systems and Control Division*, 69-2, Jan 2000.

[118] H Tan and A Pentland. Tactual displays for sensory substitution and wearable computers. *International Conference on Computer Graphics and Interactive Techniques*, Jan 2005.

[119] J Teh, A Cheok, RL Peiris, Y Choi, V Thuong, and S Lai. Huggy pajama: a mobile parent and child hugging communication system. In *IDC '08: Proceedings of the 7th international conference on Interaction design and children*, pages 250–257, New York, NY, USA, 2008. ACM.

[120] N Tsagarakis and D Caldwell. Development and control of a 'soft-actuated' exoskeleton for use in physiotherapy and training. *Autonomous Robots*, 15:21–33, Jan 2003.

[121] Å Vallbo and R Johansson. Properties of cutaneous mechanoreceptors in the human hand related to touch sensation. *Human neurobiology*, Jan 1984.

[122] Å Vallbo, H Olausson, J Wessberg, and N Kakuda. Receptive field characteristics of tactile units with myelinated afferents in hairy skin of human subjects. *Journal of Physiology*, 483(Pt 3):783, Mar 1995.

[123] MR van Ratingen, R Petterson, M.R Drost, CWJ Oomens, and JD Janssen. A mixed numerical/experimental method to find langer's lines of skin. *Advances in Bioengineering*, 26:63–65, Feb 1993.

[124] RT Verrillo. Vibrotactile thresholds measured at the finger. *Perception & Psychophysics*, 9(4):329, 1971.

[125] C Wagner and R Howe. Mechanisms of performance enhancement with force feedback. *Proceedings of the First Joint Eurohaptics Conference and Symposium on Haptic Interfaces for Virtual Environment and Teleoperator Systems*, pages 21 – 29, Feb 2005.

[126] Q Wang, V Hayward, and A Smith. A new technique for the controlled stimulation of the skin. *Proceedings of Canadian Medical and Biological Engineering Society Conference*, Jan 2004.

[127] H Wasling, U Norrsell, K Göthner, and H Olausson. Tactile directional sensitivity and postural control. *Experimental brain research Experimentelle Hirnforschung Expérimentation cérébrale*, 166(2):147–56, Oct 2005.

[128] N Weerakkody, D Mahns, J Taylor, and S Gandevia. Impairment of human proprioception by high-frequency cutaneous vibration. *The Journal of Physiology Online*, 581(3):971, Jun 2007.

[129] R ff Weir, CW Heckathorne, and DS Childress. Cineplasty as a control input for externally powered prosthetic components. *Journal of Rehabilitation Research and Development*, 38(4):357–363, 2001.

[130] A Wilksa. On the vibrational sensitivity in different regions of the body surface. *Acta physiologica scandinavica*, 31:284–289, Jul 1954.

[131] G Wu, R Ekedahl, and RG Hallin. Clustering of slowly adapting type II mechanoreceptors in human peripheral nerve and skin. *Brain*, 121(2):265, Feb 1998.

[132] L Zollo, S Roccella, E Guglielmelli, and M Carrozza. Biomechatronic design and control of an anthropomorphic artificial hand for prosthetic and robotic applications. *IEEE/ASME Transactions on Mechatronics*, 12(4):418–429, Aug 2007.

[133] J. J. Zwislocki and D. A. Goodman. Absolute scaling of sensory magnitudes: a validation. *Perception and Psychophysics*, 28(1):28–38, 1980.